MULTI-SCALE BURNED AREA MAPPING IN TALLGRASS PRAIRIE USING *IN SITU* SPECTROMETRY AND SATELLITE IMAGERY

by

RHETT L. MOHLER

B.S., Fort Hays State University, 2004
M.A., Kansas State University, 2006

AN ABSTRACT OF A DISSERTATION

submitted in partial fulfillment of the requirements for the degree

DOCTOR OF PHILOSOPHY

Department of Geography
College of Arts and Sciences

KANSAS STATE UNIVERSITY
Manhattan, Kansas

2011

Abstract

Prescribed burning in tallgrass prairie affects a wide range of human and natural systems. Consequently, managing this biome based on sound science, and with the concerns of all stakeholders taken into account, requires a method for mapping burned areas. In order to devise such a method, many different spectral ranges and spectral indices were tested for their ability to differentiate burned from unburned areas at both the field and satellite scales. Those bands and/or indices that performed well, as well as two different classification techniques and two different satellite-based sensors, were tested in order to come up with the best combination of band/index, classification technique, and sensor for mapping burned areas in tallgrass prairie. The ideal method used both the red and near-infrared spectral regions, used imagery at a spatial resolution of at least 250 m, used satellite imagery with daily temporal resolution, and used pixel-based classification techniques rather than object-based techniques. Using this method, burned area maps were generated for the Flint Hills for every year from 2000-2010, creating a fire history of the region during that time period. These maps were compared to active fire and burned area products, and these products were found to underestimate burned areas in tallgrass prairie.

MULTI-SCALE BURNED AREA MAPPING IN TALLGRASS PRAIRIE USING *IN SITU* SPECTROMETRY AND SATELLITE IMAGERY

by

RHETT L. MOHLER

B.S., Fort Hays State University, 2004
M.A., Kansas State University, 2006

A DISSERTATION

submitted in partial fulfillment of the requirements for the degree

DOCTOR OF PHILOSOPHY

Department of Geography
College of Arts and Sciences

KANSAS STATE UNIVERSITY
Manhattan, Kansas

2011

Approved by:

Major Professor
Douglas G. Goodin

Abstract

Prescribed burning in tallgrass prairie affects a wide range of human and natural systems. Consequently, managing this biome based on sound science, and with the concerns of all stakeholders taken into account, requires a method for mapping burned areas. In order to devise such a method, many different spectral ranges and spectral indices were tested for their ability to differentiate burned from unburned areas at both the field and satellite scales. Those bands and/or indices that performed well, as well as two different classification techniques and two different satellite-based sensors, were tested in order to come up with the best combination of band/index, classification technique, and sensor for mapping burned areas in tallgrass prairie. The ideal method used both the red and near-infrared spectral regions, used imagery at a spatial resolution of at least 250 m, used satellite imagery with daily temporal resolution, and used pixel-based classification techniques rather than object-based techniques. Using this method, burned area maps were generated for the Flint Hills for every year from 2000-2010, creating a fire history of the region during that time period. These maps were compared to active fire and burned area products, and these products were found to underestimate burned areas in tallgrass prairie.

Table of Contents

List of Figures

List of Tables

Acknowledgements

First and foremost, I would like to thank my committee chairperson and advisor, Dr. Douglas Goodin, for many years of guidance, encouragement, and support during my Master's and Doctoral programs. Without Doug's contributions to my educational career, this dissertation couldn't have gotten off the ground, much less morphed into the finished study on burned area mapping in tallgrass prairie that it is.

Additionally, I would like to thank my committee members, Dr. John Harrington, Jr., Dr. Kevin Price, and Dr. Marcellus Caldas, as well as my outside chairperson, Dr. Kimberly With, my undergraduate advisor, Dr. John Heinrichs, and other individuals with whom I have interacted over my academic career. Thinking back over 12 years of higher education, I cannot think of a single time when any of these individuals turned me away when I needed their help or sought their advice. I also haven't forgotten about my fellow students, who have helped me perhaps more even than my teachers have, and owe them a sincere thank you as well.

I would also like to thank the National Science Foundation for a Doctoral Dissertation Research Improvement Grant (#NS9877), which funded both the fieldwork for this project, and the dissemination of the results at professional meetings. Similarly, I would like to thank the National Aeronautics and Space Administration Kansas Space Grant Consortium for a Graduate Student Fellowship that covered some living costs while working on this dissertation. I would also like to thank the Statistical Consulting Laboratory at Kansas State University for providing statistical help with Chapter 4, as well as Kansas State Research and Extension agents Mike Holder and Jeff Davidson for providing access to private land for the purpose of collecting ground-truth data.

Finally, I would like to thank my parents, Carl and Laraine. Their support and understanding, more than any other factor, provided me with the resolve to finish this dissertation and complete my Ph.D.

CHAPTER 1 - Impacts of Prescribed Burning on Tallgrass Prairie

1.1 Impacts on Plants

Before trying to characterize and map burned areas in tallgrass prairie, it is helpful to review the links between fire and the tallgrass prairie ecosystem. Currently, spring burning of tallgrass prairie is widely prescribed as a management technique in the Flint Hills of Kansas and Oklahoma, and has been practiced since the early 1900s (Towne and Owensby 1984). Prior to settlement, lightning and Native Americans may have been responsible for igniting these fires (Anderson 1990). Regardless of how they are started, fire in tallgrass prairie continues to perform the same ecological role it has played for millennia: to influence the sustainability, species composition, and productivity of plant communities (Knapp and Seastedt 1998). This comes as no surprise, as tallgrass prairies most likely evolved into their modern form due at least partly to fire (Bragg and Hulbert 1976). In fact, it is possible that no other North American biome relies so heavily on fire to remove dead biomass and maintain ecosystem function (Knapp and Seastedt 1986).

1.1.1 Sustainability

Prescribed burning plays a primary role in preserving and sustaining the tallgrass prairie ecosystem. One way it does so is by preventing trees and other woody plants from replacing native grasses and forbs. Even in places where precipitation is sufficient to support woody species, fire allows the ecosystem to be dominated by C_4 graminoid species such as *Andropogon gerardii* (big bluestem), *Schizachyrium scoparium* (little bluestem), *Sorghastrum nutans* (indiangrass), and *Panicum virgatum* (switchgrass) (Collins 1992, Glenn *et al.* 1992, Collins and Steinauer 1998, Hartnett and Fay 1998).

In addition to suppressing trees and other woody species, fire may prevent non-native grass species from invading tallgrass prairies. Simmons *et al.* (2007) found this to be true in two midgrass Texas prairies, and Smith and Knapp (1999) found it to be true in tallgrass prairie. Specifically, the latter study suggested that fire reduced exotic species richness (which was composed of about 90% C_3 plants) by 80-90%, and reduced the cover of exotic species. The tendency of fire to reduce the abundance of some C_3 grasses has also been noted by Abrams and

Hulbert (1987) and by Towne and Kemp (2003). These traits are very important to maintaining the economic vitality of the tallgrass prairie and parts of the Flint Hills region, as prescribed burning is a relatively inexpensive means by which ranchers can control less-palatable non-native plants and woody vegetation (Bernardo *et al.* 1988).

1.1.2 Species Composition

Fire also affects the spatial and temporal heterogeneity of plant communities (Collins 1989, Hartnett and Fay 1998). Typically, plant community heterogeneity is inversely related to burn frequency, so that as burning increases, plant communities become less diverse (Abrams and Hulbert 1987, Collins 1992). This effect can be so pronounced that even some native, warm-season grasses, such as *P. virgatum*, be virtually excluded from pure stands of other warm-season grasses, such as *A. gerardii* (Knapp 1985). Collins and Smith (2006) found that both spatial and temporal community heterogeneity were lowest on annually burned sites and highest on sites burned every twenty years. Additionally, Collins (1992) and Collins and Steinauer (1998) found that a significant, positive relationship exists between spatial and temporal heterogeneity. That is, areas that are spatially homogenous, such as annually burned areas, tend to remain that way across the time span of several years, and vice versa. Collins and Steinauer (1998) noted that it is unusual to have a disturbance (fire in this case) that stabilizes and homogenizes an ecosystem. Consequently, these effects of fire may be unique, at least in North America, to tallgrass prairies.

Several factors are responsible for the homogenizing effects of fire on tallgrass prairie. Many woody species have exposed meristems and early aboveground growth that is also easily damaged by fire (Hartnett and Fay 1998), while native grasses have large root systems and belowground meristems (at least during early spring burning) that protect them from fire (Hartnett and Fay 1998). It should be noted, however, that not all published research agrees on the importance of direct mortality to woody species (Collins and Steinauer 1998). Frequent burning also favors a few species due to its tendency to volatilize nitrogen (N) in dead plant matter (Hobbs *et al.* 1991). As this N is lost to frequent burning, the store of soil N is gradually depleted. This favors a few species that can cope with reduced N levels, usually matrix species such as *A. gerardii* (Collins and Steinauer 1998). Another effect of frequent burning is that it allows consistent amounts of sunlight to reach the soil, which also favors matrix species (Collins

and Steinauer 1998). The seasonality of the burn event can also influence plant community structure. Although Towne and Kemp (2003) found that the homogenizing effects of fire occurred regardless of burn seasonality, Engle *et al.* (1998) found that late season fires tended to reduce the production of matrix grasses and increase production of forbs. However, this relationship may be more complicated than originally thought, as Engle *et al.* (1998) also found that these effects are less dramatic in years of higher precipitation, and Engle and Bidwell (2001) found that they might be routinely overestimated at larger spatial scales, such as the entire Flint Hills.

Finally, it should be noted that although frequent fire has a homogenizing effect, all of the relationships discussed above are highly dependent on spatial scale. For example, an annually burned (and therefore homogenous) five-hectare tract might only be part of a larger, more diverse several-hundred hectare pasture that is burned at varying frequencies. This issue is further complicated when the spatial variation of pre-burn biomass (and therefore burn completeness) is considered (Collins and Smith 2006).

1.1.3 Productivity

In addition to being more homogenous, burned tallgrass prairies have been shown to consistently produce more biomass than similar unburned areas, particularly if the burning is done in late spring when warm-season grasses are beginning to grow (Towne and Owensby 1984, Knapp and Seastedt 1986, Svejcar and Browning 1988). Towne and Owensby (1984) also found annual burning did not limit productivity in any way, even after being sustained for many years. One reason for this increase in productivity is that prescribed burning liberates nutrients contained in dead plant material in order to stimulate new growth. For example, Anderson *et al.* (2006) found that N availability increased (and so productivity increased) when grasslands were both burned and grazed, but that this occurred only when pastures were both burned and grazed. That is, one or the other alone did not produce the same effect; and burning alone has been shown to reduce N availability (Collins and Steinauer 1998). Additionally, Svejcar (1990) noted that *A. gerardii* produced more tillers on burned areas than on unburned areas. These additional tillers during the growing season led to more aboveground biomass production.

Another way prescribed burning stimulated more biomass growth is by increasing solar radiation and lowering leaf temperatures to the optimal range for growth. Knapp (1984)

demonstrated that standing dead biomass reduces incident radiation on new shoots by up to 58.8%, leading to a 55.4% reduction in biomass production. Additionally, Knapp (1984) showed that burned prairies maintained more optimal leaf temperatures in the range of 25-35º C, rather than the much higher temperatures maintained by unburned plots. Furthermore, Knapp (1985) showed that *A. gerardii* on burned patches showed higher rates of photosynthesis, leaf thickness, and shoot biomass compared to unburned areas.

Other research suggests that productivity increases on burned areas independently of external controls. Heisler and Knapp (2008) found that burned areas consistently out-produced unburned areas with respect to aboveground net primary production (ANPP), despite equal amounts of precipitation over several similar study sites. Finally, Towne and Kemp (2003) found that burn seasonality did significantly affect biomass (as was previously thought) because burning increased biomass in all seasons tested (fall, winter, spring).

1.2 Link Between Fire and Grazing

Although the effects of prescribed burning on plant communities are important in their own right, their effects are often interrelated with grazing in tallgrass prairies, and fire and grazing are often identified as the two most important disturbance types in tallgrass prairie (Collins and Steinauer 1998). One example of this relationship is that herbivores such as *Bison bison* (bison) and *Bos taurus* (cattle) are attracted to recently burned areas for the high quality, recently regenerated vegetation (Vinton *et al.* 1993, Coppedge and Shaw 1998). For this reason, grazing often has the opposite effect of frequent burning because it reduces the dominance of native grasses (they are preferentially grazed) and provides space for other species to colonize the area. This increases plant community heterogeneity (Collins 1987, Glenn *et al.* 1992, Hartnett *et al.* 1996, Hickman *et al.* 2004) in a manner similar to that expected from less frequently burned non-grazed areas (Collins and Steinauer 1998).

Grazing also tends to increase heterogeneity by moving N stores from aboveground plants to the soil. This prevents burning activities (even on frequently burned patches) from volatilizing the N, whereby it would be lost (Hobbs *et al.* 1991). Again, higher N concentrations allow more plant species to compete. Finally, it is worth mentioning once again that the changes in heterogeneity wrought by grazing are entirely related to the scale of the activity (Collins and

Smith 2006), and likely depend on the specific plant species that are being studied as well (Hickman *et al.* 2004).

1.3 Impacts on Wildlife

In addition to plants and grazing animals, prescribed burning affects wildlife. For example, Wilgers and Horne (2006) found that herpetofaunal community compositions within different burn treatments are significantly different from one another, and that several species showed clear preference for a specific burn treatment, though overall species diversity was similar among all treatments. It should also be noted that fires impact reptiles directly, as they are often too slow (due to cold-bloodedness) to escape fires (Kaufman *et al.* 1998a).

With regard to small mammals, Kaufman *et al.* (1990, 1998b) reported that different species respond differently to burning, with some increasing and some decreasing, though overall species richness was lower on burned areas. It is likely that small mammal responses were due to the higher biomass production associated with burning, rather than due to the direct effects of fire (Collins and Steinauer 1998).

Insect populations are closely tied to burning events as well. Jonas and Joern (2007) found that prescribed burning affected grasshopper abundances and community composition. Evans (1984, 1988) reported that overall grasshopper species diversity increases with time since fire because grasshopper diversity depends directly on plant species diversity. Furthermore this increase is more pronounced with forb-feeding species than with grass-feeding species (Evans 1988). Additionally, grass-feeding species tend to peak and decline earlier in burned areas (Evans 1984).

Regarding grassland birds, upland bird numbers were found to increase two years after an area was burned, in spite of the fact that the initial burning tended to destroy bird nests (Van Dyke *et al.* 2007). Furthermore, Fuhlendorf *et al.* (2006) found that patch burning increased bird diversity compared to homogenous burning of an entire area. Zimmerman (1992) noted that during non-drought years, burning had little effect on grassland-dependent bird species (*Ammodramus henslowii*—Henslow's Sparrow —was an exception), but that species richness decreased in drought years. Many negative effects of burning on birds have been demonstrated as well. Population models by With *et al.* (2008) show that three species of songbird could not sustain viable populations in the Flint Hills in 2004 or 2005 based on rough burned area

estimates. Their analysis suggests that even very large tracts of tallgrass prairie might not be enough to maintain viable breeding populations of some birds if the focus of fire-based management on those large areas is directed toward livestock production alone.

In the case of all species mentioned above, the trends depend on the scale at which the areas were burned, and it is possible that by constantly rotating what areas are burned (and grazed), ranchers can sustain livestock production while conserving plant biodiversity (and therefore animal biodiversity) at the same time (Anderson *et al.* 2006, Fuhlendorf *et al.* 2006, Wilgers and Horne 2006). That is, fire cannot be removed from tallgrass prairies without negative consequences for both human and natural interests, but overusing fire in order to maintain homogenous stands of matrix tallgrass species is not ideal either, as fire and grazing treatments that promote uniformity cannot maintain biodiversity in tallgrass ecosystems (Kaufman *et al.* 1998b, Fuhlendorf *et al.* 2006).

1.4 Impacts on Humans

The effects of prescribed burning in tallgrass prairie are not always limited to the plants, animals, and economic interests associated with the immediate area. Pollutants from biomass burning in general, though often considered only a nuisance, can have serious health implications for humans living within the airshed of burned areas (Radke *et al.* 2001), and these airsheds can extend for hundreds of miles (Niemie *et al.* 2005). Furthermore, these implications could become more serious as the Earth's climate continues to change (Ebi and McGregor 2008). The most common chemicals produced by biomass burning are oxocarbons (CO_X), sulfur oxides (SO_X), ozone (O_3), ammonia (NH_3), nitrogen oxides (NO_X), methane (CH_4), and other non-methane hydrocarbons (NMHC) (Dennis *et al.* 2002, Pope *et al.* 2002). Although brief exposure to these chemicals causes little risk, longer-term exposure can be harmful, particularly in the case of sulfur oxides (Pope *et al.* 2002). Biomass burning is usually responsible for only a small portion of the total budget of these chemicals in the atmosphere, though an exception may be carbon monoxide, where total emissions due to fires may be as much as 10% of the total budget according to a study by Dennis *et al.* (2002).

More likely to affect human health than chemicals are the particulates released during burning. Whereas only small percentages of the total atmospheric mass of the chemicals mentioned above are from biomass burning, a large percentage of airborne particulates are from

this activity (Dennis *et al.* 2002). Furthermore, particulates are likely to do more damage to humans, especially when they are less than 2.5 μm in size. Particles of this size, unlike larger particles of 10-15 μm, are strongly associated with elevated mortality due to lung cancer and other cardiopulmonary-related causes (Pope *et al.* 2002). Particulates are also associated with the production of O_3, and controlling particulates helps to alleviate ozone pollution problems as well (Meng et al. 1997).

CHAPTER 2 - This Place of this Study in Burned Area Mapping Research

2.1 Importance of Burned Area Mapping Research

Chapter 1 establishes that prescribed burning in tallgrass prairies affects a wide variety of both human and natural systems, including but not limited to plant species diversity and community structure, biomass production, wildlife species diversity and numbers, ranching-based economies, and local and regional human health. Furthermore, prescribed burning and its effects are important to a wide range of academic disciplines and government agencies conducting research or otherwise working in tallgrass prairies. All of these interests would benefit from knowing how much area is burned each year, and when and where that burning takes place (Pereira *et al.* 1997, Eva and Lambin 1998, personal observation). As of this writing, however, only the Bluestem Pasture Report (USDA-NASS 2011), a voluntary survey based on producer-reported estimates of burned area, exists for the Flint Hills. For this reason, the overarching goal of this research was to develop a method of accurately mapping burned areas in tallgrass prairie of the Flint Hills.

2.2 State of Burned Area Mapping Research

2.2.1 The Utility of Remotely Sensed Data

This study used remotely sensed data from both *in situ* measurements and from satellite-based sensors. Remotely sensed imagery is ideal for burned area mapping because of its relatively high temporal and spectral resolution, its cost effectiveness, and its ability to access otherwise inaccessible areas (Pereira *et al.* 1997, Al-Rawi *et al.* 2001, Roy *et al.* 2002). In fact, a large body of literature that explores the utility of remote sensing methods for mapping burned areas already exists, and forms the theoretical basis for the application of burned area mapping methods in a wide range of land cover types. Despite its large size and critical role, however, this body of knowledge could be further enriched by research that develops theories, methods, and products that are specific to mapping burned areas in grasslands, including tallgrass prairie, for the reasons outlined below.

2.2.2 Active Fire and Burned Area Products

Current satellite-derived products that show burned areas or estimate burned area from active fire data are often inaccurate and of questionable usefulness (Eva and Lambin 1998). For example, Boschetti *et al.* (2004) found little agreement between two different burned area products, particularly with regard to the areal extent of the burned patches. Giglio *et al.* (2006) found that active fires correspond poorly with actual burned areas (burned areas are severely underestimated), and that this correspondence was even poorer in cover types with few trees, such as grasslands and savannahs. Chuvieco *et al.* (2008) note similar problems with estimating burned area with active fire products.

The failure of active fire data to estimate burned areas accurately is due to a number of factors. In the case of the products evaluated by Boschetti *et al.* (2004), the estimates were made from active fires that were detected at night, when only self-sustaining fires, such as forest fires, were left burning. In contrast, prescribed grassland fires started during the day would have likely burned out by the time of satellite overpass, and only burn scars would remain (Eva and Lambin 1998, Pereira 2003). Even with an optimal overpass times and daily imagery, however, the brief nature of grassland fires would inevitably lead to significant inaccuracy, as not every pixel that is actually burned is detected as a fire pixel (Eva and Lambin 1998, Roy *et al.* 2002, Boschetti *et al.* 2004, Li *et al.* 2004, Giglio *et al.* 2006).

Another problem with using burned area products and active fire estimates is that they were developed to map burned areas regionally or globally across a wide range of biomes. Because of this, they must marginalize certain cover types to some extent (Chuvieco *et al.* 2008, Giglio *et al.* 2009). Grassland, where estimating burned area from active fires is relatively difficult, is usually the cover type that is marginalized. Nonetheless, it is important to note that Silva *et al.* (2004), Roy *et al.* (2005), and Loboda *et al.* (2007) have made headway in mapping burned areas across diverse ecosystems using adaptable detection algorithms. Similarly, Boschetti *et al.* (2008) found that two independent burned area products corresponded well to each other, though these results were in forest rather than grassland. Despite this progress, however, these studies are still far from producing global estimates that are as reliable as local ones. Consequently, the focus of this study was to directly estimate the spatial and temporal extent of burned areas, rather than derive them from active fire data or burned areas products, though it compared burned area maps produced for the Flint Hills to both of those products.

2.2.3 Current Burned Area Mapping Research

2.2.3.1 Grassland Burned Area Mapping Research

Another reason for conducting grassland burned area mapping research is that relatively little work has been done in this ecosystem type, though grasslands are specifically addressed in a few instances. For example, Cao *et al.* (2009) mapped burned areas in a semi-arid grassland with a Support Vector Machine (SVM) approach, while Rahman and Gamon (2004) characterized the evolution of a semi-arid grassland burn scar using *in situ* measurements.

Research performed in other grassland types is often of limited use for burned area mapping in tallgrass prairie. In the case of both studies mentioned above, the lower biomass of the semi-arid grassland produced far less char on the burned surface, and led to more exposed soil in both burned and unburned areas, than would be the case in tallgrass prairie (Rahman and Gamon 2004, Cao *et al.* 2009). This lessened the contrast between the burned and unburned areas, which typically makes burned area identification more difficult (Pereira *et al.* 1997). In fact, Rahman and Gamon (2004) show that with the exception of the charcoal signal (which quickly disappears) burned and unburned areas of semi-arid grassland are statistically similar until re-growth begins. Another difference between these two grassland types is that re-growth does not usually take place immediately after burning in semi-arid grasslands, but spring burning leads to immediate re-growth on tallgrass prairie.

The work of Silva *et al.* (2004) also illustrates that current grassland burn mapping research is often of only minor help to mapping burned tallgrass prairies. In this case, Silva *et al.* (2004) worked toward a global burned area-mapping algorithm using the Système Probatoire de l'Observation de la Terre (SPOT)-VEGETATION (VGT) instrument by breaking down land cover into separate classes (including grasslands). This work does provide suggestions for band and index selection for grassland burn mapping, but is limited in scope to the few bands available on the SPOT-VGT sensor. Finally, Mohler and Goodin (2010) simulated (from radiomteter data) and examined the utility of two common spectral regions and one index for differentiating burned from unburned areas in tallgrass prairie. However, this study has yet to be expanded to include the full range of potentially useful spectral regions and indices.

2.2.3.2 Burned Area Mapping In Other Cover Types

Like the grassland-specific work mentioned in the previous paragraph, burned area mapping studies in other land cover types can provide information that is useful to burned area mapping in tallgrass prairies. For example, Pereira (2003) found that the loss of telltale combustion products due to scattering by the wind, the quick recovery of the burn scars, and the persistence of cloud cover are major challenges to burned area mapping in savannahs with remotely sensed imagery. Trigg and Flasse (2000) noted a rapid removal of the char signal in savannahs poses another challenge. Shao and Duncan (2007) discuss the challenges associated burned area mapping during rapid re-growth—in their case, with Florida oak scrublands. Pereira (2003) points out that different biomass fuel loads lead to different burn signatures in savannahs. This complicates burned area mapping in that "burned surface" can refer to any number of different spectral classes (Pereira 2003). All of these challenges apply to burned area mapping in tallgrass prairie as well, because ash and char can be scattered rapidly by the wind and rain, the spectral properties of different burned areas vary, and the wet season (and therefore cloud cover) in spring corresponds to the period of highest burning activity *and* most rapid vegetation re-growth. Though they are be discussed in more detail in Chapter 4, burned area mapping studies in other cover types can also be valuable for their identification of spectral regions and indices that might be useful for burned area mapping in tallgrass prairie.

Burned area mapping work in cover types other than grasslands can be useful for its methodological findings as well. For example, Mitri and Gitas (2004a, 2004b, 2006, 2008) demonstrated the superiority of object-based classification methods over pixel-based classification methods for mapping forest fire scars. Although forests and grasslands are very different cover types, it is likely that many of the technical aspects of this work would apply to grasslands as well. A study by Hudak and Brockett (2004) is another example. They demonstrate and discuss the utility of the parallelpiped classifier for burned area mapping in a savannah, and aspects of this study could prove useful to the same pursuit in tallgrass prairie.

Despite their usefulness in many instances, caution must be exercised when applying findings from other cover types to tallgrass prairie. If the cover types are different enough, this is often intuitive. For instance, Stroppiana *et al.* (2002) found that the best spectral regions for differentiating burned from unburned forest areas could not perform the same task well in grasslands because the spectral differences between burned and unburned forest remain on the landscape longer than in grasslands. This happens because more forest biomass is burned,

because forest combustion products (char and ash) are more likely to remain on the ground longer, and because forest re-growth is very slow (Pereira 2003).

Perhaps less intuitively, savannah areas and even grassland areas (like the semi-arid ones discussed at the beginning of this section) often fail to accurately represent other grasslands, including tallgrass prairie. Furthermore, these inadequacies remain even when the grassland component of a savannah area is evaluated independently of the ecosystem as a whole (Stroppiana *et al.* 2002, Silva *et al.* 2004). Stroppiana *et al.* (2002), noted that the probability of misclassifying burned patches increased more rapidly with burn age in grasslands than in other cover types. Another example is provided by Pereira (2003), who found that if burning occurs in the understory of moderately dense tree cover, such as in a woodland savannah, the major reflectance change is a drop in the near-infrared (NIR), while burning in sparse tree cover or pure grasslands results in a decrease in reflectance across the entire spectrum. Trigg and Flasse (2000) and Dempewolf *et al.* (2007) also discuss these issues. Although most researchers maintain that the char signal of a burned savannah area disappears quickly (e.g., Trigg and Flasse 2000, Pereira 2003), Dempewolf *et al.* (2007) notes that "quickly" might mean up to two weeks or more, due in part to the absence of re-growth in many savannah studies. This may not be likely in tallgrass prairies, where most burning takes place during the wet season and wind is a constant factor. Not only do these factors rapidly decrease the char signal, but, in the case of precipitation, can also cause both burned and unburned areas to re-grow rapidly (Pereira *et al.* 1997). This process steadily eliminates the spectral differences on which burned area detection depends (Trigg and Flasse 2000, Mohler and Goodin 2010), and can lead to confusion between unburned vegetation and older burned areas (Eva and Lambin 1998).

2.2.3.3 Global Burned Area Mapping Techniques

Finally, a discussion on current burned area mapping research would not be complete without at least a brief discussion of burn mapping techniques over large, diverse regions and over the entire Earth. Many studies have concluded that applying a methodology for mapping burned areas to all land cover types, and even to specific subtypes within certain biomes, is difficult due to the great diversity of landscapes at a global level (Pereira 2003). Consequently, the automation of wide-scale burned area mapping applications is extremely difficult (Periera *et al.* 1997). Chuvieco *et al.* (2008) demonstrated this with regard to burned grasslands, which showed the least overall classification accuracy of any cover type when mapped across Central

and South America. Interestingly, these differences were regional as well, as burned areas mapped in temperate grasslands were less accurate than those in tropical grasslands (Chuvieco *et al.* 2008). It is clear, then, that global burned area mapping algorithms, if they are to be viable, must include local factors specific to the ecosystem being studied (Chuvieco *et al.* 2008). This study, therefore, used the information provided by post studies of other cover types, as well as information from tallgrass prairies, to create a body of literature that concentrates specifically on burned area mapping in tallgrass prairie.

2.3 Research Questions, Objectives, and Hypotheses

The questions and objectives of this research are based on the interrelated issues discussed above. First, that the current body of knowledge concerning burned area mapping with remotely sensed imagery in grasslands, and in tallgrass prairie in particular, will benefit from additional research. Second, that conducting this research will allow a wide range of affected entities, both human and natural, to benefit from the resulting theories, methods, and products. The specific research questions and objectives of this paper are as follows:

Research Question: Which spectral regions and indices can differentiate between burned and unburned tallgrass prairie at the individual patch scale?

Objective: Reveal the utility of various simulated bands and indices for differentiating between burned and unburned tallgrass prairie from burning through senescence at the patch scale based on hyperspectral data gathered *in situ*.

Hypothesis: A statistical difference exists between burned and unburned patches of tallgrass prairie with the simulated band/index in question for a particular time since burning took place.

Research Question: Are the bands and indices that performed well when measured in situ also effective at the satellite imagery scale?

Objective: Reveal the utility of different TM and MODIS bands and indices for differentiating burned from unburned tallgrass prairie at the satellite image scale.

Hypothesis: Those bands and indices that were successful in differentiating burned from unburned tallgrass prairie using *in situ* data will also do so effectively at the satellite image scale.

Research Question: Which bands/indices, sensors, and techniques perform best for mapping burned areas in tallgrass prairie?

Objective: Use the band/index suitability information that was obtained by accomplishing the first and second objectives to identify which bands/indices, sensors, and classification techniques work best for mapping burned areas in tallgrass prairie.

Hypothesis: Object-based classification techniques will map burned tallgrass prairie more accurately than pixel-based techniques based on prior studies in other cover types.

Hypothesis: TM will allow for more accurate burned area mapping in tallgrass prairie than MODIS due to its superior spatial resolution.

Hypothesis: Due to cloud cover, MODIS must be used in order to achieve a sample that is temporally dense enough for burned area mapping in tallgrass prairie.

Hypothesis: Bands and/or indices composed of red and NIR wavelengths will be required for optimal burned area mapping in tallgrass prairie because they represent the best compromise in spatial and temporal resolution.

Research Question: What is the burn history of the Flint Hills?

Objective: Reconstruct the spatio-temporal fire history of the Flint Hills for as far back in time as suitable imagery is available (identifying this time depends upon completion of the previous three objectives).

Research Question: How do estimates of burned areas calibrated specifically to tallgrass prairie compare to those from global burned area and active fire products?

Objective: Compare final burned area maps to MODIS active fire product and MODIS burned area product.

Hypothesis: Locally produced burned area maps will depict burned areas more accurately than active fire product.

Hypothesis: Locally produced burned area maps will depict burned areas more accurately than the monthly burned area product.

CHAPTER 3 - Study Area

The study area of this research was an 18-county region in the Flint Hills of Kansas and Oklahoma (Figure 3.1). The Flint Hills are the largest extant patch of tallgrass prairie (Kollmorgen and Simonett 1965, Knapp and Seastedt 1998). All satellite-level analysis in Chapters 5 and 6 used portions of this study area. All historical burned area mapping (Chapter 7) and the comparison of these results to active fire and burned area products (Chapter 8) was preformed across the entire 18-county region. All *in situ* hyperspectral sampling (Chapter 4) was performed solely on the Konza Prairie Biological Station (KPBS; Figure 3.1), a 3,487 ha Long-Term Ecological Research (LTER) site located in Riley County, Kansas. The KPBS was used for this purpose because it is managed so that different watersheds are burned at different, known intervals of between one and twenty years. Additionally, each watershed receives one of three grazing treatments (no grazing, grazing by *B. taurus*, and grazing by *B. bison*). Knowing these factors, as well as the spatial extent of each watershed, allowed these variables to be controlled (or at least accounted for) in the *in situ* analysis.

Precipitation for Manhattan, KS, near the KPBS in the northern part of the study area, averages 835 mm per year, with approximately 52 mm of this coming as snowfall (Hayden 1998). This precipitation is usually concentrated during the growning season (approximately 75%), though this value is highly variable from year to year (Hayden 1998). Temperature for Manhattan, KS averages –1.8 °C for the month of Januray, and 26.5 °C for the month of July.

Although tallgrass prairie dominates the study area due to thin upland soils (Freeman 1998), several other land cover types are also found there. Croplands, usually planted to corn or soybeans, are prevalent in the relatively flat floodplains of the area's streams and rivers. In addition to cropland, gallery forests follow the course of many streams and rivers. Although rare in the uplands overall, trees can be locally common in areas where fire and grazing have been suppressed. These species, despite their relative rarity, contribute greatly to the species richness of the study area (Freeman 1998). Figure 3.2 shows simplified land cover for the study area based on the Kansas Gap Analysis Program (GAP) data (Kansas Applied Remote Sensing Program 2001).

Although the vegetation of the study area can be divided roughly into the land cover classes of tallgrass prairie, tree cover, and crops, a large amount of heterogeneity exists within even the seemingly homogenous tallgrass prairie class. Although matrix species such as *A. gerardii*, *S. scoparium, S. nutans,* and *P. virgatum* dominate the Flint Hills, species typically associated with drier environments, such as *Bouteloua gracilis* (blue grama), *Bouteloua curtipendula* (sideoats grama), and *Buchloe dactyloides* (buffalograss) occur in more xeric sites (Freeman 1998). Other non-graminoid species are interspersed within the tallgrass matrix as well, including many species of forbs and woody shrubs (Freeman 1998). As mentioned in Chapter 1, these species increase or decrease with regard to burn frequency, climate, and grazing intensity. Finally, it should be noted that the main large herbivore in the study area, *B. bison*, was replaced by *B. taurus* after Euro-American settlement (Hartnett *et al.* 1996).

Figure 3.1: 18-county study area in Kansas and Oklahoma, showing KPBS in Riley County, Kansas.

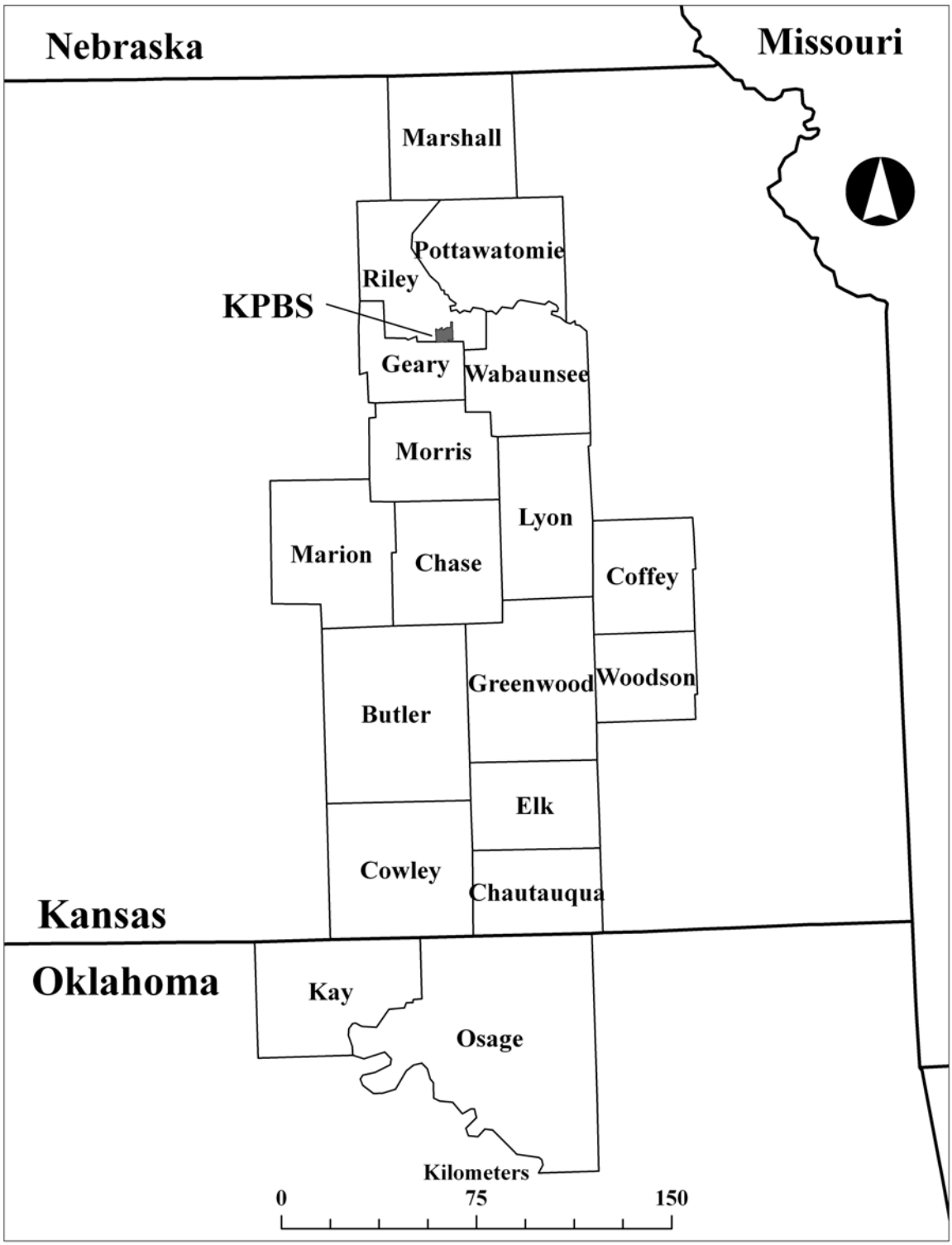

Figure 3.2: Map of grassland and non-grassland areas within the larger study area. Adapted from Kansas GAP data (Kansas Applied Remote Sensing Program 2001).

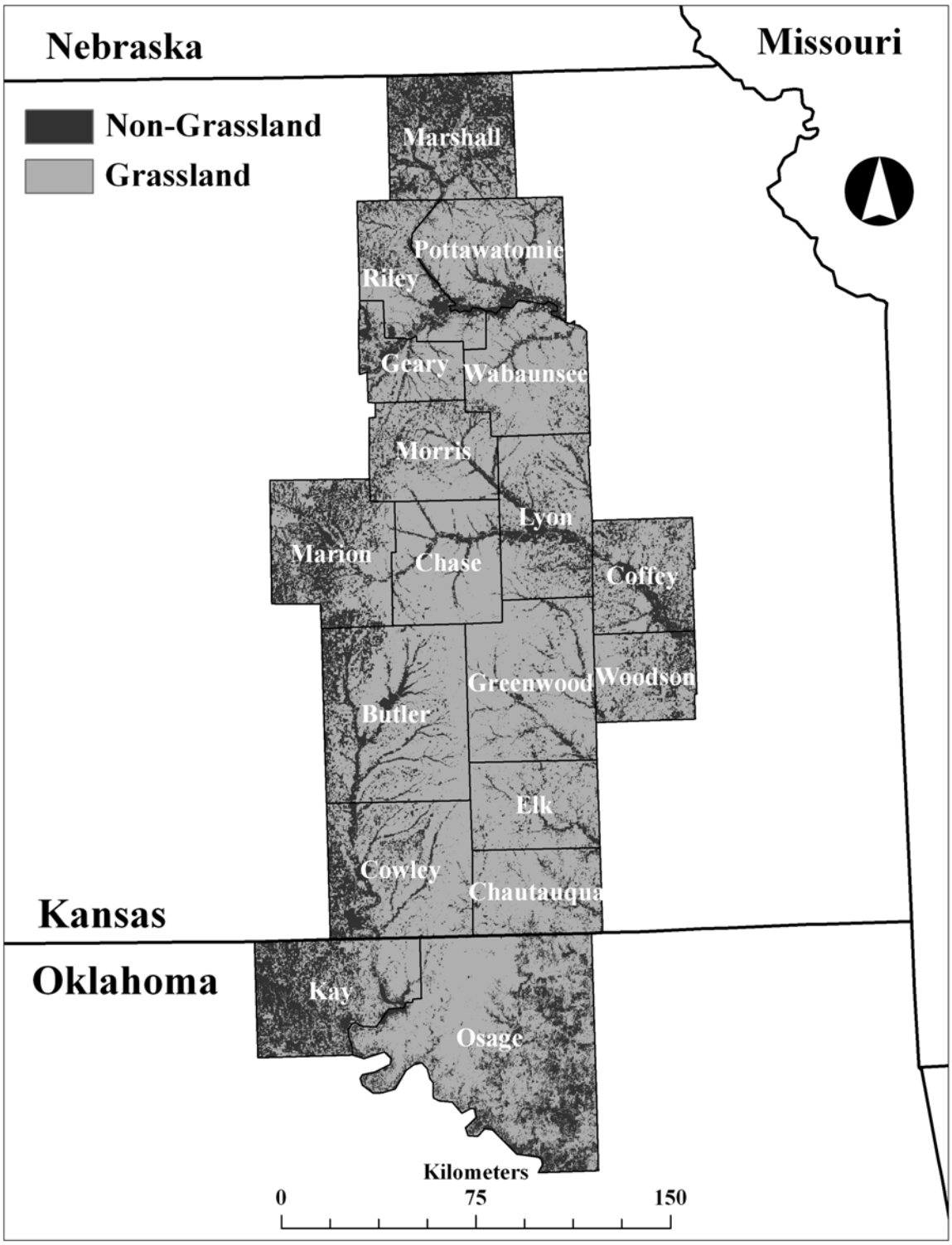

CHAPTER 4 - *In Situ* Hyperspectral Analysis

4.1 Introduction

The first objective of this study was to investigate the utility of various simulated bands and indices for differentiating between burned and unburned tallgrass prairie from burning through senescence based on hyperspectral data gathered *in situ*. This objective was accomplished by testing the hypothesis that a statistical difference exists between burned and unburned patches of tallgrass prairie with the simulated band/index in question for a particular time since burning took place. Meeting this first objective is necessary because characterizing the spectral-temporal properties of burned and unburned areas, as well as the change in these properties over time, is the logical first step toward the larger goal of mapping burned areas with satellite imagery (Chuvieco and Cognalton 1988, Pereira *et al.* 1997, Trigg and Flasse 2000). This is even more important in this case considering the lack of research in grasslands (Silva *et al.* 2004, see Chapter 2).

4.2 Methods

4.2.1 Band and Index Selection

The specific bands and indices tested were chosen based the published performance of equal or similar bands and indices in various cover types, including both tropical and boreal forest, savannahs with varying amounts of tree cover, an oak scrubland, and two semi-arid grasslands. Although these cover types are different (sometimes very different) than tallgrass prairie, little published literature evaluates the usefulness of any spectral region or index in tallgrass prairie specifically, and rarely does so in any grassland type. As a result, many spectral regions and indices were considered here, even though they are only known to be effective in cover types other than grasslands. Finally, it should be noted that all bands in this study were simulated based on their MODIS wavelength ranges only, though the exact wavelength range of similar spectral regions usually varies by sensor (Table 4.l). This is justified in section 4.2.3.

Table 4.1: Comparison of similar bands for several satellite-based sensors. The number on the left of the semicolon is the name of the band, while the range to the right is the area of the spectrum covered in micrometers. The acronym ASTER, which is not defined in the text, stands for Advanced Spaceborne Thermal Emission and Reflection Radiometer.

Band	TM	MODIS	SPOT-VGT	AVHRR	ASTER
Blue	1; 0.45-0.52	3; 0.459-0.479	BO; 0.43-0.47		
Green	2; 0.52-0.6	4; 0.545-565			1; 0.52-0.6
Red	3; 0.63-0.69	1; 0.62-0.67	R; 0.61-0.68	1; 0.58-0.68	2; 0.63-0.69
NIR	4; 0.76-0.90	2; 0.841-0.876	NIR; 0.79-0.89	2; 0.725-1	3; 0.76-0.86
LNIR		5; 1.23-1.25			
SMIR	5; 1.55-1.75	6; 1.628-1.652	MR; 1.58-1.75	3A; 1.58-1.64	5; 1.6-1.7
LMIR	7; 2.08-2.35	7; 2.105-2.155			5-9; 2.145-1.365

4.2.1.1 Bands

Among the bands that were simulated, NIR was chosen because it performed well across a wide variety of cover types (e.g., Lopez-Garcia and Caselles 1991, Koutsias and Karteris 1998, Pereira 1999, Stroppiana *et al.* 2002, Pu and Gong 2004, Shao and Duncan 2007), which should be expected (Silva *et al.* 2004). More specifically, Mohler and Goodin (2010) found that NIR could differentiate burned areas from unburned for at least a month in tallgrass prairie, while Trigg and Flasse (2000) place this figure at only a few days in a senescent savannah (likely because regrowth had not commenced and both dead and burned vegetation look the same. Additionally, the decision tree of Dempewolf *et al.* (2007) did not select NIR, though this does not speak directly to its usefulness.

Unlike NIR, the red spectral region saw mixed reports in the literature as to its usefulness. Among those studies that did not identify red as an important spectral region for burned area mapping were Koutsias and Karteris (1998) using TM in a forest area, Pereira (1999) using AVHRR in a shrubland/forest, Pu and Gong (2004), Silva *et al.* (2004) using SPOT-VGT in various cover types, Shao and Duncan (2007), and Dempewolf *et al.* (2007). Trigg and Flasse (2000) found this wavelength to be sensitive for only a few days, while Mohler and Goodin (2010) found it to be useful for up to two months. Lopez-Garcia and Caselles (1991) noted that it could separate burned areas, but did not excel at doing so, while Stroppiana *et al.* (2002), using SPOT-VGT in a savannah, echoed this sentiment.

Like NIR, long-wavelength middle infrared (LMIR) was deemed useful for burned area mapping in a wide variety of cover types (e.g., Lopez-Garcia and Caselles 1991, Koutsias and Karteris 1998, Trigg and Flasse 2000, Li *et al.* 2004, Pu and Gong 2004). In contrast to the above studies, Shao and Duncan (2007) found this band to perform only mediocre.

The performance of other TM and MODIS bands for burned area mapping varied among cover types. Koutsias and Karteris (1998) and Shao and Duncan (2007) cited TM band 5, which corresponds roughly to MODIS band 6 and is referred to as short-wavelength middle infrared (SMIR), as performing very poorly. Pu and Gong (2004) found it slightly more useful, while Lopez-Garcia and Caselles (1991) wrote that it performed well. MODIS band 6 was found by Trigg and Flasse (2000) to only differentiate burned from unburned savannah for a few days, while Li *et al.* (2004) claim that this is the poorest performing of the longer wavelength MODIS bands (bands 5-7). Stroppiana *et al.* (2002) and Silva *et al.* (2004), citing this band's counterpart on the SPOT-VGT instrument, found it useful for burned area mapping in grasslands.

Another band that was simulated was MODIS band 5—long-wavelength near infrared (LNIR). Though it has no TM counterpart, LNIR was found by Trigg and Flasse (2000) to differentiate between burned and unburned savannah for at least 13 days after burning. Li *et al.* (2004) also found this band useful. Testing the utility of these longer wavelengths is especially important because they are relatively unaffected by smoke and light clouds, and so are sometimes superior to those that use only visible and NIR spectral space (Pereira *et al.* 1997).

Unlike the above spectral regions, blue was not simulated because it is universally found to be poor at identifying burned areas (Lopez-Garcia and Caselles 1991, Trigg and Flasse 2000, Stroppiana *et al.* 2002, Pu and Gong 2004, Shao and Duncan 2007), with the exception of Koutsias and Karteris (1998), who found that it outperformed both the red and green bands of TM for burned area mapping in a forested area. Because its performance was only slightly better than blue in most studies (Lopez-Garcia and Caselles 1991, Trigg and Flasse 2000, Pu and Gong 2004, Shao and Duncan 2007) and worse than blue in one study (Koutsias and Karteris 1998), green was not simulated either.

4.2.1.2 Indices

The Normalized Difference Vegetation Index (NDVI) was chosen because it has been extensively studied for mapping burned areas in various cover types with mixed results. Al Rawi *et al.* (2001) successfully used NDVI from the Advanced Very High Resolution Radiometer

(AVHRR) in a neural network to map burned forest areas, while Mohler and Goodin (2010) found through *in situ* radiometer analysis that it could differentiate burned from unburned tallgrass prairie for up to two months. Similarly, Pu and Gong (2004) found that it was suitable for differentiating burned from unburned forest, and Shao and Duncan (2007) found that it was able to differentiate between burned and unburned oak scrubland using TM data. Despite these studies, however, NDVI was found to perform poorly for burned area mapping on several occasions in both forest and savannah using both AVHRR and MODIS imagery (e.g., Pereira 1999, Li *et al.* 2004, Dempewolf *et al.* 2007). Most likely, this inconsistency in performance is due to the variation in cover type being studied, as has been suggested by the work of Chuvieco *et al.* (2002) using AVHRR and TM data.

The Global Environmental Monitoring Index (GEMI; Pinty and Verstraete 1992) was chosen because its usefulness for burned area mapping (though it was not originally intended for this purpose) is purported in several works in a variety of cover types and with a variety of sensors (e.g., Pereira 1999, Stroppiana *et al.* 2002, Cao *et al.* 2009). However, like NDVI, Chuvieco *et al.* (2002) found that its performance depended on cover type, and the decisions tree used by Dempewolf *et al.* (2007) did not select it as an important index for mapping burned savannah areas.

Unlike NDVI and GEMI, two other indices that were chosen, the Burned Area Index (BAI) and Normalized Burn Ratio (NBR), were developed specifically for burned area detection. Like NDVI and GEMI, however, BAI has shown mixed results for burned area mapping. Chuiveco *et al.* (2002) found that it performed well in various cover types, though the authors were quick to note that its performance is based upon the existence and persistence of a char signal. Dempewolf *et al.* (2007) also found that BAI performed well. Cao *et al.* (2009), however, found that it performed poorly, likely because char in semi-arid grasslands is rare, due both to an initial lack of vegetation, and to rapid removal by wind. NBR was first published as a tool for burned area mapping Lopez-Garcia and Caselles (1991), who found that it performed well in forested areas with TM data. Pu and Gong (2004) and Loboda *et al.* (2007) reached the same conclusion in the same cover type with the ETM+ and MODIS sensors, respectively.

The final index used was the Middle-Infrared Burn Index (MIRBI) developed by Trigg and Flasse (2001) in shrub savannah from *in situ* radiometer data. All bands and indices used in this chapter are shown in Table 4.2.

Table 4.2: Bands and indices simulated using hyperspectral radiometer data and the maximum spatial resolution available for each from the MODIS sensor.

Index/Band	Abbreviation	Resolution (m)
red	red	250
Near-Infrared	NIR	250
Long-Wavelength Near-Infrared	LNIR	500
Short-Wavelength Middle Infrared	SMIR	500
Long-Wavelength Middle Infrared	LMIR	500
Normalized Difference Vegetation Index	NDVI	250
Global Environmental Monitoring Index	GEMI	250
Burned Area Index	BAI	250
Normalized Burn Ratio	NBR	500
Mid-Infrared Burn Index	MIRBI	500

4.2.2 Data Collection

In situ hyperspectral reflectance data were collected from both burned and unburned hilltop areas on KPBS for three years (2008, 2009, and 2010). Although much tallgrass prairie exists in bottomlands and on side hills, only hilltops were sampled in this study. This effectively controlled variance due to topographic position, which allowed a more meaningful comparison of results between years and between bands/indices. Additionally, concentrating samples in one area made sampling easier, which was vital on many days were measurements were made between cloud overpasses. It is likely that several days of sampling would have been sacrificed if sample points had been dispersed across hilltops, bottomlands, and side hills. Although the conclusions drawn from analysis of this data likely provide an accurate general overview of the utility of each band or index for burned area mapping in tallgrass prairie, caution should be exercised when applying these conclusions to tracts of prairie that contain bottomlands or side hills.

Data were collected using an Analytical Spectral Devices (ASD) FieldSpec Pro portable spectrometer that yields a 0.5 m diameter field of view on the canopy. Between 350 and 1050 nm, the spectral resolution varies, but is approximately 3 nm at the 700 nm wavelength. Spectral resolution from 1050 and 2500 nm is between 10 and 12 nm. All measurements were referenced to a Spectralon white target prior to sampling, which allowed conversion of the data to reflectance.

In 2008, data were sampled from a single hilltop that was divided into two watersheds. One of these was burned (treatment) and the other was unburned (control). Sampling in 2008

commenced immediately prior to the treatment watershed being burned (April 23), and continued through senescence (July 31). Due to a severe winter ice storm, the standing dead biomass of the control watershed was heavily damaged. In 2008, approximately 75 samples were taken per watershed (treatment and control).

In 2009, sampling on the treatment and control watersheds commenced on April 7 (after the treatment watershed had already been burned, though regrowth had yet to take place), and continued to August 12. Unlike in 2008, the standing dead biomass was relatively undamaged. Also, 150 points were gathered per watershed rather than 75.

In 2010, two watersheds were sampled. One of these (2010a) was the same area as in 2008, though with little winter damage. The other (2010b) had been grazed by cattle, and was the only case in which samples were taken from a grazed area. In 2010, sampling on the two grazed watersheds commenced on April 8, after the treatment watershed had already been burned and regrowth had commenced. The control watershed, due to having been grazed, exhibited relatively little standing dead biomass. Sampling of the ungrazed watershed commenced on the same date, but the treatment watershed had not yet been burned. All 2010 sampling ceased on August 23. Like in 2009, 150 samples were taken per watershed in 2010. In all three years, the treatment watershed was on an annual burn schedule, while the control watershed was on a biennial burn schedule in 2008 and 2010a, and a quadrennial burn schedule in 2009. 2010b had a variable burn schedule. General information for the three sampling years is given in Table 4.3, while locations of each set of samples within KPBS are given in Figure 4.1.

Table 4.3: Information for samples taken with the hyperspectral radiometer on KPBS.

	2008	2009	2010a	2010b
Burn date	24-Apr.	25-Mar.	20-Apr.	3-Mar.
Sampling start	23-Apr.	7-Apr.	8-Apr.	8-Apr.
Sampling end	31-Jul.	12-Aug.	23-Aug.	23-Aug.
Number of sample dates	14	14	10	12
Re-growth commenced?	No	Yes	No	Yes
Condition of standing dead biomass	Damaged	Good	Good	Grazed
Sample points per watershed	75	150	150	150
Grazed	No	No	No	Yes
Burn frequency (control)	Biennial	Quadrennial	Biennial	Variable
Burn frequency (treatment)	Annual	Annual	Annual	Variable

Figure 4.1: Location of hyperspectral samples within KPBS.

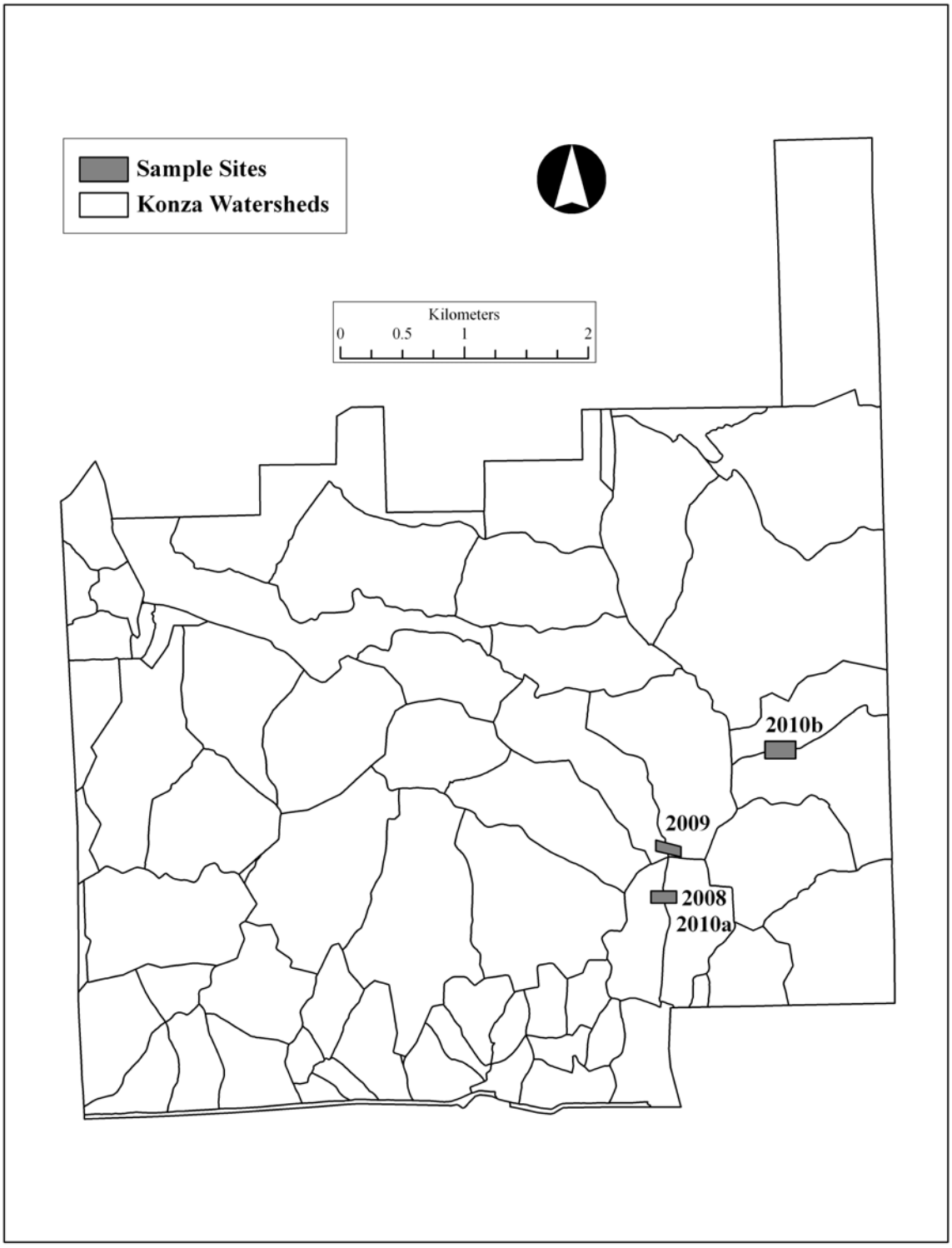

4.2.3 Data Processing and Index Calculation

In order to simulate the bands that were chosen for analysis, the 1 nm values within the upper and lower boundary of each simulated band were averaged for each sample point. Often, integration across each band's spectral response function is used for this step (e.g., Trigg and Flasse 2000). However, several tests with various simulated spectral ranges showed differences between integration and averaging to be only tenths of a percent, which is not within several significant digits, and so is negligible.

Although the exact wavelength range used to calculate each spectral region or index would be different depending on which sensor was used as the model, only MODIS was used in this chapter. This was advantageous because it reduced the amount of data preparation and analysis that was necessary. MODIS in particular was used because it covers the spectrum more completely than other sensors (Table 4.1) and so allows more bands and indices to be tested. Using only MODIS data assumed that differences between the specific wavelength ranges of similar spectral regions from sensor to sensor were negligible, and could be ignored. An Analysis of Variance (ANOVA) test that compared data as derived from both the TM and MODIS wavelength ranges (based on the 2008 and 2009 samples) confirmed this fact. In this preliminary analysis, the hypothesis that a statistical difference existed between data from the two sensors was rejected in the case of all bands and indices tested (Table 4.4). LNIR is missing from this analysis because this spectral region is not available from TM, and so could not be compared.

Table 4.4: ANOVA probabilities showing no significant difference between data from TM and MODIS, regardless of which band or index is used. Probabilities less than 0.05 meant that the null hypothesis would have been rejected at the 95% confidence interval.

Band/Index	Probability
red	0.9709
NIR	0.7349
SMIR	0.663
LMIR	0.7831
NDVI	0.8376
GEMI	0.7303
BAI	0.769
NBR	0.8927
MIRBI	0.8469

Once all bands were simulated for MODIS in all three years, these were used to calculate the appropriate indices. The specific wavelength ranges for all bands used in the equations are shown in Table 4.1. First, NDVI was calculated as

$$NDVI = (\rho_{NIR} - \rho_{red}) / (\rho_{NIR} + \rho_{red}) \quad (4.1)$$

where ρ_{NIR} and ρ_{red} are the reflectance values of the MODIS NIR and red bands, respectively.

GEMI (Pinty & Verstraete 1992) was calculated as

$$GEMI = \eta(1 - 0.25\eta) - (\rho_{red} - 0.125) / (1 - \rho_{red}) \quad (4.2)$$

where $\eta = (2(\rho^2_{NIR} - \rho^2_{red}) + (1.5\rho_{NIR} + 0.5\rho_{red}) / (\rho_{NIR} + \rho_{red} + 0.5)$, and ρ_{NIR} and ρ_{red} are defined the same as in the NDVI equation.

BAI, first published by Chuvieco *et al.* (2002) was calculated as

$$BAI = 1 / [(\rho c_{red} - \rho_{red})^2 + (\rho c_{nir} - \rho_{nir})^2] \quad (4.3)$$

where ρc_{red} and ρc_{nir} are the red and NIR reference reflectance values, respectively, and ρ_{red} and ρ_{nir} are the actual reflectance values in the same bands (defined as in NDVI and GEMI). The reference reflectance values, ρc_{red} and ρc_{nir} used constants of 0.1 and 0.6, respectively, as these tend to emphasize the charcoal signal (Chuvieco *et al.* 2002, Dempewolf *et al.* 2007).

NBR, first used for burned area mapping by Lopez Garcia and Caselles (1991) but not named until later, was calculated as

$$NBR = (\rho_{NIR} - \rho_{LMIR}) / (\rho_{NIR} + \rho_{LMIR}) \quad (4.4)$$

where ρ_{NIR} is defined as it is in the above indices and ρ_{LMIR} is the reflectance value of MODIS LMIR.

The final index used was the MIRBI proposed by Trigg and Flasse (2001), and was calculated as

$$MIRBI = 10(\rho_{LMIR}) - 9.8(\rho_{SMIR}) + 2 \quad (4.5)$$

where ρ_{LMIR} is defined as in the NBR equation and ρ_{SMIR} is the reflectance value of MODIS SMIR.

4.2.4 Assessing Band/Index Suitability

Detection of burned areas in tallgrass prairie with satellite imagery depends on a burn scar that remains on the landscape for some time after the area is burned, or at least remains distinctive from unburned grassland (Trigg and Flasse 2000). Ideally, with cloud-free daily imagery, this burn scar could persist for only 24 hours and still be detectable. However, clouds

often obscure the ground surface for up to a week at a time in the Flint Hills, particularly during spring when most burning takes place. Therefore, the longer a burned area can be differentiated from an unburned area with a given band or index, the more useful that band or index is for burned area detection (Sa *et al*. 2003). Furthermore, because most of the Flint Hills is grazed, this usefulness should persist even on grazed areas.

Additional factors affect the efficacy of certain bands or indices as well. First, rapid re-growth of burned areas is common in tallgrass prairie, and it is plausible that a clear image might be taken immediately after burning, whereby grass has not begun to re-grow on the burned area. This is the nature of performing remote sensing analysis, as clear image dates are often unevenly distributed temporally (Eva and Lambin 1998). Conversely, the first clear image of the burned area, if clouds have been persistent, might be several days after burning, and grass might be re-growing rapidly. Therefore, an ideal band or index would also distinguish between burned and unburned areas regardless of the regrowth status of the vegetation.

Finally, it should be noted that not all bands and indices are available at the same spectral resolution, and that bands or indices with a higher spatial resolution are better, all other things being equal. The purpose of this section, therefore, is to quantify how each band or index tested aligns with the ideal outlined above.

To do this, three different ANOVA tests for repeated measures were performed using SAS v. 9.2 software. All three tests used the mixed procedure (PROC MIXED). In all cases, either the autoregression 1 (AR1) or unstructured (UN) variance/covariance structure was used, depending on which provided the best fit for the band or index in question based on the Akaike Information Criterion with finite sample size adjustment (AICc; lower values are better). All three tests also used the Satterthwaite denominator degrees of freedom adjustment, and the Schaffe adjustment to control for Type 1 error. In all cases, the original sample dates were classified into six time periods, with class 0 representing all pre-burn measurement, and classes 1-5 representing a set period of time since the treatment watershed was burned (Table 4.5). Samples could not be analyzed based on their original dates because these dates were not consistent from year to year due to cloud conditions. Therefore, some temporal resolution was lost when dates were aggregated into the six classes. Classifying the original sample dates based on the time since burning was more desirable than dividing them based on absolute calendar

dates, as different watershed were not burned at the same time, and were burned well over one month apart in some cases.

Table 4.5: Categorical aggregation of sample dates.

Time Period	Weeks Since Burn
0	Pre-burn
1	1-3
2	4-7
3	8-11
4	12-15
5	> 15

The first test compared all data from 2008, 2009, and 2010a, which were similar in that none of them came from a grazed watershed. In fact, the grazed watershed (2010b) was not used here because including it would have introduced variation to the test, which would have made drawing meaningful conclusions more difficult. Variables in this test included year (2008, 2009, and 2010a), treatment (burned, unburned), and time period (0, 1, 2, 3, 4, 5).

The second test compared 2008 and 2010a, since the same burned and unburned watersheds were sampled in both of these years. This controlled for some of the variability arising from differences among watersheds (vegetation composition, burn frequency, etc), though the variables in this test are the same as in the previous test with the exception of one less year (2009).

The final test compared 2010a to 2010b in order to detect any effects that grazing might have on the ability of the bands or indices to differentiate between burned and unburned areas. In this case, the year variable is replaced by a grazing variable (yes, no), though the treatment and time period variables remain the same as in the previous two tests.

In the case of all three tests, an adjusted (Schaffe) probability value of greater than 0.05 meant that the hypothesis was rejected at the 95% confidence interval. This meant that, for the band or index in question, no statistical difference could be confirmed between burned and unburned watersheds for the variable combination in question (using time period, grazed, etc.). This significance, or lack thereof, was taken as an indication of that bandwidth or index's ability to detect burned areas under the given circumstances.

4.3 Results and Discussion

4.3.1 The First ANOVA Test (2008, 2009, and 2010a)

For each of the six time periods in the study, the combined effect of both the treatment (burned or unburned) and time (0-6) variables on the ability of each band or index to differentiate burned from unburned areas was examined. As mentioned in section 4.2.4, the ability of a band or index to differentiate burned from unburned areas for a long time after burning had taken place (a probability value of less than 0.05 in several consecutive time periods) would be ideal. Because the pre-burn time period (0) had no bearing on the efficacy of a band or index, it is not discussed here.

The LMIR band performed very poorly in this analysis, as it was the only band or index tested that did not display a significant probability value in any of the five time periods since burning (Table 4.6). That is, it was not able to distinguish burned from unburned areas at any point in the study. Additionally, it is available at a maximum spatial resolution of only 500 m from MODIS. These attributes of LMIR suggest that it is of little use for burned area mapping in tallgrass prairie. It should be noted that this is in contrast to studies in other land cover types, where LMIR was found to be useful for mapping burned areas.

Table 4.6: Probability values from the first ANOVA test (2008, 2009, and 2010a) showing the effect of treatment (burned or unburned) and time period (0-6) on the ability of each band or index to differentiate burned from unburned areas in each of the six time periods.

Band/Index	0	1	2	3	4	5
red	0.88	<0.01	0.02	<0.01	0.04	0.53
NIR	0.85	<0.01	0.40	0.04	<0.01	0.59
LNIR	0.10	<0.01	0.06	0.70	0.65	0.66
SMIR	0.57	<0.01	0.11	0.16	0.21	0.29
LMIR	<0.01	0.64	0.79	0.79	0.70	0.94
NDVI	0.86	0.54	0.03	0.00	0.04	0.28
GEMI	0.75	<0.01	0.95	0.02	0.04	0.33
BAI	0.89	0.02	0.73	0.82	0.07	0.83
NBR	0.71	<0.01	0.62	0.25	0.01	0.07
MIRBI	0.46	<0.01	<0.01	<0.01	<0.01	0.01

NDVI also performed poorly, as it was unable to differentiate burned from unburned areas in time period number 1 (Table 4.6). Interestingly, the insignificant value in the first time

period was followed by significant values in the next three time periods, meaning that although NDVI is unable to differentiate between burned and unburned areas immediately after burning, it can do so several weeks to a over a month after burning. This is due to the regrowth characteristics of the vegetation on the study sites. In the first time period, regrowth on the treatment watershed had yet to commence, allowing standing dead biomass on the unburned watershed and bare ground on the burned watershed to appear similar with NDVI. Once regrowth had commenced on the burned watershed (time periods 2-4), this watershed produced a much stronger NDVI signal than the unburned watershed, which was still dominated by standing dead biomass. Insignificant values for the last time period represent regrowth on the unburned watershed overtaking the standing dead biomass and making this watershed look similar to the burned one.

This analysis shows that the performance of NDVI for differentiating burned from unburned areas depends on whether or not regrowth has taken place. Specifically, a different relationship exists when comparing unburned prairie to charred areas that have not begun to regrow than exists when comparing unburned prairie to burned, regrowing prairie. This, along with the diverse range of cover types examined in existing NDVI studies, likely explains the wide range of opinions regarding the utility of NDVI for burned area mapping. What is clear is that this attribute of NDVI drastically reduces its usefulness in tallgrass prairie, because the researcher must know the state of vegetation regrowth in order to know what relationship between burned and unburned areas to look for. This might be possible over smaller areas, but would be impossible over wider areas, and this fact makes NDVI impractical for mapping burned areas over large tracts of tallgrass prairie.

Six of the bands or indices tested were able to distinguish between burned and unburned areas for the first time period, but could not do so for at least two consecutive time periods at the beginning of the sample (Table 4.6). They were NIR, LNIR, SMIR, GEMI, BAI, and NBR. In the case of NIR, the initial significant value during the first time period was followed by and insignificant value on the second time period, and two significant values in the third time period. Similar patterns are shown by both GEMI and NBR, both of which have NIR as a component. In the case of all three (NIR, GEMI, and NBR), the initial significance is due much higher NIR reflectance values on the unburned watershed up to three weeks after burning. However, the insignificant values in the second time period, as well as the significant values in the third and

fourth (NIR, GEMI) or fourth (NBR) time periods represent a transition to higher NIR reflectance values on the burned watershed as new vegetation growth boosts the NIR signal past that of the unburned watershed. As was the case with NDVI, the inconsistency of the relationship between burned and unburned areas means that knowledge of vegetative regrowth status would be necessary for burned area detection over large areas (and would again be impractical). However, unlike with NDVI, the relationship between burned and unburned areas with these three bands/indices is consistent for at least three weeks after burning, during which time any of them could accurately detect burned areas. The findings for NIR, GEMI, and NBR are not in direct contrast to findings from other studies, which tout the utility of all three for burned area detection in a variety of cover types. Additionally, NIR and GEMI have the added advantage of being available at 250 m spatial resolution from MODIS, while NBR can be calculated at a maximum resolution of only 500 m from MODIS.

Though their performance was, for all practical purposes, equal to the three bands/indices discussed above, BAI, LNIR, and SMIR did not exhibit any significant values other than in the first time period (Table 4.6). Nonetheless, this suggests that these bands and index are suitable for burned area detection for approximately three weeks after burning has taken place. In the case of BIA, this is consistent with what was found by Pereira (2003) in other grassland environments, and is consistent with the original intent of BAI, which was to detect the distinctive char signal of recently burned areas (Chuvieco *et al.* 2002). BAI, unlike LNIR and SMIR, also has the advantage of being available at 250 m spatial resolution from MODIS.

One of the bands (red) and one of the indices (MIRBI) excelled at differentiating burned from unburned areas (Table 4.6). The red band exhibited a significant probability value in the first four time periods, while MIRBI exhibited a significant value in all five of the time periods (Table 4.6). In the case of the red band, reflectance values on the burned watershed remained significantly lower than those on the unburned watershed until the last time period—a time span of up to 15 weeks. This makes sense, as both charred and regrowing vegetation reflect little red light compared to standing dead biomass. This analysis suggests that red, given its ability to differentiate burned from unburned areas for up to 15 weeks, shows great promise for detecting burned areas in tallgrass prairie for up to three months after an area is burned. This finding adds to the already disputed picture of the utility of the red wavelength to differentiate between burned and unburned areas in various cover types (see section 4.2.2.1), and suggests that the

overall usefulness of red depends on the cover type being studied. The red spectral region also has the advantage of being available on a wide range of sensors, and is available at 250 m resolution from the MODIS sensor. In the case of MIRBI, the significant values in all five post-burn time periods indicated that index values were higher on the treatment watershed than on the control for the entire study period. Like red, MIRBI showed great promise for detecting burned areas in tallgrass prairie, despite the fact that it is only available at 500 m spatial resolution from the MODIS sensor. The utility of MIRBI is not surprising, as it was designed specifically to amplify burn signals while minimizing spectral variability from other factors (Trigg and Flasse 2001).

4.3.2 The Second ANOVA Test (2008 and 2010a)

In the second test, which included only the samples from 2008 and 2010a that came from identical watersheds, both LMIR and NDVI performed poorly once again, with LMIR failing to record a significant value in any of the five post-burn time periods, and NDVI again having an insignificant value in the first post-burn time period before displaying significant values for the next three time periods (Table 4.7). As stated in Section 4.3.1, this effectively disqualifies both LMIR and NDVI from burn mapping applications in tallgrass prairie.

Table 4.7: Probability values from the second ANOVA test (2008 and 2010a) showing the effect of both treatment (burned or unburned) and time period (0-6) on the ability of each band or index to differentiate burned from unburned areas in each of the six time periods.

Band/Index	0	1	2	3	4	5
red	0.81	<0.01	0.11	<0.01	0.09	0.12
NIR	0.42	<0.01	0.42	0.05	0.23	0.96
LNIR	0.06	0.04	0.05	0.98	0.77	0.84
SMIR	0.63	<0.01	0.34	0.45	0.68	0.62
LMIR	0.00	0.65	0.88	0.80	0.79	0.87
NDVI	0.93	0.53	<0.01	0.02	0.43	0.39
GEMI	0.57	<0.01	0.15	0.03	0.25	0.82
BAI	0.97	<0.01	<0.01	0.70	0.71	0.29
NBR	0.34	<0.01	0.33	0.10	0.36	0.53
MIRBI	0.47	<0.01	0.24	0.01	<0.01	0.94

As in the first test, six of the bands or indices were able to distinguish burned from unburned areas for more than one consecutive time period starting with the first time period

(Table 4.7). They included red, NIR, SMIR, GEMI, NBR, and MIRBI. Interestingly, the bands that performed best in the previous test, red and MIRBI, did not perform as well in this test. All six of these bands or indices were able to differentiate burned from unburned areas for at least three weeks (the first sample period), and may still prove useful for mapping burned areas at the satellite image scale. The two bands that performed best in this analysis, LNIR and BAI, were both able to distinguish burned from unburned areas for the first two time periods (up to seven weeks), though neither displayed a significant value in the three remaining time periods. Ultimately, this second test confirmed what was shown by the first test—that LMIR and NDVI are unsuitable for detecting burned areas in tallgrass prairie, but the other eight bands or indices show varying degrees of utility depending on the circumstances tested.

4.3.3 The Third ANOVA Test (2010a and 2010b)

The third test included only the samples from 2010a and 2010b, one of which was a grazed pair of watersheds (2010b), and the other of which was a non-grazed pair of watersheds (2010a). This allowed a new variable (grazed or not), to affect the ability of a band or index to differentiate between burned and unburned areas. Once again, both LMIR and NDVI performed poorly (Table 4.8). In this case, NDVI again had an insignificant value in the first time period. When grazing was taken into account, however, NDVI only showed one significant figure in all five time periods (period 2), suggesting that NDVI performs even more poorly when trying to differentiate burned from unburned areas in grazed tallgrass prairie. This alone is detrimental to its ability to detect burned areas across the Flint Hills at large, as they are almost entirely grazed. Once again, LMIR did not have a single significant value in any of the five post-burn time periods.

Unlike in the previous two tests, LMIR and NDVI were not the only two bands that failed to have a significant value in the first time period, as GEMI, BAI, and NBR failed to do so as well (Table 4.8). In fact, none of these indices exhibited a significant value in any of the five post-burn time periods. Most likely, this is because they are overly sensitive to the fact that grazing makes burned and unburned areas more similar, as it reduced standing dead biomass on unburned areas, which allows regrowing vegetation to make up a larger portion of the canopy. As was the case with LMIR and NDVI, the inability of these indices to differentiate between

burned and unburned areas regardless of grazing practice leaves their burn detection capabilities in doubt—especially in the Flint Hills.

Table 4.8: Probability values from the third ANOVA test (2010a and 2010b) showing the effect of treatment (burned or unburned), time period (0-6), and grazing (yes or no) on the ability of each band or index to differentiate burned from unburned areas in each of the six time periods.

Band/Index	0	1	2	3	4	5
red	0.02	<0.01	<0.01	0.29	0.71	0.78
NIR	0.44	0.04	0.25	0.99	0.70	0.87
LNIR	0.23	<0.01	0.26	0.09	0.10	0.42
SMIR	0.15	<0.01	<0.01	0.03	0.16	0.37
LMIR	0.88	0.59	0.22	0.93	0.80	0.93
NDVI	0.56	0.06	0.02	0.57	0.92	0.93
GEMI	0.64	0.19	0.16	0.97	0.67	0.89
BAI	0.89	0.66	0.62	0.61	0.17	0.95
NBR	0.41	0.11	0.18	0.95	0.70	0.95
MIRBI	0.08	<0.01	0.03	0.01	0.07	0.28

As they had done in the previous two tests, NIR and LNIR were able to differentiate between burned and unburned areas in the first time period (up to three weeks after the area was burned), though neither had a significant probability value in any other time period (Table 4.8). This shows that the ability of NIR and LNIR to differentiate burned from unburned areas is not compromised by grazing practices—at least not within three weeks of an area having been burned. Consequently, both of these spectral regions show utility for detecting burned areas in tallgrass prairie.

Two bands and one index were easily able to differentiate burned from unburned areas despite the effects of grazing. They were red, SMIR, and MIRBI. In the case of red and SMIR, significant probability values were exhibited in the first two time periods. For MIRBI, these significant values extended through the third time period. This implies that MIRBI, and to a slightly lesser extent red and SMIR, are the best bands (or index) for detecting burned areas in grazed tallgrass prairie, since they performed equally well (and slightly better in the case of SMIR) regardless of whether an area had been grazed or not.

4.4 Conclusions

Two of the bands and indices tested in this analysis, LMIR and NDVI, showed little promise for detecting burned areas in tallgrass prairie, as they were unable to consistently differentiate between burned and unburned areas. The failure of LMIR was remarkable, as it did not exhibit a single significant probability value in any case during any of the three tests. That is, the hypothesis that a statistical difference existed between the burned and unburned areas was not supported in any instance. In the case of NDVI, the relationship between burned and unburned areas depended on regrowth, thereby requiring *a priori* knowledge of the condition of a burned area. Because this is impractical over large areas such as the Flint Hills, the likelihood of NDVI being useful for detecting burned areas is low.

Two other bands, GEMI and NBR, were of little use as well, as they could not differentiate between burned and unburned areas if those areas had been grazed. Because the vast majority of the Flint Hills is grazed, there is little likelihood of these two indices contributing substantially to any process of detecting burned areas in tallgrass prairies of that region at a wider scale (e.g., with satellite imagery). This is particularly true considering that better-performing bands and indices are available at equal or higher spatial resolution. Because of their poor performance, none of the four bands mentioned to this point are analyzed in subsequent chapters.

Of the remaining bands and indices, BAI was the poorest performer, as its power to differentiate burned from unburned areas is poor when those areas have been grazed. However, it is included in later analysis based on its performance in the second test, where it was able to differentiate burned from unburned areas for up to seven weeks. Other bands and indices, such as red, NIR, LNIR, SMIR, and MIRBI, were able to differentiate burned from unburned areas consistently, regardless of grazing, for at least three weeks after burning had taken place, and often much longer than that (e.g., red, LNIR, SMIR, BAI, and MIRBI). In these cases, the hypothesis that a difference existed between burned and unburned areas was accepted for at least the first time period in all three tests, and for several time periods after than in the case of some of these bands and indices. Finally, it should be noted again that all samples came from hilltops only, though they likely approximate the efficacy of these bands and indices in tallgrass prairies in general. Table 4.9 gives a summary of the performance of each band or index tested according to each of the three ANOVA tests.

Table 4.9: Consecutive length of time in weeks (calculated beginning with time period #1) over which each band or index was able to differentiate burned from unburned areas according to each of the three ANOVA tests.

Band/Index	Test #1	Test #2	Test #3
red	15	3	7
NIR	3	3	3
LNIR	3	7	3
SMIR	3	3	7
LMIR	0	0	0
NDVI	0	0	0
GEMI	3	3	0
BAI	3	7	0
NBR	3	3	0
MIRBI	> 15	3	11

CHAPTER 5 - Satellite Level Normalized Distance Analysis

5.1 Introduction

The second objective of this study was to reveal the utility of different TM and MODIS bands and indices for differentiating burned from unburned tallgrass prairie at the satellite image scale. This objective was completed by testing the hypothesis that those bands and indices that were successful in differentiating burned from unburned tallgrass prairie using *in situ* data will also do so effectively at the satellite image scale. Testing this hypothesis would give further indication of the efficacy of the bands and indices examined in Chapter 4. It would also reveal much about the similarities and differences between *in situ* measurements and satellite-based measurements, between different burned areas, and between the two sensors. The method used to test this hypothesis and accomplish this objective was a normalized distance comparison of burned and unburned areas.

5.2 Methods

5.2.1 Justification for Using the TM and MODIS Sensors

The paradox of whether to use higher temporal or spatial resolution is important in burned area studies (Eva and Lambin 1998), because burned areas can change rapidly following the burn event (Eva and Lambin 1998, Trigg and Flasse 2000). That is, the sensor used must possess high enough spatial resolution to identify the smallest burned areas in the study area, yet must produce an image of the area frequently enough to identify burned areas before the scars disappear. The TM and MODIS sensors provide an example of this paradox. TM provides better spatial resolution (30 m multi-spectral; 60 m thermal compared to 250 and 500 m for MODIS), while MODIS provides better temporal resolution (daily passes by both Aqua and Terra compared to one pass every 16 days with TM). Therefore, the use of TM and MODIS in this chapter helped identify which type of resolution (spatial or temporal) is more important to burned area mapping in tallgrass prairie, in addition to accomplishing the objective mentioned in the introduction.

5.2.2 Data Collection and Processing

The first data acquired were all path 28-row 33, path 28-row 34, path 27-row 34, and path 27-row 33 TM scenes imaged between March 1 and August 30, 2008. All scenes were downloaded through the Unites States Geological Survey's (USGS's) Global Visualization Viewer (GloVis) as georectified tagged image file format (TIFF) files. Although five different TM scenes are required to cover the entire Flint Hills study area (Figure 3.1), they were not required in this part of the analysis, as the goal was to evaluate the temporal signature of burned and unburned grasslands through the growing season at the satellite image scale. This could be done using a much smaller region, and so only subsets of the four scenes mentioned above were used. All TM imagery was calibrated to top of atmosphere reflectance using the method of Chandler and Markham (2003), which allowed for more meaningful comparison between image dates. It should be noted that not all of these scenes were used in this chapter, but were downloaded because they needed to be examined in order to determine their suitability. The justification for this is given below in section 5.2.4.

In addition to the TM scenes, all relatively cloud-free 2008 MODIS scenes captured between March 1 and August 30 from both the Aqua and Terra satellites were downloaded through the National Aeronautics and Space Administration's (NASA's) Warehouse Inventory Search Tool (WIST). These scenes were downloaded in two parts, including the red and NIR bands at 250 m spatial resolution (MOD09GQ, MYD09GQ), and all other bands at 500 m spatial resolution (MOD09GA, MYD09GA), which was the highest resolution available for each respective band. These were converted from their native Hierarchical Data Format (HDF) to TIFF files and georectified to Universal Transverse Mercator (UTM) coordinate system (zone 14) using the MODIS Reprojection Tool (MRT). Finally, they were subset to the extent of the study area. Although four TM scenes are required to cover the study areas, only one MODIS scene was necessary for this task because of its larger footprint.

5.2.3 Band/Index Selection for Normalized Distance Analysis

The bands and indices tested by normalized distance analysis in this chapter were those that proved useful for differentiating burned from unburned grasslands in Chapter 4 (BAI, MIRBI, red, NIR, LNIR, SMIR). In this case, they were calculated directly from the 2008 TM or MODIS scenes, rather than being simulated with data gathered *in situ*. All bands were

calculated using both TM and MODIS (except LNIR which is only available on MODIS), despite the fact that the two sensors mirrored each other when simulated in the 2008 and 2009 field level analysis. This was done to uncover any variation in normalized distance that may arise due to differences in the spatial resolution of the two sensors (30 m for TM vs. 250 or 500 m for MODIS), which could not be accounted for in the field level analysis. The bands and indices used in this normalized distance analysis, as well as the spatial resolution of each with both sensors, are given in Table 5.1.

Table 5.1: Indices and bands used in the normalized distance calculation.

Index/Band	TM resolution (m)	MODIS resolution (m)
BAI	30	250
MIRBI	30	500
red	30	250
NIR	30	250
LNIR	NA	500
SMIR	30	500

5.2.4 Normalized Distance Calculation

Normalized distance (*D*), sometimes called standard distance, was originally developed by Kaufman and Remer (1994), and has been used extensively to test the ability of bands and indices to differentiate between different pairs of cover classes (e.g., Pereira 1999, Chuvieco *et al.* 2002, Silva *et al.* 2004, Cao *et al.* 2009, Stroppiana *et al.* 2009). It is calculated by the equation

$$D = |\mu_B - \mu_U| / (\sigma_B + \sigma_U) \quad (5.1)$$

where D is the normalized distance, μ is the mean of the pixels included in the sample of each cover type, σ is the standard deviation of those pixels, $_B$ denotes a burned area, and $_U$ denotes an unburned area. *D*-values greater than 1 indicate good discriminatory ability, while values less than 1 indicate an unacceptable degree of overlap between the histograms of the two cover classes, and, therefore, poor discriminatory ability (Kaufman and Remer 1994; Pereira 1999). It should be noted that in the case of the *in situ* data analysis from the previous chapter, the inferential Mann-Whitney *U*-test and Student's *t*-test were warranted, as those data were samples from a larger population (Pereira 1999). In this analysis, however, entire populations

(all pixels within a burned or unburned area) were compared, making the normalized distance technique more appropriate (Pereira 1999). Furthermore, because it accounts for interclass as well as intraclass variance (Pereira 1999), normalized distance does not make the assumption of equal variance between the two samples, and so accounts for the effect of noise on the signal (Kaufman and Remer 1994).

Figure 5.1: Area of overlap between TM path 27 and path 28 showing the selected burned and unburned area pairs.

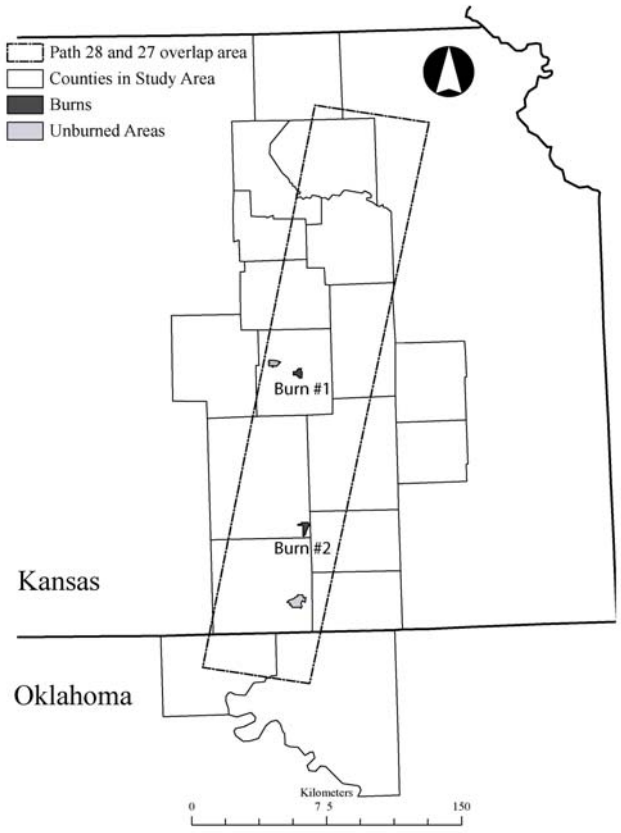

Each burned/unburned sample pair was compared using each band or index and for both sensors (except LNIR, which was available only with MODIS). This yielded two *D*-values per band or index per sensor (one for each sample pair). The sampling period covered for each pair of areas, as well as which dates were sampled, is outlined for TM in Table 5.2, and for MODIS in Table 5.3.

Table 5.2: Dates of TM imagery used in this chapter for each burned/unburned pair. Number denotes the path and row from which the scene from that date came. Total denotes the number of image dates used for each pair.

Date	Burn #1	Burn #2
4/2/08	28-33	28-34
5/4/08	28-33	28-34
5/20/08	28-33	28-34
6/14/08	27-33	27-34
6/21/08	28-33	Cloudy
6/30/08	Cloudy	27-34
7/7/08	28-33	28-34
7/23/08	28-33	28-34
8/1/08	27-33	27-34
8/8/08	28-33	28-34
Total	**9**	**9**

Table 5.3: Dates of MODIS imagery used in this chapter for each burned/unburned pair. Total denotes the number of image dates used for each pair. Missing values mean that cloud cover blocked the view of that particular sample pair. Aqua or Terra designation denotes which satellite provided the highest-resolution image for that date.

Date	Burn #1	Burn #2
3/19	Aqua	
3/20	Terra	
3/21	Aqua	
4/1		Aqua
4/2	Aqua	
4/5		Terra
4/6	Aqua	Aqua
4/13	Aqua	Aqua
4/14	Terra	Terra
4/15	Terra	Terra
4/19	Terra	Terra
4/22	Aqua	Aqua
4/25		Aqua
4/28	Terra	Terra
5/2		Aqua
5/3	Terra	Terra
5/4	Aqua	Aqua
5/5		Terra
5/8	Terra	
5/11	Aqua	Aqua
5/12	Terra	Terra
5/14	Terra	
5/15	Aqua	
5/16	Aqua	
5/17	Terra	Terra
5/18	Aqua	Aqua
5/20		Aqua
5/25	Aqua	Aqua
6/1		Aqua
6/3	Terra	Terra
6/4	Terra	Terra
6/6	Terra	Terra
6/13		Aqua
6/14	Aqua	Aqua
6/15	Terra	

Date (contd.)	Burn #1	Burn #2
6/17	Terra	Terra
6/18		Terra
6/20	Terra	Terra
6/21		Aqua
6/22	Terra	Terra
6/25	Aqua	Aqua
6/26	Terra	Terra
6/27	Terra	
6/29	Terra	Terra
6/30		Aqua
7/1	Terra	Terra
7/2		Terra
7/4	Aqua	Aqua
7/11	Terra	
7/13	Terra	
7/14	Aqua	Aqua
7/17	Terra	
7/19		Terra
7/20	Aqua	Terra
7/21	Aqua	Terra
7/22		Terra
7/23	Aqua	Aqua
7/24	Terra	Aqua
7/27		Aqua
7/31	Aqua	
8/1	Aqua	Aqua
8/2	Terra	Terra
8/3	Aqua	Aqua
8/4	Terra	Terra
8/5	Terra	Aqua
8/13	Aqua	
8/22	Aqua	Aqua
8/26		Aqua
8/28	Aqua	Terra
8/29	Aqua	
Total	**54**	**54**

5.3 Results and Discussion

5.3.1 BAI

The first normalized distance comparison was performed on BAI calculated from TM. In the case of Burn #1 and Burn #2, only the April 2, 2008 sampling date exhibited a *D*-value greater than 1 (values > 1 indicate good discriminatory power); in this case, 1.43 and 1.89, respectively. By May 5, these values had dropped to 0.74 and 0.39, respectively—well below the threshold of 1 (Figure 5.2). It should be noted that Burn #1 was known to exist on March 15, and Burn #2 existed by March 25. Furthermore, it can be safely assumed that *D*-values for both burns would have been greater than 1 prior to the April 2 sampling date, and likely would have remained above 1 for several weeks after the sampling date as well. Therefore, it is likely that BAI could discriminate between burned and unburned areas for approximately one month or slightly more. However, the temporal resolution of the TM imagery prevents this from being confirmed.

When BAI was calculated from MODIS, a similar patter emerged. In the case of Burn #1, *D*-values remained above 1 from the first sampling date on March 19 (2.25) through April 15 (1.36), before they dipped slightly below 1 on April 19 and 22 (0.94 and 0.91, respectively), then climbed above 1 again on April 28 and remained there through May 3 before dropping to 0.48. This finding is consistent with that from TM, where discrimination with BAI is possible for approximately one month after burning takes place (March 15 to April 15). Burn #2 roughly followed the signature of Burn #1, starting with a *D*-value of 1.79 on the first sampling date (April 1). Values remained above 1 until April 22, where they dropped to 0.95 before returning to 1.03 on April 25 (Figure 5.2). Once again, this finding is consistent with that of TM in that the signal is detectable for approximately one month.

In all four cases, the time period during which BAI can be reliably used to detect burned areas appears to be approximately one month or slightly longer, as both sample burns, regardless of which sensor is used, show approximately the same temporal *D*-value curve. Additionally, this finding is supported by the *in situ* analysis (Chapter 4)—specifically, that BAI, like all NIR-based indices, is typically useful for burn detection for approximately one month. Because BAI can differentiate burned from unburned areas reliably for approximately one month, and can be

calculated from both TM and MODIS (and from MODIS at 250m), it appears to be a viable option for burned area mapping in tallgrass prairie.

Figure 5.2: BAI normalized distance values for the duration of the sampling period. For all graphs in this section (5.3), values greater than 1 indicate good discriminatory power.

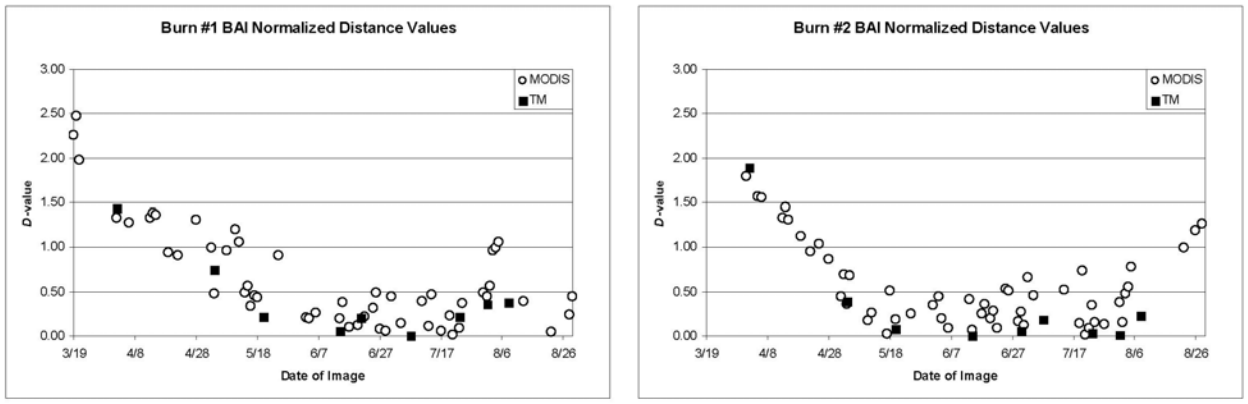

5.3.2 MIRBI

When calculated from TM, MIRBI performed better than BAI in the case of both sample burns. Burn #1 was detectable for the first three sample dates (April 2, May 4 and May 20), with values of 2.15, 1.51, and 1.17, respectively. Burn #2 exhibited *D*-values greater than 1 for the first two sampling dates (2.05 and 1.23, respectively), before the *D*-value fell below 1 on May 20, at 0.87 (Figure 5.3). As was the case with BAI, the significant *D*-values almost certainly existed immediately after the area was burned, and most likely continued for some time after it was last proven with the imagery. Therefore, MIRBI was most likely able to distinguish burned from unburned areas for at least five weeks in the case of Burn #2, and for eight weeks in the case of Burn #1, though, as was the case with BAI when taken from the TM sensor, caution must be exercised when citing these values.

The results from TM were, with a few exceptions, confirmed by MODIS. For burn #1, *D*-values remained above 1 from the first sampling date (March 19) through May 14, with the exception of March 21 (0.92). However, given the high *D*-values surrounding this date, and its proximity to 1, Adequate burned area discrimination most likely exists for the entire period ending on May 14, or for approximately eight weeks. For Burn #2, the initial *D*-value on April 1

was 0.61. However, after this date, all values remained above 1 until April 25 (Figure 5.3). The April 1 value aside, MIRBI was able to consistently detect Burn #1 for approximately four weeks.

As was the case with BAI, MIRBI showed little difference between the two sensors. This was best illustrated by Burn #1, which was detectable for approximately eight weeks regardless of which sensor was used. Burn #2 provided an exception, as it was detectable with TM for slightly longer than with MODIS, though this difference was limited to approximately one week. Unlike with BAI, however, the two sample burned areas differ in how long they could be differentiated from burned areas, with Burn #1 being detectable for nearly twice as long as Burn #2. Most likely, this phenomenon is explained by the variation that must exist between the two burned areas. However, this difference was largely unnoticed with BAI. Most likely, the shorter, month-long period during which burned and unburned areas could be detected with BAI did not allow for variation between burned areas later in the sample. This suggests that different bands or indices deal with between-burn variation differently, which should be taken into account when mapping burned areas over wider scales.

More differences become apparent when the temporal curves from this analysis are compared to those produced by the *in situ* data. While the field-level analysis suggested that MIRBI was capable of differentiating burned from unburned areas for at least five months, the normalized distance analysis limits this estimate to 4-8 weeks. Nonetheless, MIRBI is capable of detecting burned areas longer than one month—especially if the *D*-values for Burn #1 are cited—and so has the potential to outperform BAI by several months, though caution should be used due to its inconsistency. Finally, it should be noted that MIRBI, though it was able to detect burned areas for longer periods of time than BAI, is limited to 500m spatial resolution when MODIS imagery is used.

Figure 5.3: MIRBI normalized distance values for the duration of the sampling period.

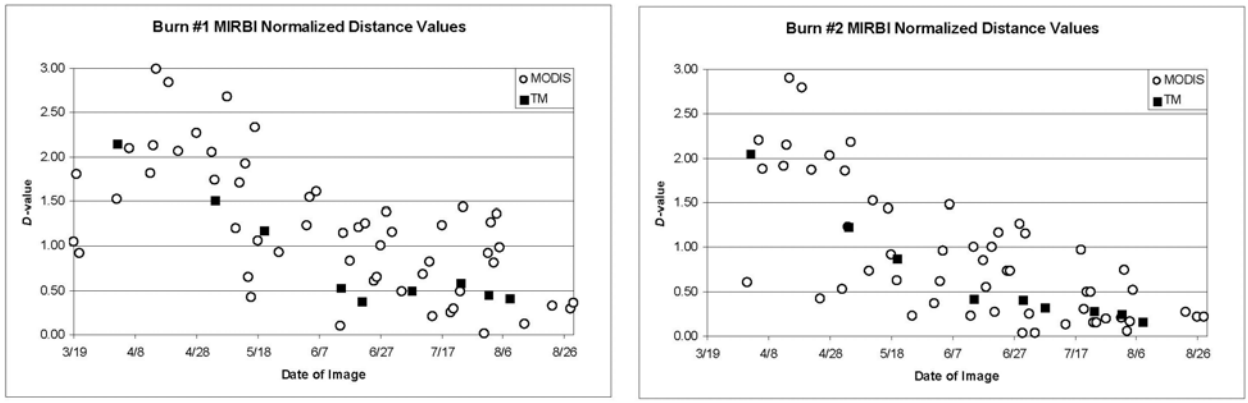

5.3.3 Red

The red TM *D*-values for Burn #1 were greater than 1 only on the April 2 image date, with a value of 1.64. For Burn #2, a value of 2.32 on April 2 was followed by a value of 1.09 on May 5, after which the values dropped to less than 1 (Figure 5.4). This suggests that red is capable of differentiating burned from unburned areas for up to four weeks in the case of Burn #1, though this again assumes that the *D*-values remained above 1 for some time after the last date on which they were known to be greater than 1. In the case of Burn #2, this time frame can be reliably extended to approximately five weeks. Again, it must be remembered that the temporal density of the TM samples prevents these time periods from being reliably estimated past what the data show.

The MODIS data for Burn #1 suggest that discrimination between burned and unburned areas in the red band are possible for more than nine weeks, as all values are above 1 until a value of 0.77 appears on June 3. Burn #2 follows a temporal curve similar to that of Burn #1, with values greater than 1 through May 17, after which two values of 0.76 and 0.86 are recorded on May 18 and 20 (Figure 5.4). It is worth noting that this time period could be further extended through June 3 if two values of 0.76 and 0.86 on May 18 and May 20 are taken to be close enough to 1 to indicate at least some level of discriminatory ability.

Like the MIRBI index reviewed above, the red band of TM and MODIS exhibited inconsistency between burned areas in the amount of time that *D*-values were greater than 1. As was the case with MIRBI, this is not surprising and is easily explained by between-burn

variation. Much different than with MIRBI or BAI, however, was the fact that estimates from the two sensors did not correspond to each other. MODIS, even if the two outliers are treated as the end of the significant differentiation period, was able to detect the burned areas from much longer than TM based on either of the two sample burns. This can be explained by either the difference in the wavelength ranges between the two sensors (Table 4.1), or by the difference in spatial resolution between the two sensors (30m for TM compared to 250m for MODIS). However, because the *in situ* analysis (which calculated bands from the same wavelength ranges as this analysis) revealed no such trends, the difference is most likely due to the effects of varying sensor spatial resolution.

Much like MIRBI, red *D*-values became insignificant much earlier than the *z* and *t*-values produced by the field-level analysis, as the field-level values are significant throughout the end of the study period in two of the four cases. Even in the two cases where significance is not maintained through the study period, they are significant well into July. Taken together, the evidence from both the field-level analysis and the satellite-based analysis suggests that red is capable of differentiating burned from unburned areas for at least four months, and up to nine months in some cases. Clearly, this suggests that it is well suited for burned area detection in tallgrass prairie. Furthermore, its usefulness is amplified by the fact that it is available on both sensors, and is available from MODIS at the maximum resolution of 250m.

Figure 5.4: Red normalized distance values for the duration of the sampling period.

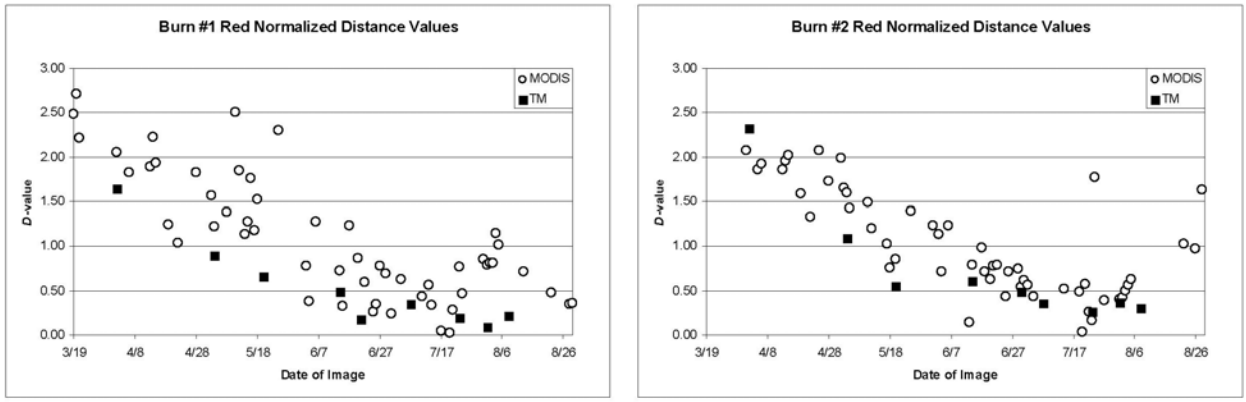

5.3.4 NIR

When TM NIR was used to calculate *D*-values for Burn #1, only the April 2 value of 1.5 was greater than 1. This is reflected by Burn #2, where the value of 1.97 on the same date was the only value greater than 1. In both cases, these values are followed by lesser values on May 4, before they fail to even approach 0.5 for the remainder of the study period (Figure 5.5). Again, the burned areas could be, and most likely are, detectable for approximately one month, though this cannot be proven.

The MODIS NIR *D*-values for Burn #1 remained above 1 until May 4, where a value of 0.95 occurred. This value was followed by three more values greater than 1 through May 12, before a value of 0.63 was recorded on May 14. Burn #2 exhibited values at or near 1 until April 22 (0.95), before a value of 1.08 on April 25, then dropped below 1 on April 28 with a value of 0.9 (Figure 5.5). From the MODIS *D*-values, it appears that NIR can distinguish burned areas for just over six weeks in the case of Burn #1, and for approximately one month in the case of Burn #2.

As was the case with BAI, its component band, NIR, showed similarity between the two sensors, as those time periods during which MODIS was able to differentiate burned from unburned can easily fall within the temporal range during which TM can be assumed to effectively perform the same task. However, unlike BAI, Burn #1 and Burn #2 varied in how long each was distinguishable, which is more characteristic of MIRBI. For the most part, these satellite level findings support those from *in situ* analysis, though Burn #1 was distinguishable for longer than any of the four field-level examples. Despite the advantage that NIR can be calculated from either sensor, and from MODIS at 250m, its utility for burned area detection in tallgrass prairie is less than MIRBI or red, though it is useful if burn detection takes place within one month of an area being burned.

Figure 5.5: NIR normalized distance values for the duration of the sampling period.

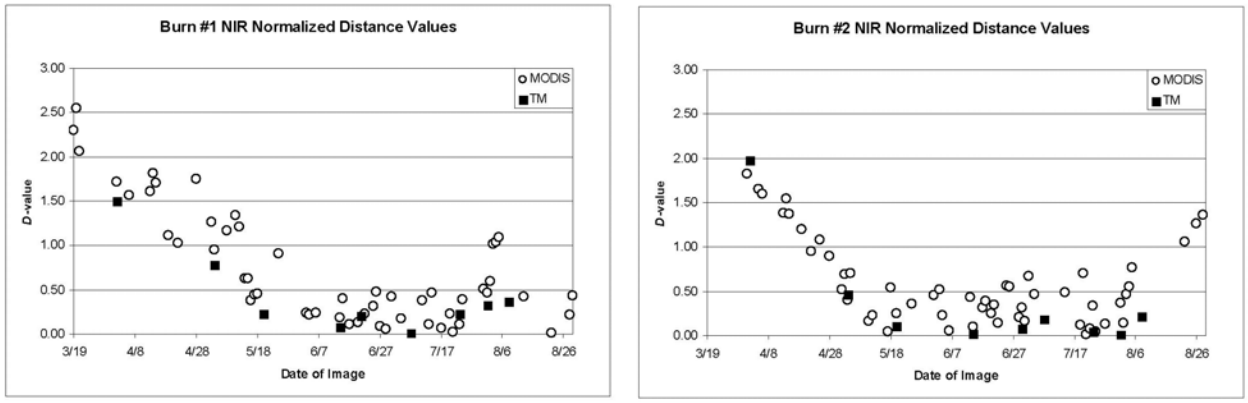

5.3.5 LNIR

LNIR, which was only available from the MODIS sensor, exhibited *D*-values of greater than 1 through May 11 for Burn #1 (Figure 5.6). This meant that Burn #1 was detectable for nearly eight weeks with LNIR. Burn #2, however, consistently showed *D*-values greater than 1 only until April 13, before this value dropped to 0.6 on April 14 (Figure 5.6), meaning that Burn #2 was only detectable for just over two weeks.

In the case of LNIR, the two burned areas show very different lengths of time over which they are detectable, (eight weeks compared to just over two). Similar inconsistencies occurred with the red band and MIRBI index reviewed earlier, though not to this extent. Compared with the *in situ* findings of the previous chapter, the LNIR *D*-values corroborated some findings and contradicted others. For example, the approximately two-week time period during which Burn #2 was detectable was shorter than all four periods in the *in situ* analysis, the shortest of which was at least four weeks long. On the other hand, Burn #1 (detectable for approximately 8 weeks in this analysis), was detectable for a shorter time period (4-5 weeks) in one *in situ* sample, for a similar time period (8 weeks) in another, and for much longer time period (through the end of August) in the remaining two.

The performance of LNIR in both the field level analysis and the normalized distance analysis suggests that the efficacy of LNIR for differentiating burned from unburned tallgrass prairie is highly subject to variability within that prairie. It is also worth noting that LNIR is disadvantaged by the fact that it is only available from the MODIS sensor, and then only at 500m

spatial resolution. For these reasons, it is likely that LNIR is of limited utility for burned area mapping at the satellite scale in tallgrass prairie.

Figure 5.6: LNIR normalized distance values for the duration of the sampling period.

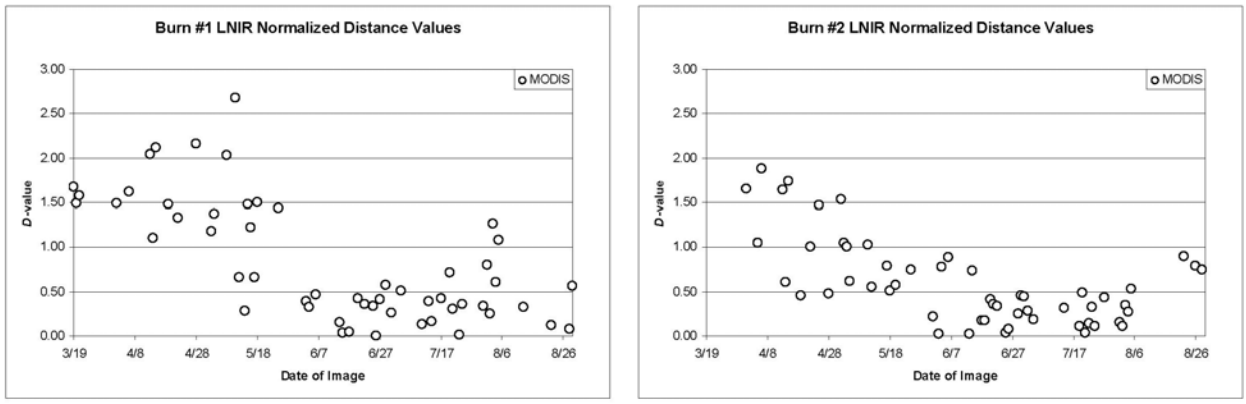

5.3.6 SMIR

The SMIR *D*-value of Burn #1, when calculated with TM, failed to reach 1 in any of the sampling dates. The closest it came was a value of 0.88 on April 2, after which no value was higher than 0.62 for the remainder of the study period. For Burn #2, only the April 2 date was significant (1.49), with the maximum value in any other TM image date being only 0.74 (Figure 5.7). From these results, it is difficult to assume that SMIR would have any utility for differentiating burned from unburned areas, except that Burn #2 might be discernable for approximately four weeks.

The MODIS SMIR *D*-values for Burn #1 were greater than 1 for only two sampling dates, March 19 and 20 with values of 1.17 and 1.87, respectively, before dropping to 0.79 on March 21. After this, *D*-values fail to consistently remain above 1 for any appreciable length of time. For Burn #2, values remain greater than 1 until May 17, after which they drop to 0.85 and 0.56 on May 18 and 20, respectively (Figure 5.7). According to the MODIS values, Burn #2 is discernable for over 7 weeks, while Burn #1 is not discernable for an appreciable length of time.

Figure 5.7: SMIR normalized distance values for the duration of the sampling period.

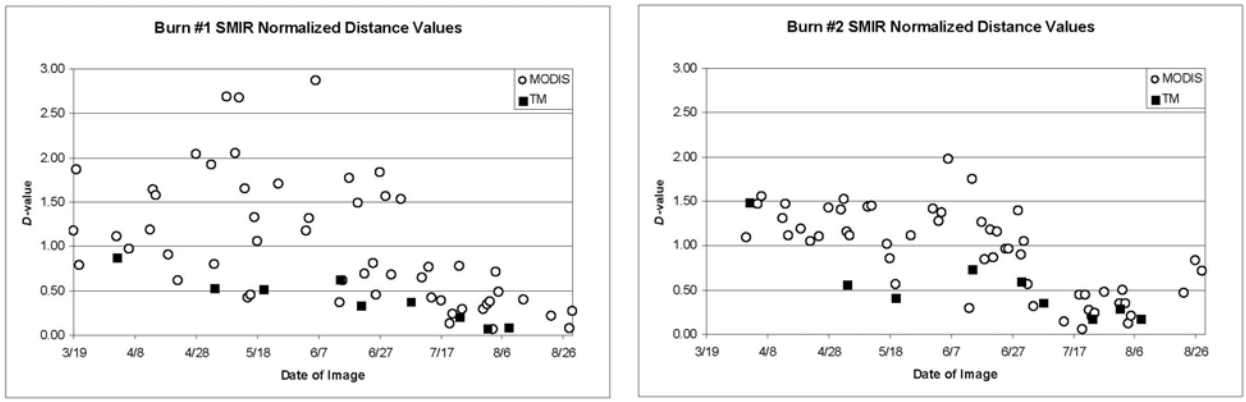

The analysis of SMIR revealed that the two sample burned areas were not similar in any way. While Burn #1 was not discernable for long, Burn #2 was discernable for more than seven weeks. This is directly in contraction to any other band where the two burn samples differed. In all of those cases, Burn #1 was detectable for much longer—sometimes for twice the amount of time. This suggests that SMIR, when it is used to distinguish between burned and unburned tracts of tallgrass prairie, focuses on different characteristics of burned areas than other indices and bands.

Although the two pairs responded differently when examined with SMIR, the two sensors showed some similarities. Neither sensor detected Burn #1 for any substantial amount of time. Burn #2 was detected by both sensors, though TM could not do so for as long as MODIS (four weeks compared to seven weeks). The satellite-based findings of neither sensor corresponded to the field-based analysis from the previous chapter. In the *in situ* analysis, SMIR values were significant for the entire study period in three of the four sample years, and significant through the end of July in the fourth. This suggests that major differences in the response of SMIR occur depending on the spatial resolution at which it is used, and on the characteristics of the burned areas to be detected. Finally, SMIR performed poorer than any other band or index tested in this satellite-level analysis, which, combined with its 500m maximum MODIS resolution, suggests that its use at this scale in tallgrass prairie is limited, despite its stellar performance in the *in situ* analysis.

5.4 Conclusions

The hypothesis proposed at the beginning of this chapter was that those bands and indices that were successful in differentiating burned from unburned tallgrass prairie using *in situ* data will also do so effectively at the satellite image scale. In most cases, this hypothesis was confirmed in that all bands or indices were able to differentiate burned from unburned areas for approximately one month or longer, and so could be said to do so effectively. The exception to this, and the band for which the hypothesis is rejected outright, is SMIR, as it performed extremely well when simulated from *in situ* data, but was only able to differentiate burned from unburned for any appreciable amount of time in one of the four scenarios tested in this chapter. Consequently, SMIR is not used for classifying burned areas in subsequent chapters of this paper.

Although the hypothesis was effectively confirmed for all bands and indices except SMIR, the length of time during which each band or index was capable of discriminating burned from unburned areas was usually different between the field-level analysis and the normalized distance analysis. In almost all cases, the *z* and *t*-values from the field-level analysis remained significant longer than the *D*-values from this analysis. This could have been caused by differences in the sensitivity of the two methods used, or by differences in the spatial scale at which the burned areas were evaluated by the two methods. However, because these differences in scale between the two methods remain constant throughout the time period of analysis, while the similarity between *t*/*z*-values and *D*-values lessens, scale differences are likely not the cause. If they were, dissimilarities would occur throughout the study period, rather than at the middle and end. Therefore, the dissimilarities most likely stem from differences in the sensitivity of the two methods. Specifically, the normalized distance method is accounting for greater sample variability (the field-level analysis techniques assumed equal variance) later in the study, which lowers the chance of having a value less than 1 during these dates. It is possible that this variance is partly related to the inclusion of bottomland and side hill grassland areas in this analysis, whereas only hilltops were sampled in Chapter 4. If this is the case, it could be argued that the conclusions regarding the efficacy of indices and bands for burned area mapping produced by this chapter are more accurate than those from Chapter 4, as they account for topographic variation within the burned area.

Because the two different burned area samples used in this chapter yielded different estimates of how long burned areas can be differentiated from unburned areas with a given band or index, one estimate must be selected to provide the baseline for further analysis. This should be the most conservative one. For example, though LNIR might be able to detect burned areas that share the characteristics of Burn #1 for more than two months after they are burned, it can only detect burned areas with the characteristics of Burn #2 for 19 days. This means that a maximum efficacy of 19 days should be assumed, as the percentage of burned areas in the entire study area that share the characteristics of Burn #2 is unknown, and might be very large.

It is also worth noting that the results of this normalized distance analysis did little to expose differences in burned area mapping capability between the TM and MODIS sensors, as the differences in spatial resolution did not seem to account for differences in the efficacy of the individual bands of indices. Those differences that were present fail to form a clear relationship, and can be mostly accounted for by temporal sample density.

All bands and indices except SMIR were retained for use in the classification of burned areas in the next chapter. These bands and indices were used because they were able to differentiate burned from unburned areas for longer periods of time than did SMIR, and/or because they contributed something (consistency between burns/sensors, high spatial resolution with MODIS, etc.) that was not also provided from a band or index with better performance. The length of time over which all bands and indices were able to differentiate burned from unburned areas is shown in Table 5.4.

Table 5.4: Length of time (at least) for each burn pair during which *D*-values remained > 1. Days of known burn existence prior to the first sampling date are counted in the total. Values in parenthesis in the table indicate a much longer period of significance that was interrupted by one or two D-values < 1.

	Resolution (m)		Length of significance in days			
Band/Index	**TM**	**MODIS**	**TM Burn #1**	**TM Burn #2**	**MOD. Burn #1**	**MOD. Burn #2**
BAI	30	250	18	8	31	25
MIRBI	30	500	66	40	5 (60)	0 (28)
red	30	250	18	40	71	53
NIR	30	250	18	8	49 (58)	25
LNIR	NA	500	NA	NA	57	19
SMIR	30	500	0	8	5	53 (73)

CHAPTER 6 - Image Classification and Accuracy Assessment

6.1 Introduction

The third objective of this study was to use the band/index suitability information that was obtained by accomplishing the first and second objectives to identify which bands/indices, sensors, and classification techniques work best for mapping burned areas in tallgrass prairie. Developing methods to identify burned areas with digital imagery is critical for two main reasons. First, fire scars that are obvious to an interpreter are usually less obvious using classification algorithms and other automated techniques (Hudak and Brockett 2004). However, these techniques must be used to some extent, as the patchiness and roughness of burned areas makes manual digitization both tedious and subjective (Hudak and Brockett 2004). Second, manual digitization can use only three-band displays, while automated methods can use a virtually unlimited amount (Hudak and Brockett 2004).

To accomplish this chapter's objective, four hypotheses were tested. First, that object-based classification techniques will map burned tallgrass prairie more accurately than pixel-based techniques based on prior studies in other cover types. Second, that TM will allow for more accurate burned area mapping in tallgrass prairie than MODIS due to its superior spatial resolution. Third, that due to cloud cover, MODIS must be used in order to achieve a sample that is temporally dense enough for burned area mapping in tallgrass prairie. Finally, that bands and/or indices composed of red and NIR wavelengths will be required for optimal burned area mapping in tallgrass prairie because they represent the best compromise in spatial and temporal resolution. Testing these hypotheses involved classifying several bands and indices both individually and in combination with two different classification techniques with both TM and MODIS.

6.2 Methods

6.2.1 Data Collection and Processing

6.2.1.1 Imagery

All 2008 TM scenes from path 28-row 33 and path 28-row 34, and all 2010 TM scenes from path 27-row 33, path 28-row 33, path 27-row 34, and path 28-row 34, that were captured

between April 1 and August 30 were downloaded through GloVis as TIFF files. They were then calibrated to top of atmosphere reflectance using the method of Chandler and Markham (2003). Only two path/row combinations from 2008 were needed because all ground-truth data (the procurement of this data is explained in section 6.2.1.2 below) were located in the footprint of these two scenes, whereas ground truth data for 2010 ranged across four scenes. Only scenes that clearly showed at least one of the aforementioned ground-truth areas in each year were retained for classification.

Also acquired were all 2008 and 2010 MODIS scenes captured between April 1 and August 30. As was the case in the previous chapter, these were downloaded through NASA WIST for both the Terra and Aqua satellites, and at spatial resolutions of both 250 m (MOD09GQ, MYD09GQ) and 500 m (MOD09GA, MYD09GA). All data were processed as in Chapter 5 using the MRT, and were subset to roughly the area covered by the TM imagery mentioned in the previous paragraph. For each year, only scenes that clearly showed all ground-truth samples that had been burned to that point were kept. Again, the image in which the ground-truth area appeared closest to nadir was used.

6.2.1.2 Ground-Truth Data

In addition to standard accuracy measures based on error matrices, the accuracy of each classification was evaluated with regard to several single, specific burned areas. In 2008, these included six burned areas in Geary and Morris Counties, Kansas, which were interpreted from oblique aerial photographs taken on April 12, 2008 by matching landmarks and burn edges to 1-meter National Aerial Imagery Program (NAIP) aerial photography. They ranged in size from approximately 46 ha to 744 ha (Figure 6.1; Table 6.1). In 2010, ground-truth areas consisted of 13 burns that were digitized *in situ* with a handheld Global Positioning System (GPS) field computer in Greenwood and Chase Counties, Kansas, between April 23 and May 5, 2010. They ranged in size from 8 ha to 958 ha (Figure 6.1; Table 6.1).

Figure 6.1: Map of the 19 ground-truth burned areas that were used to evaluate classification accuracy. The number next to each burned area identifies it according to its name in Table 6.1.

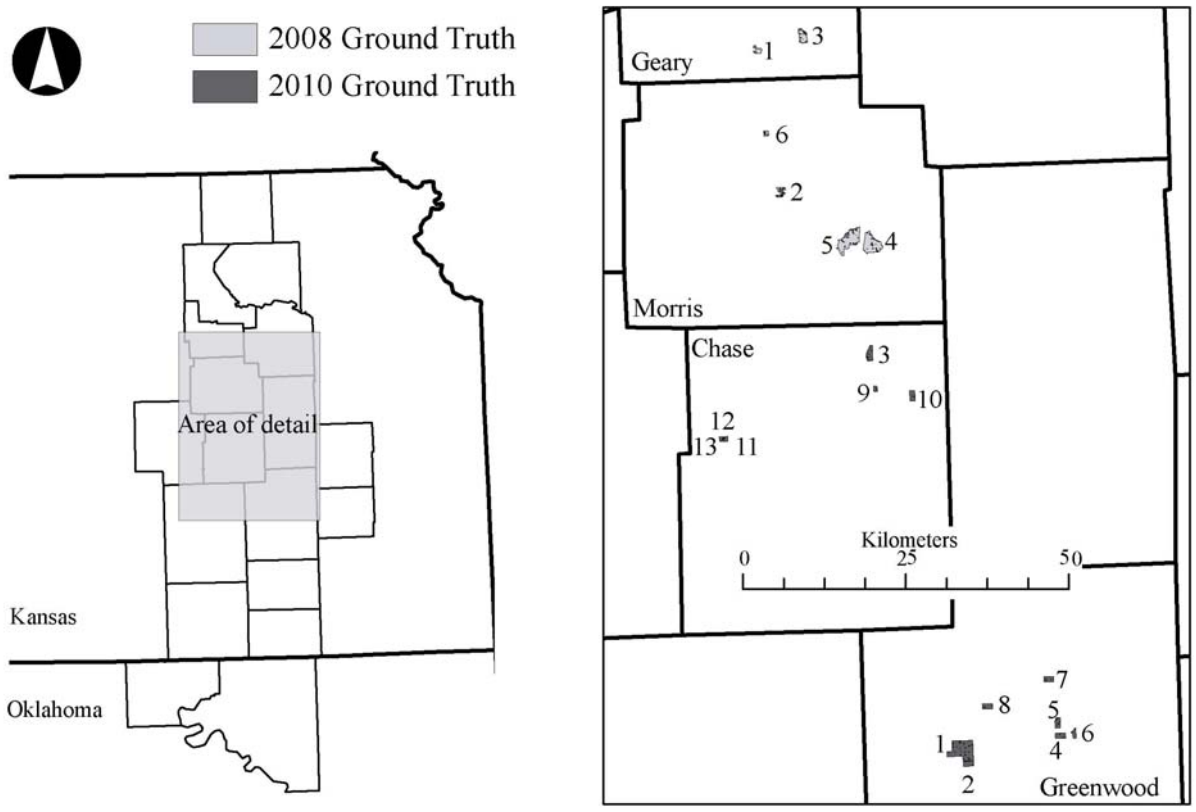

Table 6.1: Characteristics of the 19 ground-truth burned areas used in this study. Date burned was estimated based on the first confirmation of the burned area with MODIS imagery, or is known from fieldwork. The last three columns indicate how many pixels occupy an area the size of each ground-truth burned area at the given spatial resolution.

2008	Burn Date	Size (ha)	30 m	250 m	500 m
Burn #1	4/2	89	989	14	4
Burn #2	4/2	88	978	14	4
Burn #3	4/2	224	2489	36	9
Burn #4	4/1	633	7033	101	25
Burn #5	4/1	744	8267	119	30
Burn #6	4/2	46	511	7	2

2010	Burn Date	Size (ha)	30 m	250 m	500 m
Burn #1	4/10-4/11	958	10644	153	38
Burn #2	4/11	128	1422	20	5
Burn #3	4/10	182	2022	29	7
Burn #4	4/9	126	1400	20	5
Burn #5	4/9	120	1333	19	5
Burn #6	4/17	76	844	12	3
Burn #7	4/14	128	1422	20	5
Burn #8	4/9	125	1389	20	5
Burn #9	3/31	45	500	7	2
Burn #10	4/9	128	1422	20	5
Burn #11	4/9	45	500	7	2
Burn #12	4/9	8	89	1	0
Burn #13	4/9	31	344	5	1

6.2.1.3 Mask Layers

The final piece of data required was a mask layer for each of the three spatial resolutions used here (30 m, 250 m, and 500 m). These mask layers permitted the majority of each non-grassland land cover type to be excluded from consideration during the classification process, which allowed the classification to focus on differentiating burned from unburned tallgrass prairie, rather than trying to distinguish burned areas from several land-cover classes. Masking is often used prior to classification (e.g., Stroppiana et al. 2003), where it is useful for eliminating interclass variability that often causes classification problems. This is particularly true when an unburned class is composed of all land cover types other than burned areas (Pereira 1999). Additionally, some of the cover types most commonly confused with burned areas, such as water, urban, and other sparsely vegetated areas (Chuvieco and Congalton 1988, Tanaka *et al*.

1983), can be easily masked when the correct bands are used to develop the masks. Masking is also sometimes used in post-classification burned area mapping (e.g., Shao and Duncan 2007).

The images used to produce the land cover mask for the TM imagery were 11 scenes taken between March 1 and August 28 in the years from 2006 to 2010. These were from the four path/row combinations mentioned at the beginning of this section (Table 6.2). All scenes were acquired and processed in the same manner as described above for the other TM imagery used in this chapter. For each of the four TM path/row combinations, a March image was first masked in order to eliminate all land cover classes that were not grassland. First, low NIR values were masked in order to block areas of water and fallow crop. Next, low red values were masked to block areas of actively growing vegetation, such as crops and evergreen trees. A combination of low values in both NIR and green was used to mask deciduous trees (it was still too early in the year for them to have leaves) and additional areas of fallow crop. Finally, areas that had a combination of high NIR values and low green values were masked to block additional areas of active cropland. The masking of active cropland with high NIR values and low green values was then repeated for each path/row combination using three more images from April, July/August, and August/late August. Additionally, in areas were clouds were not present in an image, urban areas were masked using high green values.

MODIS masks were generated in a similar manner as the TM masks, except that only one mask was required for each spatial resolution (250m or 500m) due to the larger footprint of MODIS. Generation of all masks was performed so that an absolute minimum of grassland pixels were blocked, even at the expense of including non-grassland pixels in future classifications. In a few cases where grassland burning had occurred prior to the March image (and grassland was masked as a result), the mask was edited so that these pixels were not masked in the final product. All masks were generated from multiple image dates within the growing season because this allowed better masking of non-grassland cover types than would be possible with one or even two scenes. This is true because most cover types that appear similar to grasslands for part of the year have different temporal reflectance curves in other parts of the year. Images and criteria used to generate all masks are given in Table 6.2.

Table 6.2: Criteria used to generate each mask. Values are reflectance. Purpose denotes the primary ground cover type masked by each step, although additional masking benefits were likely realized.

TM 27-33	Purpose
3/10/2008	
NIR < 0.14	Water, Fallow Crop
Red < 0.092	Trees, Active Crop
NIR < 0.20, Green < 0.105	Trees, Fallow Crop
NIR > 0.20, Green < 0.11	Active Crop
4/14/2009	
NIR > 0.26, Red < 0.07	Active Crop
7/22/2010	
NIR > 0.31, Green < 0.04	Active Crop
Green > 0.07	Urban/Built
8/23/2010	
NIR > 0.33, Green < 0.045	Active Crop

TM 27-34	Purpose
3/10/2008	
NIR < 0.14	Water, Fallow Crop
Red < 0.092	Trees, Active Crop
NIR < 0.20, Green < 0.095	Trees, Fallow Crop
NIR > 0.20, Green < 0.11, Red < 0.12	Active Crop
4/14/2009	
NIR > 0.25, Red < 0.07	Active Crop
7/22/2010	
NIR > 0.3, Green < 0.04	Active Crop
8/28/2006	
NIR > 0.33, Green < 0.045	Active Crop

TM 28-33	Purpose
3/1/2008	
NIR < 0.14	Water/Fallow Crop
Red < 0.092	Trees, Active Crop
NIR < 0.20, Green < 0.095	Trees, Fallow Crop
NIR > 0.20, Green < 0.11	Active Crop
4/2/2008	
NIR > 0.23, Red < 0.13	Active Crop
8/8/2008	
NIR > 0.43, Green < 0.09	Active Crop
8/6/2007	
NIR > 0.32, Green < 0.04	Active Crop

TM 28-34	Purpose
3/1/2008	
NIR < 0.14	Water/Fallow Crop
Red < 0.092	Trees, Active Crop
NIR < 0.20, Green < 0.095	Trees, Fallow Crop
NIR > 0.21, Green < 0.11	Active Crop
4/21/2009	
NIR > 0.22, Red < 0.04	Active Crop
7/23/2008	
NIR > 0.33, Green < 0.09	Active Crop
Green > 0.14	Urban/Built
8/6/2007	
NIR > 0.32, Green < 0.04	Active Crop

MODIS 250m and 500m	Purpose
3/1/2008	
NIR < 0.18	Water
Red < 0.11	Active Crop
7/14/2008	
Red > 0.10	Fallow Crop
NIR < 0.28	Water
NIR > 0.48, Red < 0.045	Active Crop

6.2.2 Band/Index Selection

The next step in meeting the third objective of this study was to select the datasets that would be classified. In this case, the inputs would be single bands and indices as well as combinations of bands and indices. These are referred to as classification "scenarios" throughout

the rest of this chapter. The composition of these scenarios was ultimately based on the performance of their component band(s) and/or index in the *in situ* and normalized distance analyses performed in the preceding chapters. For example, bands or indices that demonstrated poor utility for differentiating burned from unburned grassland were not included in any scenario. Another consideration for the makeup of the scenarios was spatial resolution. For example, if three of the four bands or indices used in a scenario were available at 250 m resolution, and the fourth was available at only 500 m resolution, a 3-band version of that scenario (made up of only the 250 m spatial resolution bands) was tested as well. Finally, two scenarios were formed from all the bands from TM or MODIS. Scenarios like this are often used in burned area mapping literature, and including them here facilitates comparisons of their burned area mapping efficacy in tallgrass prairie to their efficacy in other cover types.

6.2.2.1 Single-Band/Index Scenarios

The first scenarios used were single bands and indices. Single band/index classification inputs are used here because of the simple burned/unburned nature of the classification type. If multiple land cover classes were sought, single band/index scenarios would likely be less accurate, as it is unlikely that a single band or index could discriminate between all classes well (Shao and Duncan 2007). In this study, a single band or index that performed well in both previous analyses was used if it possessed a trait that was not duplicated in another band or index, in which case only the best-performing band or index was used. NIR (Scenario #1) was the first single-band scenario used in this analysis. Although the performance of NIR was similar to BAI in the preceding two chapters, it is easier to compute, making the use of BAI unnecessary. Red (Scenario #2) was also used because it performed extremely well in both preceding chapters, and did so independently of whether or not an area was grazed. LNIR (Scenario #3) was also included based on a strong performance in Chapters 4 and 5, though it is only available from the MODIS sensor and only at 500m spatial resolution. Finally, the lone index used was MIRBI (Scenario #4), which was included on the strength of its ability to differentiate burned from unburned areas regardless of grazing intensity (Chapter 4), and because it can be calculated from both TM and MODIS.

6.2.2.2 Multiple-Band/Index Scenarios

Although single-band/index scenarios might adequately map burned areas in cases such as this (where only two classes are to be identified), multiple band/index scenarios were also tested because a mixture of bands and indices might better account for within-class variation. The first multiple-band/index scenario, Scenario #5, used all of the bands/indices that performed well in previous analysis, except for BAI. Again, BAI was not included given the similar performance of NIR. This scenario, therefore, was composed of MIRBI, LNIR, red, and NIR. Because LNIR could not be calculated from TM, a version of this scenario that was limited to MIRBI, red, and NIR was also tested (Scenario #6). Additionally, a scenario using only red and NIR was used (Scenario #7), as these are the only 250 m spatial resolution MODIS bands. Finally, two scenarios that included all bands from each of the two sensors were constructed. The first (Scenario #8) used all TM bands except the thermal band (band 6), giving it a spatial resolution of 30 m. The second (Scenario #9) used the first seven MODIS bands, giving it a spatial resolution of 500 m. Table 6.3 shows selected traits of all scenarios.

Table 6.3: Selected traits of the scenarios used as classification inputs in this chapter.

Name	Components	TM Spatial Res.	MODIS Spatial Res.
1	NIR	30	250
2	Red	30	250
3	LNIR	NA	500
4	MIRBI	30	500
5	MIRBI, LNIR, red, NIR	NA	500
6	MIRBI, red, NIR	30	500
7	red, NIR	30	250
8	TM 1-5, 7	30	NA
9	MODIS 1-7	NA	500

6.2.2.3 Scenario Generation

For each date in 2008 that a clear TM image was available from April 2 through July 23, an image representing each scenario was generated. A preliminary minimum distance classification of the scenarios from this date range showed that classification quality quickly became poor by the end of May (approximately two months after burning had taken place). Consequently, imagery after June 1 was not classified except for that already done in 2008 for TM. The results from this initial minimum distance classification of 2008 TM data is given in

this chapter to demonstrate the futility of trying to detect burned areas later in the burn season, and to justify the exclusion of this time period in all classifications except this one. However, in two of the other three cases, a final image after this cutoff date is used in order to provide an example at the end of the sample where the classification quality become poor. For example, with the MODIS imagery from 2010 the last clear image date prior to the cutoff was on May 11, on which date classification quality could still be relatively high. Therefore, a date on which the classification became poor could not be recorded unless the first clear image after the cutoff (June 22 in this case, though the classification quality would obviously be poor) was classified as well. Tables 6.4 (TM) and 6.5 (MODIS) show all imagery dates for which the scenarios were generated.

Table 6.4: Dates for which a clear TM scene was available for each of the ground-truth burned areas. Numbers in the body of the table are the path and row of the useable scene. Total is number of scenes in which a particular burned area is clearly visible.

2008	4/2	4/27	5/4	5/20	6/14	6/21	6/30	7/7	7/23	Total
Burn #1	28-33		28-33	28-33		28-33		28-33	28-33	6
Burn #2	28-33	27-33	28-33	28-33	27-33	28-33	27-33	28-33	28-33	9
Burn #3	28-33		28-33	28-33		28-33	27-33	28-33	28-33	7
Burn #4	28-33		28-33	28-33	27-33	28-33	27-33	28-33	28-33	8
Burn #5	28-33		28-33	28-33	27-33	28-33	27-33	28-33	28-33	8
Burn #6	28-33		28-33	28-33		28-33		28-33	28-33	6

2010	4/8	4/17	5/3	5/26	6/4	Total
Burn #1			27-34	28-34	27-34	3
Burn #2			27-34	28-34	27-34	3
Burn #3		27-33	27-33	28-33	27-33	4
Burn #4			27-34	28-34	27-34	3
Burn #5			27-34	28-34	27-34	3
Burn #6			27-34		27-34	2
Burn #7			27-34	28-34	27-34	3
Burn #8			27-34	28-34	27-34	3
Burn #9	28-33	27-33	27-33	28-33	27-33	5
Burn #10		27-33	27-33	28-33	27-33	4
Burn #11		27-33	27-33	28-33	27-33	4
Burn #12		27-33	27-33	28-33	27-33	4
Burn #13		27-33		28-33		2

Table 6.5: Dates of MODIS imagery used in this study. The body of the table denotes which satellite provided the scene that was used.

2008	4/2	4/6	4/13	4/15	4/19	4/22	4/28	4/29	5/4	5/11	5/17	5/20	Total
Burn #1	Aqua	Aqua	Aqua	Aqua	Terra	Aqua	Terra	Aqua	Aqua	Aqua	Terra	Aqua	12
Burn #2	Aqua	Aqua	Aqua	Aqua	Terra	Aqua	Terra	Aqua	Aqua	Aqua	Terra	Aqua	12
Burn #3	Aqua	Aqua	Aqua	Aqua	Terra	Aqua	Terra	Aqua	Aqua	Aqua	Terra	Aqua	12
Burn #4	Aqua	Aqua	Aqua	Aqua	Terra	Aqua	Terra	Aqua	Aqua	Aqua	Terra	Aqua	12
Burn #5	Aqua	Aqua	Aqua	Aqua	Terra	Aqua	Terra	Aqua	Aqua	Aqua	Terra	Aqua	12
Burn #6	Aqua	Aqua	Aqua	Aqua	Terra	Aqua	Terra	Aqua	Aqua	Aqua	Terra	Aqua	12

2010	3/31	4/9	4/14	4/17	4/19	4/29	5/4	5/5	5/6	5/7	5/11	6/22	Total
Burn #1			Aqua	Aqua	Aqua	Terra	Terra	Aqua	Terra	Aqua	Terra	Aqua	10
Burn #2			Aqua	Aqua	Aqua	Terra	Terra	Aqua	Terra	Aqua	Terra	Aqua	10
Burn #3			Aqua	Aqua	Aqua	Terra	Terra	Aqua	Terra	Aqua	Terra	Aqua	10
Burn #4		Terra	Aqua	Aqua	Aqua	Terra	Terra	Aqua	Terra	Aqua	Terra	Aqua	11
Burn #5		Terra	Aqua	Aqua	Aqua	Terra	Terra	Aqua	Terra	Aqua	Terra	Aqua	11
Burn #6				Aqua	Aqua	Terra	Terra	Aqua	Terra	Aqua	Terra	Aqua	9
Burn #7			Aqua	Aqua	Aqua	Terra	Terra	Aqua	Terra	Aqua	Terra	Aqua	10
Burn #8		Terra	Aqua	Aqua	Aqua	Terra	Terra	Aqua	Terra	Aqua	Terra	Aqua	11
Burn #9	Aqua	Terra	Aqua	Aqua	Aqua	Terra	Terra	Aqua	Terra	Aqua	Terra	Aqua	12
Burn #10		Terra	Aqua	Aqua	Aqua	Terra	Terra	Aqua	Terra	Aqua	Terra	Aqua	11
Burn #11		Terra	Aqua	Aqua	Aqua	Terra	Terra	Aqua	Terra	Aqua	Terra	Aqua	11
Burn #12		Terra	Aqua	Aqua	Aqua	Terra	Terra	Aqua	Terra	Aqua	Terra	Aqua	11
Burn #13		Terra	Aqua	Aqua	Aqua	Terra	Terra	Aqua	Terra	Aqua	Terra	Aqua	11

6.2.3 Image Classification

6.2.3.1 Minimum Distance Supervised Classification

A pixel-based, supervised, minimum distance classification technique was used because this technique works based on the "distance" (in feature space) of each pixel to the mean of each cover type's training data. This does not involve probability, as is the case with maximum likelihood, and so does not assume a Gaussian distribution. In this work, because the classes are very broad and possibly bimodal (e.g., both older and newer burned areas in the same class), the assumptions of the maximum likelihood classification would most likely be violated.

Because minimum distance is a supervised classification technique, training data for the two classes, burned areas and unburned areas, were needed. Burned area training data for 2008 and 2010 were usually selected separately for each image date, though they were reused whenever possible. Although selecting the same training data for all dates would have provided consistency, the fact that only a small portion of the respective scenes from each path

overlapped, and the fact that clouds on some dates obscured burned areas that were used in other dates rendered this approach impossible. Both recent and older burned areas were included in the sample when possible. The same burned areas used to train the TM classifications were also used to train the MODIS classifications when possible, though cloud cover sometimes dictated that new training areas be selected in these cases as well.

Training data for unburned areas in both years and for both sensors were selected in a manner similar to the burned area data, with known unburned areas used to classify other images (from either sensor) when clouds permitted. In all cases, every scenario from a given scene and date was classified with the same training data whether burned or unburned. One minimum distance classification result was generated for each scenario for each TM or MODIS image date for each of the two years (Tables 6.4 and 6.5). Non-grassland areas were masked using the masks generated previously (section 6.2.1.3).

6.2.3.2 Object-Based Classification

Object-based classification is useful because it allows for groups of similar, adjacent pixels to be treated as whole objects, rather than as an unrelated group of individual pixels (Hay *et al.* 2001). This allows for the use of geometric information that is inherent in all remotely sensed imagery. Burned areas in an image can also be thought of as discreet objects, and, consequently, object-based classification has been used extensively for mapping them, though this research is usually performed in forests (e.g., Gitas *et al.* 2004, 2008, Mitri and Gitas 2004a, 2004b, 2006, 2008). Object-based classification works by generating image objects through the process of segmentation, then classifying these objects based on various spectral and geometric properties. In this work, segmentation was performed with a Fractal Net Evolution Approach (FNEA), which builds objects using a bottom-up technique that begins with individual pixels and merges them pairwise until the resulting objects meet a user-specified threshold (Baatz *et al.* 2004, Benz *et al.* 2004). eCognition 4.0 software was used for all object-based image segmentation and classification.

Because masks cannot be applied during the classification process in eCognition, all scenarios to be classified were first saved as separate, masked, image files. For the TM images, the masked area was given a value of –5 to better separate it from the actual reflectance values contained in the rest of the image. This was not necessary for MODIS, as reflectance values were multiplied by 10,000, and would not be confused with the original mask value of zero. In

the three MODIS scenarios that used MIRBI, the single-digit index values were multiplied by 1,000. This made the radiometric range of the MIRBI values more comparable to that of the inflated MODIS reflectance values, and allowed for the use of the same segmentation parameters across all MODIS images of 500 m spatial resolution. This is necessary because segmentation of images with different radiometric resolutions (despite equal spatial resolutions and segmentation parameter values) results in different-sized objects between the two images (Baatz *et al.* 2004).

The segmentation parameters for this analysis were chosen so that the smallest burned areas could remain as separate objects (rather than be merged with other cover types—possibly unburned areas), while preventing as much as possible the division of larger individual burned areas into multiple objects. This was consistent with a primary rule of object-based classification—to produce image objects that are as large as possible but as small as necessary to preserve important details (Baatz *et al.* 2004). In cases where one or the other was unavoidable, the retention of smaller burned areas was deemed more important than keeping larger burned areas whole, as no information is actually lost by dividing larger objects into multiple parts. It should also be noted that all parameters were developed using the red and NIR image bands. The parameters which provided an optimal segmentation were different for each image type, given the different spatial and radiometric resolutions of the sensors (Table 6.6).

Table 6.6: Segmentation parameters for all three types of imagery used in this chapter.

	TM	MODIS 250m	MODIS 500m
Scale Parameter	2	60	25
Shape Factor	0.2	0.1	0.1
Compactness/Smoothness	0/1	0.5/0.5	0.5/0.5

Once segmented, the image objects were classified into one of three classes: burned, unburned, or masked. Training data were identified in the same manner as with the minimum distance classification, including reusing areas where possible and using both older and newer burned areas in the burned area training set. Typically, one major advantage of object-based classification is the ability to use geometric properties of the objects in the classification. However, burned areas (particularly later in the burn season) do not exhibit any particular geometric property that would differentiate them from unburned grassland. Consequently, the object-based technique was used here as a tool with which to avoid the misclassification of

individual pixels and small groups of pixels. That is, the advantages of object-based classification were, in this case, realized from the segmentation rather than from the classification of the resultant objects. Because a standard nearest neighbor scheme takes into account only the spectral properties of the image objects, it was used to perform the classification. Finally, it should be noted that given the futility of trying to accurately detect burned areas later in the burn season (as evidence by the pixel-based classification with the 2008 TM imagery) the imagery from this year and sensor was not classified past the June 14 image date using object-based classification.

6.2.4 Accuracy Assessment

The most reliable method for assessing the accuracy of burned area mapping results is to compare those results to results from higher-resolution imagery (Eva and Lambin 1998). In the case of both TM and MODIS, higher resolution imagery that showed burned areas was not available, and/or was not available at sufficient temporal resolution to match each image date that was classified. Consequently, two other accuracy assessment techniques were initially used to evaluate the ability of each classification scenario to detect burned areas. Once these two techniques revealed the best method for mapping burned areas, the classifications produced by this method were further evaluated for accuracy using a more objective, mainstream approach.

6.2.4.1 Error Matrix Data

A simple error matrix was constructed for each scenario for each sensor in each of the two years. The error matrix had four possibilities: correctly identified burned areas, correctly identified unburned areas, false positive burned areas, and false negative burned areas. The error matrix used between 103 and 158 ground-truth reference points to evaluate the TM data, with the number of points varying by scene. These were assigned a value of either burned or unburned based on visual interpretation of the TM images.

Because unburned areas were often burned later in the time series, some unburned points had to be manually moved from burned to unburned areas in later image dates, though most unburned area points did not have to be moved. Burned points, on the other hand, were selected and kept throughout he sampling period for the obvious reason that once an area is burned, it remains burned throughout the sampling period. Clouds obscured reference points in some images, in which case these points were simply moved to a burned or unburned area depending

on which was appropriate for that point. All points developed using the four TM scenes were merged into a composite dataset and used to evaluate the MODIS scenarios (174 points in 2008 and 227 in 2010). Again, relocating the problem points to matching cover areas (burned or unburned) solved cloud problems. Because the points in this initial analysis had to be moved to accommodate changing burn patterns and cloud cover, they could not be treated as a random sample. Consequently, all interpretations should be adjusted accordingly. It is for this reason that the more objective error matrix analysis described in section 6.2.4.3 was later performed on selected image dates from the most accurate method.

From the error matrix, producer's accuracy was calculated by dividing the correctly identified number of points for each of the two cover classes by the total points assigned to that cover class by the reference data, while user's accuracy was calculated by dividing the number of correct points in each cover class by the total points assigned to that cover class by the classification scenario. Overall accuracy was calculated by dividing the number of correctly identified points in both classes by the total number of points sampled. Finally, Kappa was estimated according to Congalton *et al.* (1983)

$$KHAT = N\sum_{i=1}^{k} x_{ii} - \sum_{i=1}^{k}(x_{i+} \times x_{+i}) / N^2 - \sum_{i=1}^{k}(x_{i+} \times x_{+i}) \tag{6.1}$$

where $KHAT$ is the estimate of Kappa, k is the number of rows in the error matrix, x_{ii} is the number of observations in row i and column i, x_{i+} and x_{+i} are the marginal totals for row i and column i, respectively, and N is the total number of observations. Kappa (and its estimate; $KHAT$) is similar to the overall accuracy in that it is a measure of agreement between the classification result and the reference data, except that it is standardized to account for any chance agreement that may be present. Ideal classifications have high Kappa values, high overall accuracy, and similar producer's and user's accuracies (Shao and Duncan 2007).

6.2.4.2 Areal Extents

Although error matrices provide a good global measure of classification accuracy, they cannot address local variation in how accurately burned areas are classified. This information would be valuable not only in its own right, but also for identifying the underlying causes of any accuracy problems exposed by the error matrix assessment, particularly errors of omission, which would result in underestimation of burned area.

The area of each of the six (2008) or thirteen (2010) ground-truth burned areas as computed from the field or aerial photography data was compared to their area as classified by each scenario. Because this was done for consecutive image dates, a temporal trend in the ability of each scenario to detect burned area size was generated. It should be noted that, because no data outside of the burned ground truth areas were evaluated, local overestimation of burned areas could not be diagnosed by this technique.

6.2.4.3 Second Error Matrix Assessment

Results from the accuracy assessment performed in the previous two sections revealed that the spatial resolution of the 500 m MODIS data was too coarse for burned area mapping in tallgrass prairie. Furthermore, the temporal resolution of the TM imagery was not sufficient for this task either. This suggests that burned area mapping in tallgrass prairie must use the 250 m MODIS bands, which are limited to the red and NIR spectral ranges. Consequently, the second accuracy assessment was performed only on the three scenarios that are comprised of the 250 m MODIS bands (Scenarios #1, #2, and #7). A more detailed discussion of the performance of all scenarios is presented beginning with section 6.3.1.

To construct these error matrices, 300 ground-truth points were randomly generated within the boundary of each 250 m MODIS image date. All points for each image date were assigned a value of either burned or unburned based on a TM scene from approximately the same date as the MODIS image date. In total, four TM dates in 2008 and three dates in 2010 corresponded to MODIS scenarios dates, give or take one day (Table 6.7). All points located in cover types other than grasslands in the TM image, including masked areas, cloudy areas, cloud shadows, border areas with no data values, forest areas, and cropland areas were deleted. Additionally, any remaining points that corresponded to clouds or their shadows in the MODIS imagery were deleted as well. In the three cases where the TM image was acquired on the day before the MODIS image, unburned area ground-truth points were examined in the MODIS image to make sure they had not been burned in the time between when the two images were taken. If so, they points were deleted. Culling unsuitable points left between 103 and 125 points depending on image date.

All accuracy measurements were calculated in the same manner as in section 6.2.4.1 above. Because no ground-truth points were manually moved, and because ground-truth data did not come from the image being classified, this accuracy assessment is more robust and reliable

than the exploratory one outlined in section 6.2.4.1, and is considered the definitive assessment of classification accuracy with 250 m MODIS data in tallgrass prairie.

Table 6.7: Dates of TM and MODIS imagery used in the error matrix.

TM Image	MODIS Image
4/2/2008	4/2/2008 (Aqua)
4/27/2008	4/28/2008 (Terra)
5/4/2008	5/4/2008 (Aqua)
5/20/2008	5/20/2008 (Aqua)
4/8/2010	4/9/2010 (Terra)
4/17/2010	4/17/2010 (Aqua)
5/3/2010	5/4/2010 (Terra)

6.3 Results and Discussion

6.3.1 Error Matrices

6.3.1.1 Scenario #1 (NIR)

Minimum distance classification of Scenario #1 from TM in both 2008 and 2010 yielded *KHAT* values greater than 80% through the first two image dates (80% or greater accuracy was considered good accuracy and was used as a baseline for discussing *KHAT* values throughout this paper). In both years, however, these values fell on the third sampling date (early May) to 50% (2008) and 74/77% (2010), from whence they fell further throughout the rest of the study period in both years (Table 6.8). Two *KHAT* values are sometimes be given for 2010, as the May 3 and 26 sampling dates included two TM scenes. The declining performance after the first two dates is explained by a rapid decrease in producer's accuracy values, which indicates underestimation of burned areas due to regeneration of grass on the burn scars. In the 2008 and 2010 MODIS minimum distance classifications, *KHAT* values were also above 80% for the first two sampling dates, before dropping to 69% (2008) and 77% (2010) by the third sampling date (Table 6.8). Again, this is due to declining Producer's accuracies from fading burn scars.

In the case of TM minimum distance, *KHAT* values for this scenario remained above 80% for at least 26 days in 2008, and for at least 10 days in 2010. The time period over which *KHAT* values are greater than 80% is likely longer than cited, as it includes only the time between when

the area was first known to be burned and last image with a *KHAT* value greater than 80%. The true length of time during which *KHAT* values were greater than 80% could actually extend much longer, given a more temporally dense imagery sample. This is more likely with TM data due to its poorer temporal resolution than with MODIS, and is particularly true in 2008 here, as the first overpass in which many of the sample burned areas are visible is immediately after burning (April 2), after which a clear image is not available until April 27. This trend occurs with all scenarios analyzed, and should be kept in mind as the results from this chapter are interpreted.

The analysis of the Scenario #1 minimum distance classifications suggests that, with NIR, TM imagery can accurately detect burned areas longer than MODIS, as the MODIS *KHAT* values remained high for only at least 5 days in 2008 and 10 days in 2010. Furthermore, unlike with TM, subsequent images mean that these periods of good *KHAT* values could not have exceeded 10 days in the case of 2008, or 14 days in the case of 2010, meaning that timing of the imagery cannot explain this difference. Most likely, the higher spatial resolution of TM is responsible for its longer period of burned area detection accuracy, as the rapidly decreasing spectral signature of burned areas creates confusion with unburned areas when the larger MODIS pixels are used. Nonetheless, reliable detection for 10 days with MODIS could be adequate, as the disadvantages previously discussed can be offset by its greater temporal resolution. Furthermore, the MODIS *KHAT* values do not necessarily reach poor levels (50-60 % range) until early to mid May, which is similar to when TM values reach this level. Finally, this scenario is very resistant to classifying non-grassland cover types as burned areas, which is more useful in cases where masking non-grassland cover types might not be feasible.

Table 6.8: Error matrix accuracy assessment of Scenario #1 (NIR) minimum distance classifications. In this chapter, producer's and user's accuracies always measure the ability of the classification to detect burned areas only, while overall accuracy and the Kappa estimate always refer to the accuracy of the whole classification.

TM 2008

Date	Producer	User	Overall	Kappa
4/2	96	100	98	96
4/27	91	100	96	92
5/4	48	100	76	50
5/20	30	63	59	15
6/14	39	59	62	19
6/21	45	50	54	6
6/30	64	51	58	17
7/7	48	48	52	3
7/23	51	41	44	-11

TM 2010

Date	Producer	User	Overall	Kappa
4/8	96	100	98	96
4/17	87	100	94	88
5/3 (27-33)	72	100	87	74
5/3 (27-34)	83	93	89	77
5/26 (28-33)	53	60	62	24
5/26 (28-34)	76	76	73	45
6/4	63	50	54	10

MODIS 2008

Date	Producer	User	Overall	Kappa
4/2	81	100	91	82
4/6	86	96	92	84
4/13	68	98	85	69
4/15	65	93	82	63
4/19	68	82	79	56
4/22	77	88	85	69
4/28	81	89	87	73
4/29	77	80	81	62
5/4	65	80	77	53
5/11	71	79	78	55
5/17	55	51	56	11
5/20	15	67	59	10

MODIS 2010

Date	Producer	User	Overall	Kappa
3/31	92	100	96	91
4/9	92	100	95	90
4/14	81	99	89	77
4/17	81	100	89	78
4/19	76	100	86	73
4/29	71	93	80	61
5/4	76	93	83	67
5/5	69	96	81	62
5/6	61	91	74	50
5/7	69	93	79	59
5/11	86	93	88	75
6/22	54	69	59	20

In both 2008 and 2010, TM object-based *KHAT* values for Scenario #1 were greater than 80% for the first two sampling dates (through April 27 and 17, respectively), and then dropped below this threshold for the third sampling date. Again, it should be noted that the 2010 range could be longer depending on image dates, especially considering that one of the two May 3 *KHAT* values is 73% (Table 6.9), which is close to the 80% threshold. In the case of 2008, low *KHAT* values are due initially to burn underestimation on May 5, then to both overestimation and underestimation beginning on May 20. In 2010, both overestimation and underestimation are responsible beginning on May 3. In the case of the 2008 MODIS object-based classifications, *KHAT* values were above 80% for the first two dates, from at least April 2 to April 6, then dropped to 75% on April 13. In 2010, however, values remained above 80% through April 19 (Table

6.9). For both MODIS years, the reduction in *KHAT* values begins with underestimation of burned areas.

The duration over which the *KHAT* values were viable for object-based classification was nearly the same as with the minimum distance classification. In fact, TM 2008 and 2010 were identical at 26 and 10 days, respectively. The 2008 MODIS duration was four days, which is comparable to five days for the minimum distance classification. In 2010, the object-based classification improved this value to 20 days, whereas for minimum distance it was only 10. In the case of both minimum distance and object-based classification techniques, NIR demonstrated great utility for identifying burned areas in tallgrass prairie, though it is most effective when burned areas are less than two weeks old.

Table 6.9: Error matrix accuracy assessment of Scenario #1 (NIR) object-based classifications.

TM 2008				
Date	**Producer**	**User**	**Overall**	**Kappa**
4/2	99	100	99	99
4/27	98	100	99	98
5/4	60	100	82	62
5/20	58	59	62	23
6/14	36	67	65	24

TM 2010				
Date	**Producer**	**User**	**Overall**	**Kappa**
4/8	99	100	99	99
4/17	96	91	94	87
5/3 (27-33)	85	86	87	73
5/3 (27-34)	97	71	79	59
5/26 (28-33)	67	51	55	12
5/26 (28-34)	97	58	59	7
6/4	61	54	58	17

MODIS 2008				
Date	**Producer**	**User**	**Overall**	**Kappa**
4/2	87	100	94	88
4/6	83	96	91	81
4/13	76	97	88	75
4/15	82	88	87	73
4/19	81	62	70	40
4/22	86	64	72	46
4/28	78	59	66	32
4/29	74	67	72	45
5/4	82	63	70	41
5/11	78	57	64	34
5/17	47	53	57	13
5/20	47	49	54	7

MODIS 2010				
Date	**Producer**	**User**	**Overall**	**Kappa**
3/31	100	100	100	100
4/9	95	100	97	95
4/14	96	98	96	93
4/17	93	98	95	89
4/19	91	98	93	87
4/29	79	83	79	57
5/4	83	81	79	58
5/5	80	86	81	62
5/6	68	83	74	48
5/7	82	88	83	65
5/11	77	98	86	72
6/22	72	67	63	24

6.3.1.2 Scenario #2 (red)

For the 2008 TM minimum distance classifications, Scenario #2 (red) *KHAT* values remained above 80% through the first three sampling dates. This lasted until May 20, on which *KHAT* values were still relatively high at 75%. 2010 TM *KHAT* values were similar, and did not drop below 80% until May 26 (Table 6.10). In the case of 2008, lower *KHAT* values are explained by both overestimation and underestimation of burned areas on the May 20 sampling date. In 2010, lower *KHAT* values are explained by severe underestimation of burned areas (poor producer's accuracies for burned areas) on the May 26 sampling date. The 2008 MODIS minimum distance *KHAT* values remained above 80% for the first three sampling dates, before decreasing to 78% on April 15. As was the case with TM, this was due to underestimation of burned areas beginning with this date. 2010 *KHAT* values, however, remained above 80% through May 6 (Table 6.10).

Overall, Scenario #2 outperformed Scenario #1 (NIR) in terms of how long it could accurately detect burned areas with minimum distance classification. Unlike with Scenario #1, however, TM and MODIS performed almost equally, with TM having *KHAT* values above 80% for 33 or 25 days, and MODIS for 12 or 37 days, depending on year. Despite its seemingly stellar performance, it should be noted that that Scenario #2 consistently confuses burned areas with patches of actively growing vegetation, as both of these cover types reflect very little in the red spectral range. This led to major overestimation of burned areas, particularly with active cropland, because not all of these areas were masked. This trend is not reflected in the accuracy assessment figures, however, because growing vegetation was not included in the ground truth points for unburned area. Because of its tendency to confuse green vegetation with burned areas, the red spectral range should not be used to identify burned areas unless all but target land cover types are sufficiently masked in order to prevent this overestimation. Additionally, the background unburned cover type (in this case dead vegetation) must not be green, or it will appear similar to its burned counterpart. It should be noted that this is not a problem with a dead vegetation canopy, and so is not a problem in the tallgrass prairies of the Flint Hills until later in the growing season.

Table 6.10: Error matrix accuracy assessment of Scenario #2 (red) minimum distance classifications.

TM 2008				
Date	**Producer**	**User**	**Overall**	**Kappa**
4/2	99	100	99	99
4/27	98	100	99	98
5/4	88	97	93	86
5/20	88	85	87	75
6/14	89	76	83	67
6/21	37	66	62	21
6/30	75	69	75	49
7/7	71	54	59	19
7/23	67	48	51	5

TM 2010				
Date	**Producer**	**User**	**Overall**	**Kappa**
4/8	100	100	100	100
4/17	89	100	95	90
5/3 (27-33)	92	96	94	88
5/3 (27-34)	85	100	92	85
5/26 (28-33)	54	81	73	45
5/26 (28-34)	68	94	79	60
6/4	59	64	66	31

MODIS 2008				
Date	**Producer**	**User**	**Overall**	**Kappa**
4/2	88	100	95	89
4/6	91	96	94	88
4/13	83	96	91	81
4/15	81	94	89	78
4/19	79	78	81	62
4/22	94	91	93	86
4/28	95	94	95	90
4/29	92	88	91	81
5/4	92	88	91	81
5/11	96	93	95	90
5/17	91	85	89	77
5/20	94	72	80	62

MODIS 2010				
Date	**Producer**	**User**	**Overall**	**Kappa**
3/31	95	99	97	94
4/9	95	100	97	95
4/14	94	98	96	91
4/17	95	98	96	92
4/19	93	98	95	89
4/29	98	93	95	89
5/4	94	93	93	85
5/5	95	92	93	85
5/6	98	88	91	81
5/7	95	87	89	77
5/11	99	90	93	86
6/22	72	60	56	8

KHAT values from the object-based classification of Scenario #2 remained above 80% through May 4 in 2008, and through May 3 in 2010, which is comparable to the minimum distance results (Table 6.11). The 2008 and 2010 MODIS results were much different than with minimum distance classification, however, as *KHAT* values never rose above 80% for more than one consecutive sampling date (Table 6.11). For the 2008 TM classification, underestimation of burned areas is the primary cause of low *KHAT* values. For 2010 TM, both overestimation and underestimation beginning on the May 26 image date cause low *KHAT* values. For both years of MODIS, low *KHAT* values values were cause by underestimation of burned areas.

Although the number of consecutive days with TM *KHAT* values above 80% was approximately equal to that of the minimum distance classification, this date range was reduced with MODIS (no consecutive values above 80%). This suggests that MODIS performs more poorly when object-based classification is used than when minimum distance classification is

used. Because producer's accuracy for the burned area class is low, this means that this technique is failing to find many burned areas. Likely, this results from smaller burned areas being included into objects with unburned pixels, and therefore being classified as unburned, whereas pixel-based classification techniques would classify these separately as burned pixels. Therefore, the smoothing effects of object-based classification, particularly when used with larger pixels such as MODIS, might miss smaller burned areas, which would be a major drawback of object-based classification for mapping burned areas in tallgrass prairie. This does not necessarily matter in this case, as Scenario #2 showed the same problems with object-based classification as it did with minimum distance, such as classifying all green vegetation as burned, and so is of limited use with either classification technique unless a very complete mask of all other cover types is constructed. Nonetheless, it is something that should be considered when using larger pixels not only in general, but particularly with object-based classification methods.

Table 6.11: Error matrix accuracy assessment of Scenario #2 (red) object-based classifications.

TM 2008				
Date	**Producer**	**User**	**Overall**	**Kappa**
4/2	100	100	100	100
4/27	95	100	98	96
5/4	89	92	91	82
5/20	81	95	89	78
6/14	84	54	62	28

TM 2010				
Date	**Producer**	**User**	**Overall**	**Kappa**
4/8	99	100	99	99
4/17	94	100	97	95
5/3 (27-33)	86	100	94	87
5/3 (27-34)	95	91	93	86
5/26 (28-33)	56	47	51	3
5/26 (28-34)	58	55	50	-2
6/4	79	48	52	8

MODIS 2008				
Date	**Producer**	**User**	**Overall**	**Kappa**
4/2	88	99	94	88
4/6	79	95	89	78
4/13	79	95	89	78
4/15	72	89	83	66
4/19	51	69	68	33
4/22	71	89	83	64
4/28	56	98	80	58
4/29	72	71	74	48
5/4	60	63	66	31
5/11	87	92	91	81
5/17	83	67	74	49
5/20	59	64	67	32

MODIS 2010				
Date	**Producer**	**User**	**Overall**	**Kappa**
3/31	70	100	83	67
4/9	89	100	94	88
4/14	63	98	78	58
4/17	90	91	89	78
4/19	65	100	80	62
4/29	78	98	86	73
5/4	68	94	79	60
5/5	85	76	76	50
5/6	85	67	67	29
5/7	78	75	72	43
5/11	88	77	78	53
6/22	67	59	54	4

6.3.1.3 Scenario #3 (LNIR)

In both 2008 and 2010, Scenario #3 (LNIR) minimum distance *KHAT* values failed to reach 80% in either initial image date. This alone does not necessarily disqualify Scenario #3 from usefulness in differentiating burned and unburned areas. However, *KHAT* values begin at only 70% in 2008 and never climb above this value. In 2010, this initial *KHAT* value is only 72%, and those few values that improve upon it come later in the sample, with lower values in between (Table 6.12).

Object-based *KHAT* values were poor in both years as well, and only reached 80% once—on April 19, 2010 (Table 6.13). In the case of both classification types in both years, poor performance was due to underestimation of burned areas. Striping of the MODIS LNIR band on the Terra satellite caused the extremely low *KHAT* values, such as those on May 4 and May 6, 2010. Considering that the performance of this scenario was poor, that striping exists on its sole band when one of two satellites are used (roughly half of the sample), that it is not comparable with a band on TM or many other sensors, and that it is available at a maximum spatial resolution of only 500m, it cannot be considered a viable option for burned area mapping in tallgrass prairie with either classification technique.

Table 6.12: Error matrix accuracy assessment of Scenario #3 (LNIR) minimum distance classifications.

MODIS 2008				
Date	**Producer**	**User**	**Overall**	**Kappa**
4/2	69	98	86	70
4/6	71	90	83	66
4/13	69	92	83	66
4/15	58	83	76	50
4/19	53	71	69	36
4/22	60	70	71	40
4/28	73	74	76	52
4/29	71	67	71	42
5/4	64	70	72	43
5/11	69	76	76	52
5/17	62	57	62	24
5/20	49	67	66	30

MODIS 2010				
Date	**Producer**	**User**	**Overall**	**Kappa**
3/31	75	100	85	72
4/9	39	91	63	31
4/14	77	93	83	67
4/17	78	94	85	69
4/19	82	94	86	73
4/29	70	87	77	54
5/4	3	40	42	-3
5/5	89	94	90	80
5/6	4	45	42	-2
5/7	90	89	88	75
5/11	79	93	85	69
6/22	85	80	79	56

Table 6.13: Error matrix accuracy assessment of Scenario #3 (LNIR) object-based classifications.

MODIS 2008				
Date	**Producer**	**User**	**Overall**	**Kappa**
4/2	77	100	90	79
4/6	73	88	83	66
4/13	82	88	87	73
4/15	77	69	74	48
4/19	55	69	69	36
4/22	86	64	72	45
4/28	72	75	76	52
4/29	37	49	55	6
5/4	60	58	63	25
5/11	78	63	70	40
5/17	42	70	66	29
5/20	64	65	68	36

MODIS 2010				
Date	**Producer**	**User**	**Overall**	**Kappa**
3/31	68	99	81	64
4/9	78	95	85	71
4/14	89	89	88	75
4/17	91	89	89	77
4/19	96	88	90	80
4/29	68	86	76	52
5/4	86	82	81	62
5/5	82	95	87	74
5/6	84	78	77	53
5/7	88	83	83	65
5/11	53	97	72	47
6/22	85	67	67	29

6.3.1.4 Scenario #4 (MIRBI)

The 2008 TM Scenario #4 (MIRBI) minimum distance classifications yielded *KHAT* values that were above 80% through the first three sampling dates before falling to 74% on May 20. 2010 *KHAT* values were greater than 80% through May 3 in the case of the row 34 scenes, and through May 26 in the case of the row 33 scenes. However, the path 34 scene *KHAT* values did reach 78% on May 26, which is close to the 80% threshold, and could be considered as having acceptable accuracy (Table 6.14). In the case of both years, decreasing *KHAT* values were due to increases in both overestimation and underestimation of burned areas. MODIS minimum distance *KHAT* values in either year did not reach 80% except once in 2010, and were not even above 70% for any image date in 2008 (Table 6.14). The reason for this was major underestimation of burned areas in the earliest image dates, and both over and underestimation beginning around the middle of April.

With minimum distance classification of Scenario #4, results obtained from TM were clearly superior to those obtained from MODIS, with periods of *KHAT* values greater than 80% for at least 33 days in 2008 and either 25 or 49 days in 2010, depending on which TM path is cited. For MODIS, only one *KHAT* value greater than 80% was observed, and this on May 5, 2010, which is nowhere near the beginning of the sample. As was the case with Scenario #1, the poorer spatial resolution of MODIS seems to prevent accurate burned area detection, as burned

areas are being overlooked by the classification. Scenario #4 also had a tendency to confuse urban/built environments and roads (particularly with TM where even smaller roads were discernable) with burned areas, as both have similar MIRBI index values. This led to overestimation of burned areas, but was not a major problem due to the limited presence of this land cover class in the study area. Nonetheless, these cover types should be masked if MIRBI alone is used for classifying burned areas. Furthermore, the limited ability of Scenario #4 to detect burned areas when calculated with MODIS suggests that it should be used for burned area detection in tallgrass prairie only with TM imagery (if at all), which could be problematic given the relatively poor temporal resolution of the TM sensor.

Table 6.14: Error matrix accuracy assessment of Scenario #4 (MIRBI) minimum distance classifications.

TM 2008				
Date	**Producer**	**User**	**Overall**	**Kappa**
4/2	99	97	98	96
4/27	84	100	93	86
5/4	88	98	94	87
5/20	84	88	87	74
6/14	84	71	79	57
6/21	73	85	82	63
6/30	59	74	74	45
7/7	60	80	75	48
7/23	75	72	75	50

TM 2010				
Date	**Producer**	**User**	**Overall**	**Kappa**
4/8	93	100	97	94
4/17	97	95	96	92
5/3 (27-33)	97	93	96	91
5/3 (27-34)	95	90	92	85
5/26 (28-33)	86	93	90	81
5/26 (28-34)	89	91	89	78
6/4	90	82	87	73

MODIS 2008				
Date	**Producer**	**User**	**Overall**	**Kappa**
4/2	60	100	78	53
4/6	68	87	81	61
4/13	76	87	84	67
4/15	82	76	80	61
4/19	81	89	87	73
4/22	78	68	74	47
4/28	81	82	83	66
4/29	79	76	79	58
5/4	78	73	77	54
5/11	62	56	61	23
5/17	76	86	83	66
5/20	65	68	71	41

MODIS 2010				
Date	**Producer**	**User**	**Overall**	**Kappa**
3/31	70	95	81	62
4/9	90	98	93	87
4/14	75	84	77	54
4/17	81	93	85	71
4/19	91	91	90	79
4/29	88	84	83	66
5/4	95	87	89	78
5/5	90	86	86	71
5/6	93	85	87	73
5/7	88	80	81	61
5/11	97	89	92	83
6/22	78	77	74	48

In 2008, object-based *KHAT* values for Scenario #4 (MIRBI) were above 80% only for the first image date on April 2. In 2010, however, this length of time extended throughout the entire

sample to June 4 (Table 6.15). In 2008, low producer's accuracy values, indicative of burned area underestimation, were responsible. In the case of MODIS, object-based *KHAT* values were not above 80% for consecutive image dates (Table 6.15) due to underestimation of burned areas, particularly early in the sample.

2010 Scenario #4 object-based *KHAT* values remained above 80% for the entire length of the study—at least 58 days—which is longer than any other period in the study, regardless of sensor, scenario, or year. However, 2008 TM object-based *KHAT* values did not remain above 80% for consecutive image dates, and MODIS object-based *KHAT* values were lower than 80% from the beginning of sampling in both years. This means that Scenario #4 was inconsistent between sensors, between years, and between classification types. No other scenario showed this much inconsistency, and this, combined with its overall poor performance with MODIS imagery, suggests that MIRBI alone is of limited use in classifying burned areas in tallgrass prairie, unless it is used in a limited capacity with the minimum distance classification of TM data, in which case the main problem with using TM data—inadequate temporal resolution—applies.

Table 6.15: Error matrix accuracy assessment of Scenario #4 (MIRBI) object-based classifications.

TM 2008				
Date	**Producer**	**User**	**Overall**	**Kappa**
4/2	100	100	100	100
4/27	61	100	83	65
5/4	86	100	94	87
5/20	82	92	89	77
6/14	77	74	79	57

TM 2010				
Date	**Producer**	**User**	**Overall**	**Kappa**
4/8	99	93	96	92
4/17	100	88	94	87
5/3 (27-33)	100	95	97	95
5/3 (27-34)	98	93	95	91
5/26 (28-33)	100	90	95	90
5/26 (28-34)	100	88	92	84
6/4	97	88	93	86

MODIS 2008				
Date	**Producer**	**User**	**Overall**	**Kappa**
4/2	54	88	76	49
4/6	68	85	80	60
4/13	88	79	84	69
4/15	78	80	82	63
4/19	74	89	84	68
4/22	60	69	70	39
4/28	71	89	83	64
4/29	59	72	71	41
5/4	60	73	72	43
5/11	45	54	58	14
5/17	37	88	70	35
5/20	35	75	66	27

MODIS 2010				
Date	**Producer**	**User**	**Overall**	**Kappa**
3/31	72	95	81	64
4/9	85	98	90	81
4/14	84	83	81	60
4/17	76	93	83	66
4/19	88	89	87	74
4/29	82	85	81	62
5/4	78	94	84	69
5/5	84	82	80	59
5/6	82	86	82	63
5/7	88	78	79	56
5/11	64	92	76	54
6/22	53	68	59	18

6.3.1.5 Scenario #5 (MIRBI, LNIR, red, NIR)

In both 2008 and 2010, minimum distance *KHAT* values for Scenario #5 (MIRBI, LNIR, red, NIR) failed to reach 80% in every case except on one date in 2010 (Table 6.16). As was the case with Scenario #4 (LNIR), underestimation of burned areas caused the low *KHAT* values, particularly during the first part of the sample in each year. With object-based classification, Scenario #5 (MIRBI, LNIR, red, and NIR) yielded *KHAT* values that were greater than 80% for only the initial date in 2008, and for two consecutive dates in 2010 (Table 6.17). As with minimum distance, underestimation of burned areas was responsible for *KHAT* values below 80%.

Interestingly, this scenario performed slightly better with object-based classification than with minimum distance classification. Nonetheless, this performance was not good enough to overcome the other shortcomings of the scenario that stem from its LNIR component band.

Consequently, it is of very little use for burned area mapping in tallgrass prairie regardless of classification technique.

Table 6.16: Error matrix accuracy assessment of Scenario #5 (MIRBI, LNIR, red, NIR) minimum distance classifications.

MODIS 2008				
Date	**Producer**	**User**	**Overall**	**Kappa**
4/2	73	100	88	75
4/6	73	90	84	68
4/13	74	95	87	73
4/15	63	86	79	56
4/19	50	80	72	41
4/22	62	72	72	42
4/28	76	78	79	58
4/29	78	73	77	54
5/4	64	77	75	49
5/11	65	82	78	55
5/17	58	62	65	29
5/20	47	67	66	30

MODIS 2010				
Date	**Producer**	**User**	**Overall**	**Kappa**
3/31	78	100	88	76
4/9	67	93	78	57
4/14	77	95	85	69
4/17	81	97	88	76
4/19	79	94	85	71
4/29	79	87	81	62
5/4	5	54	43	-1
5/5	88	95	90	80
5/6	5	54	43	-1
5/7	88	88	86	71
5/11	82	93	86	73
6/22	84	80	79	56

Table 6.17: Error matrix accuracy assessment of Scenario #5 (MIRBI, LNIR, red, NIR) object-based classifications.

MODIS 2008				
Date	**Producer**	**User**	**Overall**	**Kappa**
4/2	82	96	90	80
4/6	79	87	86	71
4/13	65	86	80	58
4/15	71	85	81	61
4/19	87	82	86	71
4/22	87	66	74	49
4/28	85	83	85	70
4/29	62	77	75	48
5/4	87	73	80	60
5/11	77	72	76	53
5/17	40	82	69	34
5/20	76	73	76	53

MODIS 2010				
Date	**Producer**	**User**	**Overall**	**Kappa**
3/31	93	96	94	87
4/9	88	95	91	81
4/14	82	91	85	69
4/17	88	93	89	78
4/19	93	88	89	77
4/29	82	83	80	60
5/4	89	83	83	65
5/5	91	89	88	76
5/6	72	88	78	57
5/7	87	83	82	64
5/11	92	90	89	78
6/22	67	70	64	28

6.3.1.6 Scenario #6 (MIRBI, red, NIR)

2008 and 2010 TM minimum distance *KHAT* values for Scenario #6 (MIRBI, red, NIR) closely resembled those from Scenario #4 (MIRBI alone), as they remained above 80% through

May 4 in 2008, and through May 3 or 26 in 2010,depending on which scene is cited (Table 6.18). As was the case with Scenario #4, decreases in *KHAT* values were due to increases in both overestimation and underestimation of burned areas. Also similar to Scenario #4, MODIS minimum distance *KHAT* values in 2008 for Scenario #6 did not climb above 80% at any point in the study. However, unlike with Scenario #4, 2010 values were above 80% for the first two sampling dates (Table 6.18). Again, early underestimation of burned areas, and both overestimation and underestimation beginning in middle and late April, led to the low *KHAT* values.

Along with similar accuracy values, this scenario shared other problems with Scenario #4, including a tendency to confuse burned areas with urban areas and roads, and poor performance with MODIS imagery. Nonetheless, consistency problems associated with using MIRBI alone might create a niche for this scenario if used with the TM sensor, and if used where an adequate mask can be created for non-target cover types. However, as with any scenario that works well only when used with TM, it is likely to be of limited use in tallgrass prairie, where sensor return times must be relatively high.

Table 6.18: Error matrix accuracy assessment of Scenario #6 (MIRBI, red, NIR) minimum distance classifications.

TM 2008				
Date	**Producer**	**User**	**Overall**	**Kappa**
4/2	99	97	98	96
4/27	84	100	93	86
5/4	88	98	94	87
5/20	84	88	87	74
6/14	89	74	82	63
6/21	73	84	81	61
6/30	59	74	74	45
7/7	62	80	75	50
7/23	78	72	76	52

TM 2010				
Date	**Producer**	**User**	**Overall**	**Kappa**
4/8	93	100	97	94
4/17	97	96	97	94
5/3 (27-33)	97	93	96	91
5/3 (27-34)	95	90	92	85
5/26 (28-33)	86	93	90	81
5/26 (28-34)	89	91	89	78
6/4	90	82	87	73

MODIS 2008				
Date	**Producer**	**User**	**Overall**	**Kappa**
4/2	77	100	90	79
4/6	72	95	86	70
4/13	73	93	86	70
4/15	64	83	78	55
4/19	53	85	75	47
4/22	71	77	78	54
4/28	83	81	84	68
4/29	86	77	82	64
5/4	63	75	74	48
5/11	67	91	82	63
5/17	53	60	63	25
5/20	49	75	70	36

MODIS 2010				
Date	**Producer**	**User**	**Overall**	**Kappa**
3/31	84	100	91	82
4/9	85	97	90	80
4/14	75	96	84	69
4/17	78	96	86	72
4/19	80	96	87	74
4/29	78	86	80	60
5/4	84	89	85	70
5/5	85	97	90	80
5/6	76	88	81	61
5/7	80	88	82	65
5/11	85	93	88	76
6/22	70	79	72	44

In 2008, Scenario #6 (MIRBI, red, NIR) TM object-based *KHAT* values remained above 80% for four of the five image dates, including the first three (through May 4). In 2010, this was the case through May 3 for one TM row, and through May 26 for the other, as well as for the last image date on June 4. In fact, the May 26, 2010 value that did not reach 80% was close, at 75% (Table 6.19). In 2008, dates with lower *KHAT* values were caused by underestimation of burned areas. In 2010, the opposite was true, and overestimation was responsible. For MODIS, only the initial *KHAT* value in 2008 (April 2) was greater than 80%, and was followed by a value of 71% on April 6. In 2010, the two initial *KHAT* values on March 31 and April 9 were greater than 80% (Table 6.19). In both years, both overestimation and underestimation, dependent on which image was examined, were responsible for low *KHAT* values.

The performance of this scenario using object-based classification resembles its performance when used with minimum distance classification. If only the minimum distance

classification findings are considered, Scenario #6 would not provide any advantage over Scenario #4 (MIRBI alone). Furthermore, because it is more computationally intensive due to more components, it would not be needed when MIRBI alone is available. However, given the inconsistency of MIRBI alone, this scenario could have a niche because it performs slightly better, and is more consistent and predictable across different sensors, classification techniques, and years. Even if it does show some utility with TM data, however, MIRBI's 500 m maximum spatial resolution with MODIS is a major disadvantage, and likely renders is of little use for burned area mapping in tallgrass prairie.

Table 6.19: Error matrix accuracy assessment of Scenario #6 (MIRBI, red, NIR) object-based classifications.

TM 2008				
Date	**Producer**	**User**	**Overall**	**Kappa**
4/2	100	99	99	99
4/27	91	100	96	92
5/4	95	97	96	92
5/20	70	91	83	65
6/14	95	86	91	82

TM 2010				
Date	**Producer**	**User**	**Overall**	**Kappa**
4/8	97	100	99	97
4/17	100	92	96	92
5/3 (27-33)	100	96	98	96
5/3 (27-34)	100	94	97	94
5/26 (28-33)	100	87	93	86
5/26 (28-34)	100	83	88	75
6/4	100	85	92	83

MODIS 2008				
Date	**Producer**	**User**	**Overall**	**Kappa**
4/2	81	98	91	81
4/6	73	92	85	69
4/13	72	93	85	69
4/15	74	85	83	65
4/19	90	83	87	75
4/22	82	70	76	52
4/28	88	82	86	72
4/29	69	67	71	41
5/4	86	71	78	56
5/11	82	73	78	56
5/17	83	75	80	60
5/20	71	69	72	44

MODIS 2010				
Date	**Producer**	**User**	**Overall**	**Kappa**
3/31	86	100	92	84
4/9	89	97	92	84
4/14	85	86	83	66
4/17	88	92	89	78
4/19	92	94	93	85
4/29	81	86	81	63
5/4	84	92	87	73
5/5	88	88	86	72
5/6	65	85	74	48
5/7	88	85	84	67
5/11	80	74	73	43
6/22	72	66	63	22

6.3.1.7 Scenario #7 (red, NIR)

The 2008 TM minimum distance *KHAT* values for Scenario #7 (red, NIR) remained above 80% for the first two sampling dates, after which they dropped to 59% by May 5. In 2010, these

values remained significant through the third sampling date on May 3, though one scene on this date had a value of 79% (Table 6.20). 2008 MODIS minimum distance *KHAT* values for Scenario #7 were above 80% for the first two sampling dates, after which they dropped to 77% on April 13, and only reached 80% on May 11 after several image dates with lower values. In 2010, *KHAT* values were greater than 80% through April 17, and, with the exception of a value of 78% on April 19, remained above 80% through May 5 (Table 6.20). For both sensors in both years, lower *KHAT* values were caused mostly by underestimation of burned areas.

Using TM, this scenario performed similar to Scenario #1 in 2008 (at least 26 days between dates with *KHAT* values above 80% of for both scenarios) and outperformed Scenario #1 in 2010 (25 days compared to 10). However, it did not perform as well as Scenario #2. For MODIS, performance was also better than Scenario #1 and not as good as Scenario #2 in both years. However, unlike Scenario #2, the mix of red and NIR does not overestimate burned areas due to actively growing vegetation in the study area. At the same time, it improves upon the abilities of NIR by detecting burned areas longer. Consequently, Scenario #7 shows great promise for burned area mapping in tallgrass prairie, exhibiting the advantages of both red and NIR, while minimizing the disadvantages of both as well. Additionally, it can be calculated from a wide range of sensors and from MODIS at 250 m spatial resolution.

Table 6.20: Error matrix accuracy assessment of Scenario #7 (red, NIR) minimum distance classifications.

TM 2008				
Date	**Producer**	**User**	**Overall**	**Kappa**
4/2	99	100	99	99
4/27	98	100	99	98
5/4	58	100	80	59
5/20	55	80	73	44
6/14	39	59	62	19
6/21	44	51	54	28
6/30	66	53	60	21
7/7	48	49	53	4
7/23	52	41	44	-11

TM 2010				
Date	**Producer**	**User**	**Overall**	**Kappa**
4/8	97	100	99	97
4/17	89	100	95	90
5/3 (27-33)	83	100	92	84
5/3 (27-34)	82	96	89	79
5/26 (28-33)	56	69	68	35
5/26 (28-34)	80	81	79	57
6/4	65	62	66	32

MODIS 2008				
Date	**Producer**	**User**	**Overall**	**Kappa**
4/2	82	100	92	83
4/6	87	96	93	85
4/13	77	98	89	77
4/15	68	93	83	65

MODIS 2010				
Date	**Producer**	**User**	**Overall**	**Kappa**
3/31	93	100	96	92
4/9	94	100	96	93
4/14	87	99	92	84
4/17	86	100	92	84

4/22	82	89	87	74	**4/29**	88	96	91	81
4/28	87	89	90	79	**5/4**	88	95	90	80
4/29	87	84	87	73	**5/5**	87	98	92	83
5/4	81	91	88	75	**5/6**	83	97	89	78
5/11	94	91	93	86	**5/7**	85	96	89	78
5/17	91	80	86	71	**5/11**	90	95	92	83
5/20	35	82	67	30	**6/22**	55	69	60	22

In 2008, TM object-based *KHAT* values for Scenario #7 (red, NIR) were greater than 80% for the first two sampling dates (through April 27) before dropping to 79% on May 4. In 2010, values were above 80% for the first three sampling dates, through May 3 (Table 6.21). In 2008, reduced *KHAT* values were the product of burned area underestimation. In 2010, however, lower values were the product of overestimation of burned areas. In the case of MODIS, 2008 object-based *KHAT* values were greater than 80% for the first two sampling dates, before falling to 78% on April 13. 2010 values remained above 80% for five sampling dates, finally falling to 77% on April 29 (Table 6.21). In both MODIS cases, reduced *KHAT* values were caused by underestimation of burned areas.

This scenario performed very well with both classification types, and the duration over which *KHAT* values remained greater than 80% with the object-based technique was similar to the minimum distance duration in all four cases. For the these reasons, the performance of this scenario suggests that it is very useful for burned area mapping in tallgrass prairie with either classification type. In fact, this scenario might represent a way to extend (temporally) the burn mapping capabilities of Scenario #1 (NIR), while preventing some of the overestimation problems of Scenario #2 (red).

Table 6.21: Error matrix accuracy assessment of Scenario #7 (red, NIR) object-based classifications.

TM 2008				
Date	**Producer**	**User**	**Overall**	**Kappa**
4/2	100	100	100	100
4/27	98	100	99	98
5/4	84	94	90	79
5/20	75	90	85	69
6/14	75	70	76	51

TM 2010				
Date	**Producer**	**User**	**Overall**	**Kappa**
4/8	100	99	99	99
4/17	92	100	96	92
5/3 (27-33)	99	100	99	99
5/3 (27-34)	89	100	95	89
5/26 (28-33)	79	54	59	21
5/26 (28-34)	87	82	82	63
6/4	75	60	65	32

MODIS 2008				
Date	**Producer**	**User**	**Overall**	**Kappa**
4/2	82	100	92	83
4/6	85	96	91	82
4/13	81	94	89	78
4/15	86	77	82	64
4/19	77	72	76	53
4/22	82	82	84	67
4/28	85	86	87	73
4/29	74	69	74	47
5/4	83	60	68	37
5/11	82	76	80	61
5/17	72	62	67	35
5/20	59	66	68	34

MODIS 2010				
Date	**Producer**	**User**	**Overall**	**Kappa**
3/31	97	100	98	96
4/9	95	99	97	94
4/14	95	99	97	94
4/17	92	98	95	89
4/19	88	96	91	82
4/29	85	94	89	77
5/4	85	94	88	76
5/5	81	95	87	74
5/6	92	90	89	78
5/7	97	82	86	70
5/11	96	93	93	86
6/22	46	50	43	-14

6.3.1.8 Scenario #8 (TM 1-5, 7) and Scenario #9 (MODIS 1-7)

Using Scenario #8 (TM bands 1-5, 7) yielded minimum distance *KHAT* values that remained above 80% through April 27 in 2008, and through May 3 in 2010 (Table 6.22). The reduction in TM *KHAT* values in both 2008 and 2010 is due to underestimation of burned areas. Minimum distance *KHAT* values for Scenario #9 (MODIS bands 1-7) did not reach 80% in either 2008 or 2010, except for the May 5 image date in 2010 (Table 6.22). As was the case with TM, underestimation of burned areas is responsible.

Scenario #9, like other 500 m spatial resolution MODIS scenarios, failed to match the accuracy of its TM counterpart (Scenario #8), though it should be noted that in this case their component wavelength ranges differed more than did the component ranges of other scenarios. The usefulness of Scenario #9, therefore, can be ruled out immediately for burned area mapping in tallgrass prairie with minimum distance techniques, as it performed poorly and is available at a

maximum spatial resolution of only 500 m. However, even the better performance of Scenario #8 is not as good as some other scenarios, such as Scenarios #1 and #7, which are less computationally intensive due to fewer components. Furthermore, Scenarios #8 and #9 tend to overestimate burned areas for the same reason as red, though not to the same extent, which makes extensive masking of other cover types necessary.

Table 6.22: Error matrix accuracy assessment of Scenario #8 (TM 1-5, 7) and Scenario #9 (MODIS 1-7) minimum distance classifications.

TM 2008				
Date	**Producer**	**User**	**Overall**	**Kappa**
4/2	96	100	98	96
4/27	95	100	98	96
5/4	71	100	87	73
5/20	81	91	87	74
6/14	55	71	71	39
6/21	48	69	66	30
6/30	82	67	75	50
7/7	55	51	54	9
7/23	63	46	49	-1

TM 2010				
Date	**Producer**	**User**	**Overall**	**Kappa**
4/8	96	100	99	96
4/17	87	97	93	86
5/3 (27-33)	100	96	95	90
5/3 (27-34)	82	98	90	80
5/26 (28-33)	46	92	73	44
5/26 (28-34)	80	98	88	76
6/4	73	67	71	42

MODIS 2008				
Date	**Producer**	**User**	**Overall**	**Kappa**
4/2	68	98	85	69
4/6	69	89	82	63
4/13	73	95	86	71
4/15	63	86	79	56
4/19	51	78	72	41
4/22	65	66	70	38
4/28	81	78	81	62
4/29	87	74	80	61
5/4	65	77	76	50
5/11	81	78	81	62
5/17	83	64	71	44
5/20	50	74	70	37

MODIS 2010				
Date	**Producer**	**User**	**Overall**	**Kappa**
3/31	79	100	88	77
4/9	72	92	80	61
4/14	75	93	83	66
4/17	81	96	87	75
4/19	85	92	87	74
4/29	89	87	86	71
5/4	10	68	46	3
5/5	92	92	91	81
5/6	26	79	54	15
5/7	92	83	85	68
5/11	89	91	89	78
6/22	88	71	73	43

In 2008, TM Scenario #8 (TM 1-5, 7) object-based *KHAT* values were greater than 80% for all but the last image date on June 14. In 2010, these values remained above 80% through the May 3 sampling date, but dropped below this threshold for the May 26 date (Table 6.23). In 2008, the lower *KHAT* values on the last date were due to underestimation of burned areas. In 2010, these low values were caused by both overestimation and underestimation of burned areas. For Scenario #9 (MODIS 1-7), a single object-based *KHAT* value was above 80% for the first date

in 2008, and two values were above this threshold in 2010 (Table 6.23). In both years, underestimation of burned areas was initially responsible for the low *KHAT* values, though both overestimation and underestimation are responsible later in the sample.

In all four cases, the number of days with *KHAT* values above 80% was greater for object-based classification than for minimum distance classification, with 2008 TM posting the largest difference (23 days). Additionally, 2010 MODIS *KHAT* values were above 80% for at least 10 consecutive days, whereas with minimum distance, this number was zero. These figures clearly suggest that object-based classification is better than minimum distance classification for mapping burned areas of tallgrass prairie when all bands of a sensor are used. However, it should be noted that this scenario shares one disadvantage with Scenario #1 (red)—that it overestimates burned areas due to green vegetation. Nonetheless, if used with object-based classification methods and other cover types are masked, it holds some promise for burned area mapping in tallgrass prairie, though other, higher-resolution options exist when using MODIS.

Table 6.23: Error matrix accuracy assessment of Scenario #8 (TM 1-5, 7) and Scenario #9 (MODIS 1-7) object-based classifications.

TM 2008

Date	Producer	User	Overall	Kappa
4/2	100	100	100	100
4/27	98	100	99	98
5/4	90	100	96	91
5/20	90	94	93	86
6/14	75	92	86	72

TM 2010

Date	Producer	User	Overall	Kappa
4/8	99	99	99	97
4/17	100	95	97	95
5/3 (27-33)	97	95	96	92
5/3 (27-34)	100	97	98	97
5/26 (28-33)	90	70	78	56
5/26 (28-34)	86	90	87	73
6/4	75	58	63	28

MODIS 2008

Date	Producer	User	Overall	Kappa
4/2	82	100	92	83
4/6	78	90	86	72
4/13	76	83	82	64
4/15	63	82	77	52
4/19	81	79	82	63
4/22	83	66	73	47
4/28	85	78	82	64
4/29	73	48	53	9
5/4	83	71	77	54
5/11	85	61	69	39
5/17	82	60	67	36
5/20	50	70	68	33

MODIS 2010

Date	Producer	User	Overall	Kappa
3/31	86	100	92	84
4/9	88	95	90	80
4/14	82	93	86	73
4/17	88	90	88	75
4/19	93	89	89	78
4/29	78	88	81	62
5/4	83	87	83	66
5/5	87	88	86	71
5/6	75	84	78	55
5/7	80	81	78	54
5/11	80	93	85	70
6/22	79	69	67	32

6.3.1.9 Summary of Scenarios' Utility Based on Error Matrices

Because of their poor performance, three of the scenarios tested should not be used for burned area mapping in tallgrass prairie, regardless of which sensor or technique is used. Two of these, Scenario #3 (LNIR) and Scenario #5 (MIRBI, LNIR, red, NIR), performed poorly due to their use of the LNIR band, with its myriad problems, including striping, poor resolution, and limited availability. Scenario #4 (MIRBI), was of limited use because it showed inconsistency between years, sensors, and classifications techniques.

Three other scenarios in this study were accurate only when the TM sensor was used, including Scenario #6 (MIRBI, red, NIR), Scenario #8 (TM 1-5, 7), and Scenario #2 (red). In the case of Scenario #2, this relationship was true only with object-based classification, as its minimum distance performance was good with both sensors. Another drawback of these three sensors is that they require a detailed mask of non-grassland cover types, though this problem is most evident with Scenario #2. Perhaps most important to grassland burned area mapping, however, is that, because of their poor performance with MODIS, all of these scenarios (red only with object-based classification) must rely only on the 16-day temporal resolution of TM to accurately map burned areas in tallgrass prairie throughout the year. Considering this relatively long return time and the high likelihood of cloud cover during the spring burn season, identifying all or even most burned areas with TM is usually not possible in the Flint Hills. Therefore, the matrix accuracy results suggest that MODIS imagery is more reliable for burned area mapping in tallgrass prairie due to its greater temporal resolution.

Although Scenario #9 (MODIS 1-7) showed some promise for burned area mapping in tallgrass prairie, it had several problems, including that it is only available from the MODIS sensor, that it is only available at 500 m resolution, and that it requires masking of other cover types. Consequently, other scenarios would be better suited for burned area mapping in tallgrass prairie.

The final two scenarios, #1 (NIR) and #7 (red, NIR) performed better overall than any other scenario. Furthermore, they performed consistently well regardless of sensor, year, or technique. Although periods of good performance were longer with TM than with MODIS (a trend that persisted throughout the study), this was expected. The performance of these two scenarios allows them to be used with either or both sensors, creating the most temporally dense sample possible for burned area mapping. Additionally, these scenarios are available on both

sensors, and are available at the highest possible resolution of 250 m from MODIS. Additionally, they do not require masking of actively growing vegetation (as is the case with red wavelengths alone) or urban areas (in the case of MIRBI and its associated scenarios). Therefore, according to the accuracy data gleaned from the error matrices, burned area mapping in tallgrass prairie should concentrate on these two scenarios, regardless of which technique or sensor is used. Tables 6.24 and 6.25 contain the criteria used to evaluate the different scenarios.

Table 6.24: Comparison of results for both classification types. Columns indicate consecutive days (at least) from the beginning of the sample during which *KHAT* values were greater than 80%.

	Minimum Distance Classification				Object-Based Classification			
	TM		MODIS		TM		MODIS	
Scenario (components)	**2008**	**2010**	**2008**	**2010**	**2008**	**2010**	**2008**	**2010**
1 (NIR)	26	10	5	10	26	10	4	20
2 (red)	33	25	12	37	33	26	1	0
3 (LNIR)	NA	NA	0	0	NA	NA	0	0
4 (MIRBI)	33	49	0	0	1	58	0	0
5 (MIRBI, LNIR, red, NIR)	NA	NA	0	0	NA	NA	1	10
6 (MIRBI, red, NIR)	33	49	0	10	33	49	1	10
7 (red, NIR)	26	25	5	18	26	26	4	20
8 (TM 1-5, 7)	26	25	NA	NA	49	26	NA	NA
9 (MODIS 1-7)	NA	NA	0	0	NA	NA	1	10

Table 6.25: Summary of each scenario's usefulness for burned area mapping in tallgrass prairie based on error matrices. "Sensor" denotes which sensor a given scenario can be used with; while "technique" denotes which classification type is best suited for the scenario. A yes in the "mask" column denotes a scenario that should only be used with a mask that eliminates other cover types.

Scenario (components)	TM Res. (m)	MODIS Res. (m)	Sensor	Technique	Mask
1 (NIR)	30	250	Both	Both	No
2 (red)	30	250	Both	Min. Dist.*	Yes
3 (LNIR)	NA	500	Not Useful	NA	NA
4 (MIRBI)	30	500	Not Useful	NA	NA
5 (MIRBI, LNIR, red, NIR)	NA	500	Not Useful	NA	NA
6 (MIRBI, red, NIR)	30	500	TM	Both	Yes
7 (red, NIR)	30	250	Both	Both	No
8 (TM 1-5, 7)	30	NA	TM	Both	Yes
9 (MODIS 1-7)	NA	500	Not Useful	Object	Yes

* Red wavelengths performed well with object-based classification, but only when used with TM data

6.3.2 Areal Extents

6.3.2.1 Scenario #1 (NIR)

The performance of TM Scenario #1 (NIR) with minimum distance classification varied between years, as it was only able to detect greater than 80% of all sample burned areas for one image date in 2008, but was able to do so for more than a month in the case of most 2010 sample burns. It should be noted, however, that the 2008 time periods might be longer (nearly a month) if suitable imagery had been available to prove this was the case. Nonetheless, this does not account for the difference between years, and this issue remains beyond explanation. The performance of MODIS Scenario #1 with minimum distance was similar to that of TM, in that it was able to detect most burned areas for at least 1-2 weeks. In most cases in 2010, however, it was not able to detect burned areas for as long as TM did (Table 6.26). Although MODIS seemed to outperform TM in 2008, this could be a product of poor temporal density on the part of the 2008 TM imagery.

One major issue that exists with both sensors in both years is that smaller burned areas are either not detect at all, or are able to be detected for less time than larger burned areas. This is not surprising with MODIS, as the four smaller burned areas only contain from one to seven of these larger pixels. However, several burned areas are missed with TM as well, including Burn #6 in 2008, which is the size of 511 TM pixels. This seems to show that quantifying the area of smaller burned areas is much more difficult than doing so for larger burned areas regardless of sensor—at least where NIR is concerned. For the most part, the findings of this accuracy assessment method match the findings of the matrix data, though the utility of NIR using TM is more inconsistent between years. However, considering that the 2008 TM performance would likely be better with more suitably dated imagery, nothing can be deduced from this analysis that suggests NIR is unfit for burned area mapping in tallgrass prairie, other than the fact that smaller burned areas might be missed. Most likely, the extremely short duration over which these areas can be detected speaks to the rapid degradation in the effectiveness of NIR—it appears that the usefulness of NIR extends only for about two weeks after an area is burned.

Table 6.26: Consecutive days (at least) where Scenario #1 (NIR) detected at least 80% of the burned area with the minimum distance technique. In this section the "max" column indicates the length of time from burning to the date when < 80% of a burned area was detected. Question marks indicate that > 80% was detected through the end of the sampling period, while an asterisk indicates that one date with a value close to 80% interrupted an otherwise long period where > 80% of the burned area was detected.

2008	Date Burned	Size (ha)	TM	TM (max)	MODIS	MODIS (max)
Burn #1	4/2	89	1	32	12	13
Burn #2	4/2	88	1	25	0	0
Burn #3	4/2	224	1	32	5*	11*
Burn #4	4/1	633	2	33	29	33
Burn #5	4/1	744	2	33	29	33
Burn #6	4/2	46	0	0	0	0
2010						
Burn #1	4/11	958	46	?	31	72
Burn #2	4/11	128	46	?	73	?
Burn #3	4/10	182	56	?	25*	25*
Burn #4	4/9	126	25	47	1	5
Burn #5	4/9	120	25	47	9	10
Burn #6	4/17	76	17	39	0	0
Burn #7	4/14	128	43	?	70	?
Burn #8	4/9	125	48	?	75	?
Burn #9	3/31	45	9	17	0	0
Burn #10	4/9	128	25	47	1	5
Burn #11	4/9	45	9	24	6	8
Burn #12	4/9	8	0	8	0	0
Burn #13	4/9	31	0	8	11	20

The performance of Scenario #1 (NIR) with object-based classification was excellent in both years and with both sensors. Even in 2008 with TM, where the analysis showed only one- and two-day ranges over which at least 80% of the burned areas could be detected, the real values are likely much longer than this—possibly up to one month—for the same reasons mentioned in section 6.3.1.1 (Table 6.27). Because performance was good across the board, no trend could be detected regarding burned area size. The areal accuracy assessment results from both classification types suggest that NIR is very useful for burned are mapping in tallgrass prairie regardless of classification technique, as long as it is done relatively quickly after an area is burned (within two weeks).

Table 6.27: Consecutive days (at least) where Scenario #1 (NIR) detected at least 80% of the burned area with the object-based technique.

2008	Date Burned	Size (ha)	TM	TM (max)	MODIS	MODIS (max)
Burn #1	4/2	89	1	32	5	11
Burn #2	4/2	88	26	32	5	11
Burn #3	4/2	224	1	32	32	39
Burn #4	4/1	633	2	33	33	40
Burn #5	4/1	744	2	33	33	40
Burn #6	4/2	46	0	0	0	0
2010						
Burn #1	4/11	958	46	?	31	72
Burn #2	4/11	128	46	?	25	25
Burn #3	4/10	182	56	?	10	19
Burn #4	4/9	126	25	47	9	10
Burn #5	4/9	120	25	47	11	20
Burn #6	4/17	76	17	?	1	2
Burn #7	4/14	128	43	?	70	?
Burn #8	4/9	125	48	?	75	?
Burn #9	3/31	45	18	33	0	0
Burn #10	4/9	128	48	56	1	5
Burn #11	4/9	45	9	24	26	26
Burn #12	4/9	8	9	24	0	0
Burn #13	4/9	31	0	8	11	20

6.3.2.2 Scenario #2 (red)

Scenario #2 (red), when derived from either sensor and classified using minimum distance classification, was able to detect at least 80% of each sample burn for a longer period of time than did Scenario #1 (NIR). In fact, it performed better than any other scenario in this analysis, regardless of year. Furthermore, the size of the sample burn had much less of an affect than with Scenario #1, though some smaller burns were still missed (Table 6.28). However, given the tendency of this scenario to overestimate burned areas (as identified with the error matrix data), this performance was most likely achieved at the expense of burned area overestimation, though this cannot be proven by this accuracy analysis technique.

The suspiciously high values for Scenario #2 suggest that, as was the case with the error matrix data, it is of limited utility to burned area mapping in tallgrass prairie. Its advantages, including availability on a wide variety of sensors, and 250 m MODIS spatial resolution, can be achieved by using Scenario #1 or Scenario #7, neither of which have overestimation problems, and therefore do not require extensive masking.

Table 6.28: Consecutive days (at least) where Scenario #2 (red) detected at least 80% of the burned area with the minimum distance technique.

2008	Date Burned	Size (ha)	TM	TM (max)	MODIS	MODIS (max)
Burn #1	4/2	89	49	80	49	?
Burn #2	4/2	88	49	73	5	11
Burn #3	4/2	224	49	80	49	?
Burn #4	4/1	633	50	74	49	?
Burn #5	4/1	744	50	74	49	?
Burn #6	4/2	46	49	80	0	0
2010						
Burn #1	4/11	958	46	?	31	72
Burn #2	4/11	128	46	?	73	?
Burn #3	4/10	182	24	46	32	73
Burn #4	4/9	126	25	47	33	74
Burn #5	4/9	120	25	47	33	74
Burn #6	4/17	76	17	39	3	12
Burn #7	4/14	128	19	42	28	69
Burn #8	4/9	125	25	47	33	74
Burn #9	3/31	45	66	?	0*	0*
Burn #10	4/9	128	57	?	75	?
Burn #11	4/9	45	25	47	75	?
Burn #12	4/9	8	0	8	0	0
Burn #13	4/9	31	9	47	75	?

The performance of Scenario #2 was poorer with object-based classification than with minimum distance classification, and this difference existed regardless of year or sensor (Table 6.29). Furthermore, though the three largest burned areas were still detectable for at least a week with the object-based classification, they were not detectable as long as with the minimum distance technique, so this problem does not appear to be related to burn size. Due to its persistent overestimation, the utility of the red wavelength is limited, regardless of classification technique, unless an accurate and comprehensive mask is used during classification. For this reason, its lower accuracy when used in conjunction with object-based classification is ultimately inconsequential, as Scenario #1 and Scenario #7 (red, NIR) perform nearly as well with little need for masking.

Table 6.29: Consecutive days (at least) where Scenario #2 (red) detected at least 80% of the burned area with the object-based technique.

2008	Date Burned	Size (ha)	TM	TM (max)	MODIS	MODIS (max)
Burn #1	4/2	89	33	48	14	17
Burn #2	4/2	88	26	32	1	4
Burn #3	4/2	224	33	48	14	17
Burn #4	4/1	633	50	74	50	?
Burn #5	4/1	744	50	74	19	21
Burn #6	4/2	46	49	?	1	4
2010						
Burn #1	4/11	958	23	45	9	18
Burn #2	4/11	128	46	?	73	?
Burn #3	4/10	182	24	46	0	4
Burn #4	4/9	126	25	47	6	8
Burn #5	4/9	120	25	47	21	25
Burn #6	4/17	76	17	?	3	12
Burn #7	4/14	128	43	?	16	20
Burn #8	4/9	125	25	47	1	5
Burn #9	3/31	45	34	56	0	0
Burn #10	4/9	128	48	56	1	5
Burn #11	4/9	45	25	47	1	5
Burn #12	4/9	8	0	8	0	0
Burn #13	4/9	31	48	?	1	5

6.3.2.3 Scenario #3 (LNIR)

As was the case with the error matrix assessment, Scenario #3 (LNIR) performed poorly regardless of year or classification technique (Tables 6.30, 6.31), and is not suitable for burned area mapping in tallgrass prairie.

Table 6.30: Consecutive days (at least) where Scenario #3 (LNIR) detected at least 80% of the burned area with the minimum distance technique.

2008	Date Burned	Size (ha)	MODIS	MODIS (max)
Burn #1	4/2	89	0	0
Burn #2	4/2	88	0	0
Burn #3	4/2	224	0	0
Burn #4	4/1	633	2	5
Burn #5	4/1	744	6	12
Burn #6	4/2	46	0	0
2010				
Burn #1	4/11	958	9	18
Burn #2	4/11	128	0	3
Burn #3	4/10	182	0	4
Burn #4	4/9	126	0	0
Burn #5	4/9	120	0	0
Burn #6	4/17	76	3	12
Burn #7	4/14	128	16	20
Burn #8	4/9	125	0	0
Burn #9	3/31	45	0	0
Burn #10	4/9	128	0	0
Burn #11	4/9	45	21	25
Burn #12	4/9	8	NA	NA
Burn #13	4/9	31	11	20

Table 6.31: Consecutive days (at least) where Scenario #3 (LNIR) detected at least 80% of the burned area with the object-based technique.

2008	Date Burned	Size (ha)	MODIS	MODIS (max)
Burn #1	4/2	89	1	4
Burn #2	4/2	88	0	0
Burn #3	4/2	224	0	0
Burn #4	4/1	633	2	5
Burn #5	4/1	744	0*	0*
Burn #6	4/2	46	1*	4*
2010				
Burn #1	4/11	958	9*	18
Burn #2	4/11	128	0	3
Burn #3	4/10	182	0	4
Burn #4	4/9	126	0	0
Burn #5	4/9	120	0	0
Burn #6	4/17	76	3	12
Burn #7	4/14	128	70	?
Burn #8	4/9	125	0	0
Burn #9	3/31	45	0	0
Burn #10	4/9	128	0	0
Burn #11	4/9	45	29	32
Burn #12	4/9	8	NA	NA
Burn #13	4/9	31	11	20

6.3.2.4 Scenario #4 (MIRBI)

For both TM years, Scenario #4 (MIRBI) was very good at identifying at least 80% of the sample burned areas when the minimum distance classification technique was used. In 2008, these values were less consistent than in 2010, though they were able to detect burned areas at least as well as Scenario #1 (NIR) did in this year, and usually outperformed that scenario. In 2010, the performance of Scenario #4 was similar to that of both Scenario #1 and Scenario #2 (red). When the minimum distance technique was used with the MODIS sensor, however, performance in both years was very poor compared to that of either Scenario #1 or Scenario #2, with only 7 of the 19 total burned areas having at least 80% of their area accounted for in the first image date. Furthermore, this performance was inconsistent across burned area sizes, with one of the largest burned areas, as well as some smaller areas, going undetected (Table 6.32).

The contrasting performance of Scenario #4 depending on sensor is similar to the inconsistency suggested by the error matrix accuracy analysis. This finding suggests that MIRBI alone should not be trusted for burned area mapping in tallgrass prairie. Furthermore, the inconsistency between sensors illustrates the effect that spatial resolution plays in burned area mapping accuracy, which was also demonstrated with the error matrix data. Specifically, it shows that classifications of coarser spatial resolution data are less accurate—in some cases even when burned areas are large and should be less vulnerable to scale changes. This adds further credibility to the idea that 500 m spatial resolution is too coarse for burned area mapping in tallgrass prairie.

Table 6.32: Consecutive days (at least) where Scenario #4 (MIRBI) detected at least 80% of the burned area with the minimum distance technique.

2008	Date Burned	Size (ha)	TM	TM (max)	MODIS	MODIS (max)
Burn #1	4/2	89	1	32	0	0
Burn #2	4/2	88	1	25	18	20
Burn #3	4/2	224	113	?	0	0
Burn #4	4/1	633	2	33	28	28
Burn #5	4/1	744	34	49	0	1
Burn #6	4/2	46	0	0	0	0
2010						
Burn #1	4/11	958	46	?	9*	18*
Burn #2	4/11	128	46	?	0	3
Burn #3	4/10	182	56	?	0*	4*
Burn #4	4/9	126	25	47	0	0
Burn #5	4/9	120	25	47	0	0
Burn #6	4/17	76	17	39	1	2
Burn #7	4/14	128	43	?	70	?
Burn #8	4/9	125	48	?	0	0
Burn #9	3/31	45	0	8	0	0
Burn #10	4/9	128	57	?	0	0
Burn #11	4/9	45	57	?	6	8
Burn #12	4/9	8	57	?	NA	NA
Burn #13	4/9	31	9	47	6	8

Similar to when classified with the minimum distance technique, Scenario #4 (MIRBI) performed better with TM than with MODIS (Table 6.33). Consequently, this scenario is not useful for burned area mapping in tallgrass prairie with either classification technique, as other scenarios perform much better, and do so without the drawback of poor MODIS resolution.

Table 6.33: Consecutive days (at least) where Scenario #4 (MIRBI) detected at least 80% of the burned area with the object-based technique.

2008	Date Burned	Size (ha)	TM	TM (max)	MODIS	MODIS (max)
Burn #1	4/2	89	1	32	0	0
Burn #2	4/2	88	1*	25*	1	4
Burn #3	4/2	224	49	?	0	0
Burn #4	4/1	633	2	33	20	21
Burn #5	4/1	744	34	48	0	0
Burn #6	4/2	46	0	0	0	0
2010						
Burn #1	4/11	958	46	?	9	18
Burn #2	4/11	128	46	?	0	3
Burn #3	4/10	182	56	?	0	4
Burn #4	4/9	126	25	47	0	0
Burn #5	4/9	120	25	47	0	0
Burn #6	4/17	76	17	?	1	2
Burn #7	4/14	128	43	?	24	27
Burn #8	4/9	125	48	?	0	0
Burn #9	3/31	45	57	65	0	0
Burn #10	4/9	128	57	?	0	0
Burn #11	4/9	45	57	?	6	8
Burn #12	4/9	8	57	?	NA	NA
Burn #13	4/9	31	48	?	6	8

6.3.2.5 Scenario #5 (MIRBI, LNIR, red, NIR)

For similar reasons as Scenario #3, Scenario #5 is not useful for burned area mapping in tallgrass prairie (Tables 6.34, 6.35).

Table 6.34: Consecutive days (at least) where Scenario #5 (MIRBI, LNIR, red, NIR) detected at least 80% of the burned area with the minimum distance technique.

2008	Date Burned	Size (ha)	MODIS	MODIS (max)
Burn #1	4/2	89	1	4
Burn #2	4/2	88	0	0
Burn #3	4/2	224	0	0
Burn #4	4/1	633	15*	18*
Burn #5	4/1	744	47	49
Burn #6	4/2	46	0	0
2010				
Burn #1	4/11	958	9*	18*
Burn #2	4/11	128	0	3
Burn #3	4/10	182	0*	4*
Burn #4	4/9	126	0	0
Burn #5	4/9	120	0	0
Burn #6	4/17	76	3	12
Burn #7	4/14	128	16	20
Burn #8	4/9	125	0	0
Burn #9	3/31	45	0	0
Burn #10	4/9	128	0	0
Burn #11	4/9	45	21	25
Burn #12	4/9	8	NA	NA
Burn #13	4/9	31	11	20

Table 6.35: Consecutive days (at least) where Scenario #5 (MIRBI, LNIR, red, NIR) detected at least 80% of the burned area with the object-based technique.

2008	Date Burned	Size (ha)	MODIS	MODIS (max)
Burn #1	4/2	89	1	4
Burn #2	4/2	88	1	4
Burn #3	4/2	224	0	0
Burn #4	4/1	633	41	46
Burn #5	4/1	744	41	46
Burn #6	4/2	46	1	4
2010				
Burn #1	4/11	958	9	18
Burn #2	4/11	128	0	3
Burn #3	4/10	182	5*	7*
Burn #4	4/9	126	0	0
Burn #5	4/9	120	0	0
Burn #6	4/17	76	3	12
Burn #7	4/14	128	70	?
Burn #8	4/9	125	0	0
Burn #9	3/31	45	0	0
Burn #10	4/9	128	1*	5*
Burn #11	4/9	45	33	74
Burn #12	4/9	8	NA	NA
Burn #13	4/9	31	11	20

6.3.2.6 Scenario #6 (MIRBI, red, NIR)

In both years with TM, the performance of Scenario #6 (MIRBI, red, NIR) with minimum distance was the same as that of Scenario #4 (MIRBI), which was relatively good. With the MODIS sensor, however, performance was better than with Scenario #4. Also, unlike with Scenario #4, the three sample burned areas larger than 500 ha were all classified accurately for several weeks (Table 6.36). Performance with object-based classification was similar (Table 6.37).

As was the case with most scenarios (particularly when 500 m MODIS bands are used), TM outperformed MODIS in both years. Along with the findings from the error matrix analysis, this accuracy assessment suggests that Scenario #6 is more suitable for mapping burned areas than MIRBI alone, and could prove useful when used with the TM sensor, or with MODIS if only larger burned areas are sought, though this renders this scenario effectively useless in the tallgrass prairie of the Flint Hills, regardless of which classification technique is employed.

Table 6.36: Consecutive days (at least) where Scenario #6 (MIRBI, red, NIR) detected at least 80% of the burned area with the minimum distance technique.

2008	Date Burned	Size (ha)	TM	TM (max)	MODIS	MODIS (max)
Burn #1	4/2	89	1	32	1	4
Burn #2	4/2	88	1	25	0	0
Burn #3	4/2	224	113	?	0	0
Burn #4	4/1	633	2	33	29	33
Burn #5	4/1	744	34	49	34	40
Burn #6	4/2	46	0	0	0	0
2010						
Burn #1	4/11	958	46	?	24	24
Burn #2	4/11	128	46	?	0	3
Burn #3	4/10	182	56	?	74	?
Burn #4	4/9	126	25	47	1	5
Burn #5	4/9	120	25	47	0	0
Burn #6	4/17	76	17	39	3	12
Burn #7	4/14	128	43	?	70	?
Burn #8	4/9	125	48	?	0	0
Burn #9	3/31	45	0	8	0	0
Burn #10	4/9	128	57	?	0	0
Burn #11	4/9	45	57	?	29	32
Burn #12	4/9	8	57	?	NA	NA
Burn #13	4/9	31	9	47	27	27

Table 6.37: Consecutive days (at least) where Scenario #6 (MIRBI, red, NIR) detected at least 80% of the burned area with the object-based technique.

2008	Date Burned	Size (ha)	TM	TM (max)	MODIS	MODIS (max)
Burn #1	4/2	89	1	32	1	4
Burn #2	4/2	88	74	?	1	4
Burn #3	4/2	224	49	?	0	0
Burn #4	4/1	633	33	49	50	?
Burn #5	4/1	744	33	49	50	?
Burn #6	4/2	46	0	0	1	4
2010						
Burn #1	4/11	958	46	?	7	8
Burn #2	4/11	128	46	?	0	3
Burn #3	4/10	182	56	?	5*	7*
Burn #4	4/9	126	25	47	0	0
Burn #5	4/9	120	25	47	0	0
Burn #6	4/17	76	17	?	3	12
Burn #7	4/14	128	43	?	70	?
Burn #8	4/9	125	48	?	0	0
Burn #9	3/31	45	66	?	0	0
Burn #10	4/9	128	57	?	1	5
Burn #11	4/9	45	8*	24	27	27
Burn #12	4/9	8	25	47	NA	NA
Burn #13	4/9	31	48	?	26	26

6.3.2.7 Scenario #7 (red, NIR)

The performance of Scenario #7 (red, NIR) with minimum distance was similar to that of Scenario #1 (NIR) in both years when TM was used, and was better than Scenario #1 in both years when MODIS was used. Furthermore, this performance was consistent regardless of burn size (Table 6.38). The utility of Scenario #7 for burned area mapping in tallgrass prairie is high, as it can identify a large percentage of each burned area like Scenario #2 (red), but without the overestimation problems associated with that scenario. As was the case with the error matrix analysis, this analysis suggests that Scenario #7 is among the best in this study for burned area mapping in tallgrass prairie. Furthermore, the fact that it can be calculated from many sensors, and from MODIS at 250 m spatial resolution, are added advantages.

Table 6.38: Consecutive days (at least) where Scenario #7 (red, NIR) detected at least 80% of the burned area with the minimum distance technique.

2008	Date Burned	Size (ha)	TM	TM (max)	MODIS	MODIS (max)
Burn #1	4/2	89	1	32	12	13
Burn #2	4/2	88	1	25	1	4
Burn #3	4/2	224	1	32	33	39
Burn #4	4/1	633	2	33	47	49
Burn #5	4/1	744	2	33	47	49
Burn #6	4/2	46	0	0	0	0
2010						
Burn #1	4/11	958	46	?	31	72
Burn #2	4/11	128	46	?	73	?
Burn #3	4/10	182	56	?	74	?
Burn #4	4/9	126	25	47	9	10
Burn #5	4/9	120	25	47	9	10
Burn #6	4/17	76	17	39	0	0
Burn #7	4/14	128	43	?	70	?
Burn #8	4/9	125	47	?	75	?
Burn #9	3/31	45	9	17	0	0
Burn #10	4/9	128	25	47	11	20
Burn #11	4/9	45	9	24	6	8
Burn #12	4/9	8	0	8	1	5
Burn #13	4/9	31	0	8	21	25

As was the case with minimum distance, Scenario #7 (red, NIR) performed well with object-based classification regardless of sensor, year, burn size, or accuracy assessment technique (Table 6.39). However, a very important trend is present in this data. Specifically, the MODIS data performed best when subjected to a minimum distance classification, while the TM sensor performed best when subjected to an object-based classification. This further illustrates the trend that has been shown throughout this chapter—that the reliability of object-based classification becomes poorer as the spatial resolution becomes coarser. This has major implications for burned area mapping in tallgrass prairie, as the analysis contained in this chapter suggest that only MODIS can provide an imagery record that is temporally dense enough to account for all burned areas. Under these circumstances, it appears that the use of object-based techniques is unnecessary at best, and likely hurts classification accuracy.

Table 6.39: Consecutive days (at least) where Scenario #7 (red, NIR) detected at least 80% of the burned area with the object-based technique.

2008	Date Burned	Size (ha)	TM	TM (max)	MODIS	MODIS (max)
Burn #1	4/2	89	1	32	5	11
Burn #2	4/2	88	26	32	1	4
Burn #3	4/2	224	49	?	14	17
Burn #4	4/1	633	50	74	1*	1*
Burn #5	4/1	744	50	74	47	49
Burn #6	4/2	46	1	32	0	0
2010						
Burn #1	4/11	958	46	?	31	72
Burn #2	4/11	128	46	?	73	?
Burn #3	4/10	182	56	?	74	?
Burn #4	4/9	126	25	47	33	74
Burn #5	4/9	120	25	47	0	0
Burn #6	4/17	76	17	?	1	2
Burn #7	4/14	128	43	?	28	69
Burn #8	4/9	125	48	?	32	74
Burn #9	3/31	45	18	33	18	19
Burn #10	4/9	128	48	56	0	0
Burn #11	4/9	45	48	56	27	27
Burn #12	4/9	8	9	24	NA	NA
Burn #13	4/9	31	9	47	21	25

6.3.2.8 Scenario #8 (TM 1-5, 7) and Scenario #9 (MODIS 1-7)

The performance of Scenario #8 (TM 1-5, 7) with minimum distance classification was better in 2008 than in 2010, though this could be due to the lack of temporal resolution in 2008 as noted earlier. Scenario #9 (MODIS 1-7), however, did not perform well in either year, mainly because it missed many burned areas. Although the performance of the TM scenario was not affected by burn size, the MODIS scenario was, as the largest three burned areas were identified more accurately than many smaller burned areas (Table 6.40).

This analysis, like the error matrix analysis, showed that other scenarios such as Scenario #1 (NIR) and Scenario #7 (red, NIR) easily outperform Scenarios #8 and #9. Therefore, it is unlikely that scenarios made up of all bands in a given sensor have much utility for burned area mapping in tallgrass prairie.

Table 6.40: Consecutive days (at least) where Scenario #8 (TM 1-5, 7) and Scenario #9 (MODIS 1-7) detected at least 80% of the burned area with the minimum distance technique.

2008	Date Burned	Size (ha)	TM	TM (max)	MODIS	MODIS (max)
Burn #1	4/2	89	1	32	1	4
Burn #2	4/2	88	26	32	0	0
Burn #3	4/2	224	1	32	0	0
Burn #4	4/1	633	2	33	29	33
Burn #5	4/1	744	2	33	47	49
Burn #6	4/2	46	1	32	0	0
2010						
Burn #1	4/11	958	46	?	9	24
Burn #2	4/11	128	46	?	0	3
Burn #3	4/10	182	47	55	0	4
Burn #4	4/9	126	25	47	11	20
Burn #5	4/9	120	25	47	0	0
Burn #6	4/17	76	17	39	3	12
Burn #7	4/14	128	43	?	16	20
Burn #8	4/9	125	47	?	0	0
Burn #9	3/31	45	9	17	0	0
Burn #10	4/9	128	57	?	0	0
Burn #11	4/9	45	25	47	21	25
Burn #12	4/9	8	25	47	NA	NA
Burn #13	4/9	31	9	47	21	25

Using object-based classification, the performances of Scenario #8 (TM 1-5, 7) and Scenario #9 (MODIS 1-7) were similar to Scenario #7 (red, NIR) in that TM was more accurate. This is particularly true in 2008 (Table 6.41). However, like its performance with minimum distance classification, MODIS performed more poorly than TM regardless of year, and this performance was affected by burn size. Unlike its assessment with the error matrix data suggested, however, Scenario #9 (MODIS 1-7) showed no promise for burned area mapping in tallgrass prairie with either classification technique, and regardless of whether or not a mask is used.

Table 6.41: Consecutive days (at least) where Scenario #8 (TM 1-5, 7) and Scenario #9 (MODIS 1-7) detected at least 80% of the burned area with the object-based technique.

2008	Date Burned	Size (ha)	TM	TM (max)	MODIS	MODIS (max)
Burn #1	4/2	89	1	32	1	4
Burn #2	4/2	88	49	73	1	4
Burn #3	4/2	224	49	?	0	0
Burn #4	4/1	633	75	?	2	5
Burn #5	4/1	744	50	74	22	27
Burn #6	4/2	46	1	32	5	11
2010						
Burn #1	4/11	958	46	?	9	18
Burn #2	4/11	128	46	?	0	3
Burn #3	4/10	182	56	?	0*	4*
Burn #4	4/9	126	25	47	1	5
Burn #5	4/9	120	25	47	0	0
Burn #6	4/17	76	17	?	3	12
Burn #7	4/14	128	43	?	70	?
Burn #8	4/9	125	48	?	0	0
Burn #9	3/31	45	18	33	0	0
Burn #10	4/9	128	48	56	1	5
Burn #11	4/9	45	57	?	75	?
Burn #12	4/9	8	57	?	NA	NA
Burn #13	4/9	31	48	?	75	?

6.3.2.9 Summary of Scenarios' Utility Based on Areal Extents

As was the case with the error matrices, the areal extent accuracy assessment showed that some scenarios would not be useful for mapping burned areas in tallgrass prairie. These included Scenario #3 (LNIR), Scenario #4 (MIRBI), Scenario #5 (MIRBI, LNIR, red, and NIR), and Scenario #9 (MODIS 1-7). All of these scenarios not only performed poorly, but also possessed other traits that limited their usefulness. For example, all four scenarios mentioned above are available at a maximum resolution of 500 m when calculated from the MODIS sensor. Additionally, the two scenarios that contain LNIR are not even available on the TM sensor, and have striping problems with the MODIS instrument aboard the Terra satellite. It is likely that these additional problems were largely responsible for the poor performance of all but Scenario #4.

Similar to what was revealed with the error matrix data, three of the remaining scenarios appear to be useful only under certain circumstances. Scenario #6 (MIRBI, red, NIR) and Scenario #8 (TM 1-5, 7) are only useful when taken from the TM sensor. However, they are

effectively rendered useless by the fact that the temporal density of the TM sensor is not great enough to map all burned areas during a typical burn season. Furthermore, these sensors have other problems, such as the 500 m maximum MODIS spatial resolution in the case of Scenario #6, the limitation of Scenario #8 to the TM sensor, and the need to mask non-grassland cover types when using either sensor. Although it appears to perform well on first examination, the overestimation problems associated with Scenario #2 (red), and its subsequent need for extensive masking, limit its usefulness to certain circumstances as well.

The final two scenarios, Scenario #1 (NIR) and Scenario #7 (red, NIR), performed well regardless of year, sensor, classification technique, or accuracy assessment technique. They also do not require extensive masking like other scenarios, and are available from a wide range of sensors, and at the maximum spatial resolution of 250 m from MODIS. For this reason, these two scenarios show the most promise for burned area mapping in tallgrass prairie. Finally, it is worth noting that the two accuracy assessment techniques were consistent with each other, as shown in the similarities between Tables 6.25 and 6.42.

Table 6.42: Usefulness of each scenario for burned area mapping in tallgrass prairie based on the areal accuracy assessment technique. Column headings retain the same meaning as in Table 6.25.

Scenario (components)	TM Res. (m)	MODIS Res. (m)	Sensor	Technique	Mask
1 (NIR)	30	250	Both	Both	No
2 (red)	30	250	Both	Min. Dist.*	Yes
3 (LNIR)	NA	500	Not Useful	NA	NA
4 (MIRBI)	30	500	Not Useful	NA	NA
5 (MIRBI, LNIR, red, NIR)	NA	500	Not Useful	NA	NA
6 (MIRBI, red, NIR)	30	500	TM	Both	Yes
7 (red, NIR)	30	250	Both	Both	No
8 (TM 1-5, 7)	30	NA	TM	Both	Yes
9 (MODIS 1-7)	NA	500	Not Useful	NA	NA

* Red wavelengths performed well with object-based classification, but only when used with TM data

6.3.3 Second Error Matrix Assessment

When the minimum distance classification technique was used, all three 250 m MODIS scenarios from 2008 had *KHAT* values greater than 80% through April 27 (and through May 4 in the case of Scenarios #2 and #6). This is in contrast to the *KHAT* values from the object-based

classification, which were only greater than 80% for the first sampling date on April 2. The difference between the two classification types was not as pronounced in 2010 except in the case of Scenario #2, which had low *KHAT* values for all image dates. As was the case with the other two accuracy assessment methods, this one suggests that object-based classification is not necessary, and possibly less accurate than pixel-based methods, for burned area mapping in tallgrass prairie.

It is worth noting here that the actual *KHAT* values for the first image date in each year (April 2, 2008 and April 8, 2010) would almost certainly be higher than indicated if only relatively recent burned areas were used as ground truth. However, the random sample created some ground-truth points that fell in areas that had been burned for as long as one month prior to the earliest image date. Because these older burned areas made up a disproportionately high percentage of the relatively few burned ground-truth areas in the early images, and because these older burned areas are much harder to identify as burned, it can be safely assumed that more recent burned areas would be detected at a much higher rate than indicated by *KHAT* values in the mid to low 80% range. The evidence for this is relatively low producer's accuracy values for these dates. In fact, a visual examination of these false negative ground-truth points for Scenario #7 in 2008 reveals that two of the four are located in areas that were clearly burned on, or prior to, March 1, according to another TM image. Removing these two points raises *KHAT* values in 2008 from 84% to 90%, to say nothing of the other two points, for which a burn estimate date cannot be assumed due to insufficient TM imagery. In 2010, this adjustment would raise the *KHAT* value from 81% to 89% based on three similar ground truth points (of a total of six false negatives) that were present within burned areas that already appeared to be a few weeks old on a March 23, 2010 image. Although these new, higher *KHAT* values represent a deviation from those indicated by the purely random sample, they are more likely representative of true burn mapping accuracy, as it is unlikely that month-long gaps between subsequent clear images exist with twice-daily MODIS imagery, meaning that older burned areas, such as those that were removed from this accuracy assessment, would have already been mapped with a previous image.

Whether old or new values area cited for the first two image dates, Scenario #7 (red, NIR) maintains higher *KHAT* values than the other two scenarios throughout the time period of burn recovery (or at least until *KHAT* values for all scenarios drop too far to be useful for burned

area mapping). These results suggest that using MODIS bands 1 (red) and 2 (NIR) in combination provides the most accurate results, though performance drops dramatically after several weeks. In fact (assuming the adjustments to two initial imagery dates in each year are correct), approximately 90% accuracy can be expected when classifying burned areas up to two weeks old (Table 6.43), with most of the inaccuracy due to underestimation of burned areas. This lends further support to the findings of the two previous accuracy assessment techniques: that a combination of red and NIR provides the most utility for burned area mapping in tallgrass prairie.

Table 6.43: Unmodified *KHAT* estimates for all image dates for all three 250 m scenarios.

2008 Minimum Distance			
Date	**Scenario #1 (NIR)**	**Scenario #2 (red)**	**Scenario #7 (red, NIR)**
4/2	84	88	84
4/27	80	84	90
5/4	79	83	89
5/20	11	53	23

2008 Object-Based			
Date	**Scenario #1 (NIR)**	**Scenario #2 (red)**	**Scenario #7 (red, NIR)**
4/2	88	81	84
4/27	42	54	76
5/4	60	22	52
5/20	18	25	45

2010 Minimum Distance			
Date	**Scenario #1 (NIR)**	**Scenario #2 (red)**	**Scenario #7 (red, NIR)**
4/8	81	82	81
4/17	83	86	91
5/3	60	46	72

2010 Object-Based			
Date	**Scenario #1 (NIR)**	**Scenario #2 (red)**	**Scenario #7 (red, NIR)**
4/8	82	57	84
4/17	84	57	93
5/3	48	30	73

6.4 Conclusions

The results of this chapter revealed many things about the utility of various sensors, scenarios, and classification techniques for mapping burned areas in tallgrass prairie. First, they revealed that poorer spatial resolution results in a loss of classification accuracy, as TM consistently outperformed MODIS with most scenarios. Furthermore, those MODIS scenarios

that were calculated at 250 m spatial resolution performed much better than those calculated at 500 m spatial resolution. This supports that hypothesis proposed at the beginning of this chapter, that TM will allow for more accurate burned area mapping in tallgrass prairie than MODIS due to its superior spatial resolution. In fact, these findings take this a step further and suggest that 500 m spatial resolution MODIS data is too coarse for burned area mapping in tallgrass prairie.

The main problem with coarser spatial resolution was underestimation of burned areas. This was illustrated by the error matrix analysis, which showed that shrinking *KHAT* values later in the sampling period occurred when underestimation of burned areas increased. Most likely, this is due to the regrowth of vegetation on both burned and unburned areas, which makes these two areas appear more similar and prevents mixed edge pixels from being classified as burned. The other problem with coarse resolution was that it missed smaller burned areas, most likely due to edge effects, which are well documented when they lead to overestimation of burned areas (Al Rawi *et al*. 2001, Loboda *et al*. 2007) and so are somewhat surprising here only because underestimation of burned areas was the problem, rather than overestimation. However, it is likely that a conservative classification of burned areas such as this one could cause these edge effects to trend toward underestimation instead of overestimation—particularly when amplified by the heterogeneity of many burned areas (Loboda *et al*. 2007). In this case, within-burn heterogeneity is caused by unburned or lightly burned inclusions, as well as rocky soil surface inclusions in burned areas.

The lesson to be taken from these two characteristics is obvious—that burned area mapping in tallgrass prairie should not use 500 m MODIS data, and should use the more accurate TM data. However, even if burned areas were detectable for months at a time, as was the case with some scenarios, this only allows for a few TM passes. Combined with the high likelihood of cloud cover (particularly during the spring burn season), this means that TM cannot be relied upon to produce enough useable images during the burn season, which not only has the obvious effect of many burned areas going undetected, but also prevents any precise identification of when an area was burned. Consequently, this need for higher temporal resolution dictates that a 250 m MODIS scenario must be used. This supports another hypothesis stated at the beginning of this chapter—that due to cloud cover, MODIS must be used in order to achieve a sample that is temporally dense enough for burned area mapping in tallgrass prairie.

Aside from dictating which sensor and resolution would perform best for mapping burned areas in tallgrass prairie, the analysis in this chapter also showed that minimum distance classification is better than object-based classification, and this was especially true with coarser resolution imagery. Consequently, since 250 m resolution MODIS imagery must be used in order to get a sample of sufficient temporal density, minimum distance classification should be used rather than object-based classification. This does not support the hypothesis given at the beginning of this chapter—that object-based classification techniques will map burned tallgrass prairie more accurately than pixel-based techniques.

The final major piece of information provided by this chapter is which scenario would perform best for classifying burned areas in tallgrass prairie. Because the scenario must be available from MODIS at 250 m spatial resolution, only Scenarios #1 (NIR), #2 (red), and #7 (red, NIR) were viable options, which supports the hypothesis that bands and/or indices composed of red and NIR wavelengths will be required for optimal burned area mapping in tallgrass prairie because they represent the best compromise in spatial and temporal resolution. Scenario #2, however, has the overestimation problems mentioned in previous sections, which requires extensive and accurate masking of cover types other than grasslands. Of the remaining two, Scenario #1 is not able to detect burned areas for as long as Scenario #7. Therefore, burned area mapping in tallgrass prairie should use both the red and NIR bands taken from the MODIS sensor (possibly with additional dates taken from the TM sensor where possible), and should employ a minimum distance classification technique, or at lease a pixel-based classification technique. This combination gives the best balance of temporal resolution, spatial resolution, and classification accuracy for burned area mapping in tallgrass prairie, and it can achieve approximately 90% accuracy if burned areas are two weeks old or less.

CHAPTER 7 - Flint Hills Burn History (2000-2010)

7.1 Introduction

The fourth objective of this paper was to reconstruct the spatio-temporal fire history of the Flint Hills as far into the past as suitable imagery was available. This objective was accomplished by applying the method suggested by the analysis in chapter 6, including using the 250 m spatial resolution red and NIR MODIS bands, using minimum distance classification, and masking non-grassland land cover types. Analysis was performed back to and including the year 2000 (the first from which MODIS imagery was available). Using these methods resulted in maps with accuracies that consistently reach 90%. Furthermore, these values were greater than 90% in most cases, and increased as the time between successive clear images decreased. Accuracy was less when larger gaps between successive images existed, and likely fell below 90% after 2-3 weeks, and fell rapidly thereafter as well. Most inaccuracy resulted from underestimation of burned areas.

7.2 Methods

7.2.1 Image Acquisition and Processing

The first step in accomplishing this chapter's objective was downloading the necessary MODIS imagery. For each of the 11 years (2000 to 2010), all 250 m red and NIR Terra (MOD09GQ) and Aqua (MYD09GQ) images between March 1 and May 10 (though an image from February 28, 2002 was also used) were downloaded and processed using the same procedure described in section 5.2.2 of Chapter 5. Unlike in Chapter 5, all images were subset to the 18-county study area shown in Figure 3.1. Images in which cloud cover obscured the entire study area were not used. It should be noted that in 2000, 2001, and 2002, only scenes from Terra were available, as the Aqua satellite was not launched until May 4, 2002. When a clear image from both sensors was available on the same date, the one in which the study area was closest to nadir was kept. On the rare occasions that both satellites produced an image with approximately the same resolution, the Aqua image was chosen because it is taken later in the day, and therefore captures more burned areas from that day. In the case of three dates, all in 2005, burned areas that were obscured by clouds in one image (from either Aqua or Terra) were

visible in the other image. Consequently, both images were used in these three cases. Table 7.1 shows the date and satellite of origin for all scenes used in this burned area reconstruction.

Table 7.1: List of MODIS scenes classified in this reconstruction. Letters beside each scene denote whether it was from Aqua (A) or Terra (T), or both (B). All scenes from 2000-2002 are from Terra.

2000	2001	2002	2003		2004		2005		2006		2007		2008		2009		2010	
3/5	3/8	2/28	3/2	A	3/7	T	3/1	T	3/2	T	3/3	A	3/1	A	3/1	T	3/2	A
3/25	3/13	3/9	3/6	A	3/9	T	3/4	A	3/3	A	3/4	T	3/4	T	3/8	A	3/3	T
3/28	3/20	3/29	3/9	T	3/11	A	3/5	T	3/16	A	3/8	A	3/8	A	3/16	T	3/4	A
3/30	3/22	4/1	3/13	A	3/12	A	3/11	A	3/24	T	3/9	T	3/10	A	3/17	A	3/18	A
4/2	3/31	4/3	3/15	A	3/14	T	3/12	T	3/27	T	3/16	T	3/11	T	3/19	A	3/25	A
4/4	4/7	4/5	3/23	T	3/18	T	3/13	A	3/28	A	3/17	A	3/15	A	3/21	T	3/26	T
4/7	4/9	4/9	3/24	A	3/21	T	3/19	T	3/31	T	3/18	T	3/19	A	3/24	A	3/29	T
4/8	4/11	4/10	3/26	A	3/23	T	3/20	T	4/2	A	4/1	T	3/20	T	3/30	T	3/31	T
4/10	4/12	4/17	3/29	A	3/28	A	3/27	A	4/9	A	4/2	A	3/21	A	3/31	A	4/1	A
4/11	4/13	4/22	3/30	T	3/31	A	4/1	A	4/10	A	4/3	T	3/23	T	4/3	A	4/2	T
4/14	4/18	4/23	3/31	A	4/1	T	4/2	T	4/12	T	4/4	A	3/25	A	4/4	T	4/3	A
4/17	4/21	4/24	4/1	T	4/2	A	4/4	T	4/13	A	4/7	A	3/27	T	4/7	A	4/4	T
4/18	4/25	4/25	4/2	A	4/4	A	4/7	B	4/16	T	4/8	T	4/1	A	4/8	T	4/5	A
4/19	4/27	4/28	4/7	A	4/8	T	4/14	A	4/17	A	4/15	T	4/2	A	4/10	A	4/6	A
4/22	5/9	5/5	4/9	T	4/11	A	4/16	A	4/18	T	4/16	A	4/4	A	4/11	T	4/9	T
5/10		5/9	4/10	A	4/16	A	4/17	B	4/19	T	4/19	T	4/5	T	4/14	A	4/10	A
			4/11	T	4/17	T	4/23	A	4/21	T	4/20	A	4/6	A	4/20	T	4/14	A
			4/12	A	4/19	T	4/24	T	4/22	A	4/21	A	4/13	A	4/21	A	4/17	A
			4/14	A	4/27	A	4/27	T	4/23	T	4/28	T	4/14	T	4/22	T	4/19	A
			4/18	A			5/1	T	4/27	A	4/29	A	4/15	A	4/23	A	4/23	A
			4/21	A			5/2	B					4/19	T	4/24	T	4/27	T
			4/22	T			5/4	T					4/22	A	4/28	A	4/29	T
			4/26	T									4/25	A	5/8	T		
			5/5	A									4/28	T				
													4/29	A				
													5/3	T				

7.2.2 Masking

Prior to classification, a mask was built in manner similar to that described in section 6.2.1.3. Pixels with red reflectance values less than 0.11 were excluded from a March 1, 2008 image. This mask eliminated some actively growing crops and water bodies, but its primary purpose was to mask evergreen vegetation. NIR reflectance values less than 0.16 were then masked in a March 5, 2000 image. This allowed masking of water areas and darker areas of fallow cropland. Next, pixels with NIR reflectance values greater than 0.25 and red reflectance

values less than 0.09 were masked from a March 28, 2000 image. This allowed active crops and cool-season grasses to be masked without excluding native, warm-season grasses (which were not actively growing at the time). Water areas were further masked from a later, June 14, 2008 image that showed no recently burned areas, thereby allowing all NIR pixels with reflectance values less than 0.235 to be masked (in earlier images, burned areas could fall below this threshold, thereby incidentally allowing grasslands to be masked). Additionally, this late June image allowed masking of fallow cropland. During this time, fallow croplands and harvested winter wheat fields have spectral properties similar to non-vegetated areas, while grasslands are actively growing, thereby allowing differentiation. These principles were also applied to a July 14, 2008 image to further mask fallow cropland and water, as well as to mask additional areas of active cropland. Finally, a mask was generated that excluded all areas outside of the 18-county study area described in Chapter 3. All masks were meticulously checked to ensure that grassland areas were not masked, or, if they were, that this was kept to an absolute minimum. In rare cases where burned grasslands were masked, they were manually removed from the mask. Finally, all masks were combined in order to create a single mask that eliminated all of the areas mentioned above, and this mask was used in the classification.

Table 7.2: Image dates used to mask non-grassland areas and the rationale for using each.

Masking Element	Feature Masked
Study area shapefile	everything but the study area
3/1/2008 (Aqua)	
Red < 0.11	active crop, water, evergreen trees
3/5/2000 (Terra)	
NIR < 0.16	fallow crop, water
3/28/2000 (Terra)	
NIR > 0.25, Red < 0.09	active crop
6/14/2008 (Aqua)	
NIR < 0.235	water
NIR < 0.4, Red > 0.1	fallow crop
7/14/2008 (Aqua)	
Red > 0.1	fallow crop
NIR < 0.28	water
NIR > 0.48, Red < 0.045	active crop

7.2.3 Classification

A supervised, minimum distance classification was performed on each bi-spectral (red and NIR) scene in each year. Burned area training data were selected only from the most recent

burned areas in each image so that burned area estimates would be conservative. This minimized false positives, since unburned areas and older burned areas sometimes share spectral similarities, and assured that accuracies would be 90% or greater. The application of this technique relied on the assumption that older burned areas did not need to be classified in the current image, as they would already have been accounted for by the previous image. Burned areas that were identified in consecutive images were given credit for being burned only in the earliest image.

In many cases, clouds covered a portion of the image, though burned areas could still be seen in cloudless areas of the image. In these cases, all burned areas that were located in areas with cloud cover were deleted. This prevented cloud shadows from accidentally being classified as burned areas. The drawback to this, however, is that those burned areas located next to, or mixed in with, cloud shadows must be detected in the next scene, which makes assigning a precise burn date to these burned areas even more difficult. That is, just because a burned area is first identified in an image does not necessarily mean that it did not exist by the previous image date, only that it could not be detected yet. Nonetheless, the main purpose of this exercise was to map total burned areas in a given year. Identifying when an area was burned was a secondary priority. Deleting cloudy areas also meant that some sections of the study area might escape the mapping procedure for longer than the 2-3 week threshold of reliable burned area detection, even though this would not always be immediately apparent by looking only at the dates of imagery used. This is because the fact that each date was used does not necessarily mean all sections of the study area were free of clouds on that date.

7.3 Results and Discussion

7.3.1 Study Area Results

7.3.1.1 Total Area Burned

Total annual area burned varied from as few as 414,456 ha in 2007 to as many as 1,320,556 ha in 2005 (Table 7.3). Interestingly, high or low values were not clustered in any particular part of the range of years, but were distributed relatively evenly throughout. This shows that burning in the Flint Hills is neither decreasing nor increasing through time, though it is highly variable from year to year.

In addition to this year-to-year variability in total area burned, year-to-year spatial variability is present in the data as well. In 2006 and 2007, for example, more burning took place in the northern half of the study area than in the southern half. This stands in contrast to many other years, where burning was more evenly distributed north and south throughout the study area. It is worth noting here that in 2006 and 2007, cloudy imagery did not allow burned areas to be detected past April 27 and April 29, respectively. This might partially account for the low total burned area detected in these years, but likely does not account for all of it.

Table 7.3: Total burned area, percent of total study area that was burned, and percent of grassland within the study area that was burned for each of the 11 years in the study.

Year	Total (ha)	% Total	% Grassland
2000	1,064,994	25	70
2001	760,769	18	50
2002	543,119	13	36
2003	1,077,588	26	71
2004	696,594	17	46
2005	1,320,556	31	87
2006	755,813	18	50
2007	414,456	10	27
2008	1,074,944	26	70
2009	1,212,281	29	79
2010	905,738	22	59

7.3.1.2 Percentage of Total Area and of Grassland Area Burned

When total burned area is normalized by the size of the study area, annual percentages of the study area that were burned range from 10% to 31% (2007 and 2005, respectively). When total burned area is divided by the total amount of grassland in the study area, the percentages burned range from a low of 27% in 2007 to a high of 87% in 2005 (Table 7.3, Figure 7.1). This serves to further illustrate the high year-to-year variability in area burned. It should be noted that deducing the percentage of grassland burned by dividing total hectares burned by total grassland might provide inflated estimates of total grassland burned, as cover types other than grassland are burned within the study area. However, no effective means by which to exclude all non-grassland burned areas exists, meaning that neither a reliable estimate of this problem's extent, nor a method by which to correct it, are addressed in this paper.

Figure 7.1: Percent of total grassland in the study area that was burned in each year. Note that high and low values are not clustered together in any part of the sample.

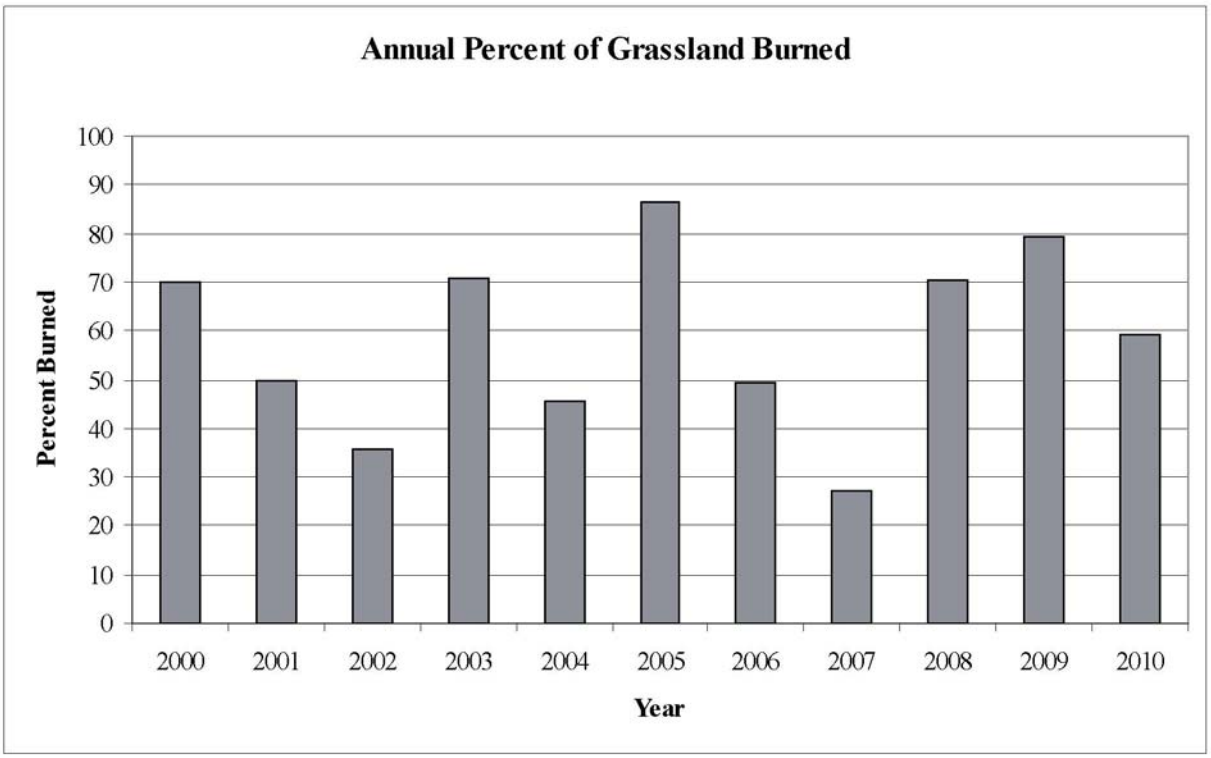

7.3.1.3 Burn Frequency

Examining the frequency with which the study area is burned reveals several interesting patterns. First, approximately 45% of the entire 18-county study area was not burned in any of the eleven years of the study. The remaining 55% is distributed according to a negative relationship with number of years burned, and ranges from 10% of the study area being burned once to only 1% of the study area being burned the maximum of eleven times (Table 7.4, Figure 7.2). Given the predominant philosophy that burning annually or at least every two years increases productivity (see Chapter 1), these findings are surprising, and indicate that much burning takes place at intervals that are much longer than this. When this frequency is applied only to grassland areas within the study area, these percentages rise, as grasslands are more likely to be burned than other cover types (especially given that other cover types were mostly masked during classification). Once again, caution should be used when interpreting the percentage of grassland burned, as these values are produced with the assumption that all burned

areas were grasslands, even though other cover types are often burned. Furthermore, this problem is likely to be worse than with the annual calculations above, since non-grassland burned areas are reflected here in total for all eleven years, rather than being spread among them.

Table 7.4: Cumulative burning statistics for all 11 years of the study. Total percent of grassland burned equals more than 100% because land cover types other than grassland were sometimes burned.

Years Burned	Total (ha)	% Total	%Grassland
0	1,905,949	45	NA
1	419,738	10	28
2	347,031	8	23
3	305,219	7	20
4	260,356	6	17
5	228,906	5	15
6	202,813	5	13
7	172,006	4	11
8	153,838	4	10
9	119,913	3	8
10	61,200	1	4
11	24,419	1	2

Figure 7.2: Cumulative burning totals throughout the study area for the study period. Value in the legend indicates the number of years out of 11 that an area was burned.

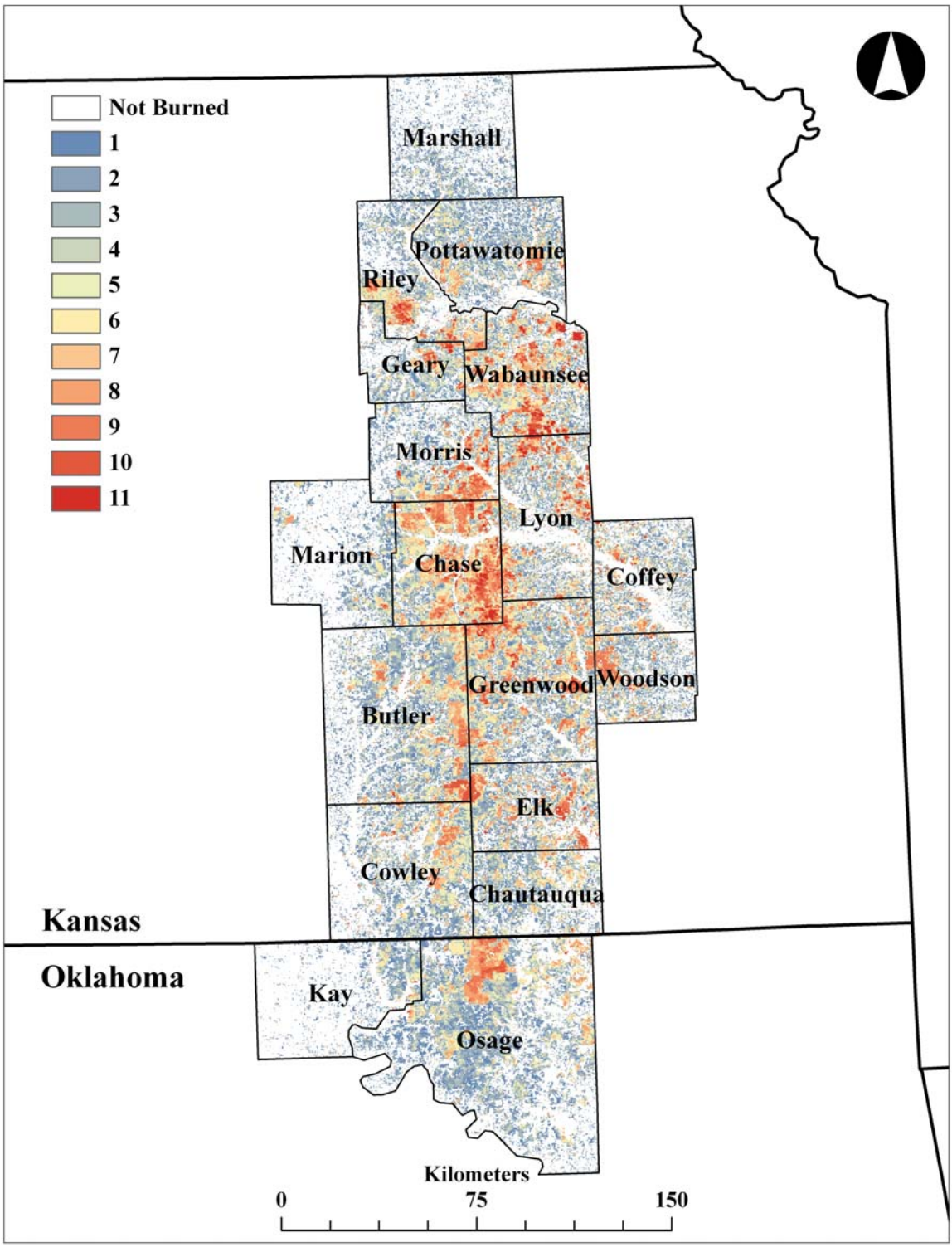

7.3.1.4 Temporal Distribution of Burned Areas

When the temporal distribution of burned areas within each year is examined, it becomes immediately apparent that most burning takes place in April (Figure 7.3). Burning increases steadily but slowly until April when it begins to increase very rapidly. Furthermore, the plateau shown at the end of April on the graph shows that burning is nearly complete before the first of May. Other years of the study showed a similar trend, with the vast majority of burns in all years detected in April (Table 7.5). 2008 was used as an example here because it had the most temporally dense sample of any year, and its images were distributed relatively evenly throughout the study period with no large data gaps.

Figure 7.3: Temporal distribution of cumulative and absolute burned areas detected in 2008.

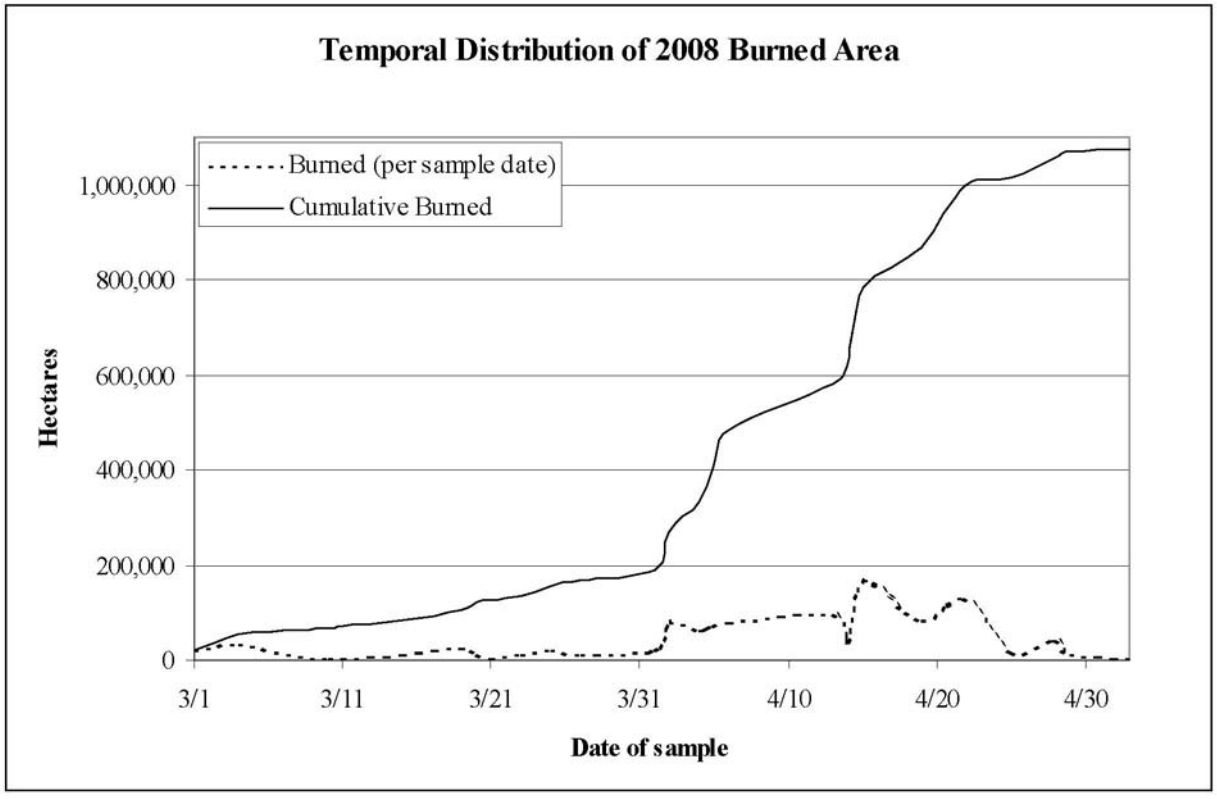

Table 7.5: Temporal distribution of all burned areas detected for each year. Date indicates the date in which the burned areas were detected. Value beside each date indicates the percentage of the total burned area for a given year that was detected on that date.

2000		2001		2002		2003		2004		2005		2006		2007		2008		2009		2010	
3/5	1	3/8	2	2/28	3	3/2	1	3/7	1	3/1	1	3/2	3	3/3	2	3/1	2	3/1	1	3/2	1
3/25	4	3/13	3	3/9	2	3/6	1	3/9	1	3/4	1	3/3	1	3/4	3	3/4	3	3/8	3	3/3	0
3/28	10	3/20	2	3/29	7	3/9	3	3/11	2	3/5	0	3/16	6	3/8	1	3/8	1	3/16	1	3/4	1
3/30	3	3/22	1	4/1	4	3/13	1	3/12	1	3/11	1	3/24	2	3/9	1	3/10	0	3/17	1	3/18	2
4/2	8	3/31	3	4/3	3	3/15	1	3/14	1	3/12	0	3/27	2	3/16	2	3/11	0	3/19	1	3/25	1
4/4	7	4/7	22	4/5	2	3/23	1	3/18	2	3/13	1	3/28	2	3/17	1	3/15	1	3/21	1	3/26	0
4/7	15	4/9	11	4/9	5	3/24	1	3/21	3	3/19	2	3/31	4	3/18	1	3/19	2	3/24	4	3/29	1
4/8	11	4/11	27	4/10	5	3/26	3	3/23	3	3/20	1	4/2	2	4/1	4	3/20	1	3/30	2	3/31	6
4/10	1	4/12	2	4/17	6	3/29	3	3/28	2	3/27	2	4/9	15	4/2	8	3/21	0	3/31	1	4/1	1
4/11	10	4/13	6	4/22	20	3/30	2	3/31	6	4/1	4	4/10	3	4/3	3	3/23	1	4/3	4	4/2	1
4/14	11	4/18	10	4/23	3	3/31	3	4/1	6	4/2	7	4/12	12	4/4	8	3/25	2	4/4	2	4/3	4
4/17	4	4/21	5	4/24	11	4/1	4	4/2	9	4/4	16	4/13	15	4/7	9	3/27	1	4/7	6	4/4	3
4/18	6	4/25	3	4/25	6	4/2	2	4/4	13	4/7	6	4/16	9	4/8	4	4/1	2	4/8	8	4/5	1
4/19	6	4/27	1	4/28	14	4/7	8	4/8	19	4/14	28	4/17	4	4/15	18	4/2	7	4/10	11	4/6	1
4/22	2	5/9	1	5/5	2	4/9	11	4/11	8	4/16	3	4/18	3	4/16	4	4/4	6	4/11	6	4/9	19
5/10	1			5/9	9	4/10	10	4/16	13	4/17	7	4/19	3	4/19	9	4/5	7	4/14	13	4/10	12
						4/11	8	4/17	2	4/23	11	4/21	4	4/20	3	4/6	7	4/20	14	4/14	15
						4/12	9	4/19	3	4/24	3	4/22	2	4/21	4	4/13	9	4/21	5	4/17	16
						4/14	7	4/27	5	4/27	1	4/23	2	4/28	13	4/14	3	4/22	4	4/19	8
						4/18	7			5/1	1	4/27	5	4/29	1	4/15	16	4/23	5	4/23	4
						4/21	5			5/2	2					4/19	8	4/24	1	4/27	2
						4/22	2			5/4	1					4/22	12	4/28	1	4/29	1
						4/26	6									4/25	1	5/8	5		
						5/5	1									4/28	4				
																4/29	1				
																5/3	1				

7.3.2 County Level Results

7.3.2.1 Total Area Burned

As expected, the total amount of burned area in a county usually depended on the amount of grassland available for burning in that county, and on county size (Table 7.6). Chase County, because it is made up largely of tallgrass prairie, often had nearly as many acres burned per year as much larger counties, such as Greenwood, Butler, and Osage. Conversely, Marshall County, though a relatively large county, had much less grassland area than most counties in the study area, and so consistently displayed relatively low burned area values.

Table 7.6: Total burned area (in hectares) by county for each of the 11 sampling years.

County	2000	2001	2002	2003	2004	2005	2006	2007	2008	2009	2010
Marshall	16,694	32,344	11,706	5,975	8,919	18,863	11,931	8,925	13,525	19,156	9,075
Riley	36,725	31,450	28,900	25,525	28,763	51,819	39,313	28,513	37,425	47,150	35,088
Pottawatomie	43,569	53,275	28,519	17,088	41,938	68,750	37,556	23,675	50,281	51,063	48,475
Geary	18,750	16,738	12,188	12,338	17,950	41,863	23,944	9,350	27,594	30,694	25,056
Wabaunsee	79,094	52,100	55,306	70,250	63,681	113,906	110,756	37,119	97,481	105,963	74,269
Morris	54,375	31,113	32,800	43,194	27,825	69,444	55,869	7,500	50,669	45,300	51,231
Lyon	66,888	34,144	58,438	76,431	42,094	86,719	89,488	25,025	64,188	82,306	49,250
Marion	26,288	10,650	4,856	21,825	10,794	32,738	6,469	4,200	21,363	25,144	24,544
Chase	128,981	74,600	68,206	112,700	75,619	137,906	79,913	22,025	115,988	125,650	113,363
Coffey	27,781	11,419	38,444	35,825	16,869	45,488	40,906	24,800	30,538	49,719	17,100
Greenwood	122,413	61,063	72,231	135,094	61,625	144,181	73,938	55,544	124,313	143,156	110,019
Butler	120,456	71,788	30,144	104,819	51,056	125,438	36,900	49,306	108,469	118,881	97,606
Woodson	29,881	29,650	19,581	34,550	25,131	40,081	21,313	22,250	34,925	39,506	24,263
Elk	52,175	46,481	23,700	63,744	42,513	64,563	26,950	24,419	59,919	71,956	51,281
Cowley	69,450	44,856	8,869	80,713	45,663	78,575	25,794	26,313	76,538	60,350	51,481
Chautauqua	37,031	19,288	10,869	49,963	30,400	46,619	26,350	8,731	34,556	49,794	15,750
Osage (OK)	122,900	128,900	35,669	164,838	97,556	140,238	41,519	31,800	110,988	135,150	96,231
Kay (OK)	11,581	10,950	2,719	22,763	8,231	13,438	6,950	4,969	16,250	11,388	11,694

7.3.2.2 Percentage Burned of Total Area and Grassland Area

The pattern displayed by total burned area is also apparent in the percentage of each county that was burned in each year (Table 7.7). In this case, Chase County displayed percentages of total area burned that averaged 49%, which was the highest value of any county in the study, while counties with less grassland, such as Marshall, Marion, and Kay (all larger than Chase), averaged only 6%, 7%, and 5% of total area burned, respectively.

It is interesting that this difference is also apparent when only the percentages of each county's grassland acres that were burned are compared. One could reasonably expect that percentages of grassland burned would be similar among the different counties, as any piece of grassland throughout the Flint Hills might be as likely to be burned as the next. However, the value for Chase County is again the highest in the study at 56%, while the values for Marshall, Marion, and Kay Counties are again the lowest in the study, at 18%, 15%, and 11%, respectively (Table 7.8). This is illustrated graphically in Figure 7.4. This phenomenon is linked to burn frequency, which will be discussed further in section 7.3.2.3.

Although it is beyond the scope of this study to identify the reason for this discrepancy, several plausible explanations follow. First, counties with lower grassland percentages tend to

exist on the periphery of the Flint Hills proper, which also leads to smaller, fractured grasslands (since they are interspersed with croplands) in which case the risk and time required for consistent burning might mitigate any positive effects. Another possibility is that many of these grasslands might be enrolled in the Conservation Reserve Program (CRP), in which case the landowner does not need to burn for cattle production, and so burns only as often as stipulated in the CRP contract. Yet another possibility is that burned areas in these counties might be from cover types other than grasslands, such as crop residue, which might not be burned as frequently as grasslands. A final possibility might be that land ownership/tenure affects burning frequencies.

Table 7.7: Percentage of total county area burned in each year of the study.

County	Area (ha)	2000	2001	2002	2003	2004	2005	2006	2007	2008	2009	2010	Mean
Marshall	232,721	7	14	5	3	4	8	5	4	6	8	4	**6**
Riley	159,443	23	20	18	16	18	32	25	18	23	30	22	**22**
Pottawatomie	221,865	20	24	13	8	19	31	17	11	23	23	22	**19**
Geary	106,740	18	16	11	12	17	39	22	9	26	29	23	**20**
Wabaunsee	206,796	38	25	27	34	31	55	54	18	47	51	36	**38**
Morris	181,102	30	17	18	24	15	38	31	4	28	25	28	**24**
Lyon	222,711	30	15	26	34	19	39	40	11	29	37	22	**28**
Marion	243,462	11	4	2	9	4	13	3	2	9	10	10	**7**
Chase	197,692	65	38	35	57	38	70	40	11	59	64	57	**49**
Coffey	170,580	16	7	23	21	10	27	24	15	18	29	10	**18**
Greenwood	296,191	41	21	24	46	21	49	25	19	42	48	37	**34**
Butler	376,394	32	19	8	28	14	33	10	13	29	32	26	**22**
Woodson	131,777	23	23	15	26	19	30	16	17	27	30	18	**22**
Elk	167,261	31	28	14	38	25	39	16	15	36	43	31	**29**
Cowley	291,020	24	15	3	28	16	27	9	9	26	21	18	**18**
Chautauqua	163,096	23	12	7	31	19	29	16	5	21	31	10	**18**
Osage (OK)	588,530	21	22	6	28	17	24	7	5	19	23	16	**17**
Kay (OK)	242,427	5	5	1	9	3	6	3	2	7	5	5	**5**

Table 7.8: Percentage of county grassland area burned in each year of the study.

County	Grass (ha)	% Grass	2000	2001	2002	2003	2004	2005	2006	2007	2008	2009	2010	Mean
Marshall	77,514	33	22	42	15	8	12	24	15	12	17	25	12	**18**
Riley	101,515	64	36	31	28	25	28	51	39	28	37	46	35	**35**
Pottawatomie	154,836	70	28	34	18	11	27	44	24	15	32	33	31	**27**
Geary	71,259	67	26	23	17	17	25	59	34	13	39	43	35	**30**
Wabaunsee	165,161	80	48	32	33	43	39	69	67	22	59	64	45	**47**
Morris	132,198	73	41	24	25	33	21	53	42	6	38	34	39	**32**
Lyon	149,519	67	45	23	39	51	28	58	60	17	43	55	33	**41**
Marion	116,515	48	23	9	4	19	9	28	6	4	18	22	21	**15**
Chase	172,128	87	75	43	40	65	44	80	46	13	67	73	66	**56**
Coffey	96,821	57	29	12	40	37	17	47	42	26	32	51	18	**32**
Greenwood	252,354	85	49	24	29	54	24	57	29	22	49	57	44	**40**
Butler	269,743	72	45	27	11	39	19	47	14	18	40	44	36	**31**
Woodson	85,772	65	35	35	23	40	29	47	25	26	41	46	28	**34**
Elk	138,170	83	38	34	17	46	31	47	20	18	43	52	37	**35**
Cowley	193,548	67	36	23	5	42	24	41	13	14	40	31	27	**27**
Chautauqua	132,105	81	28	15	8	38	23	35	20	7	26	38	12	**23**
Osage (OK)	369,597	63	33	35	10	45	26	38	11	9	30	37	26	**27**
Kay (OK)	96,340	40	12	11	3	24	9	14	7	5	17	12	12	**11**

Figure 7.4: Comparison of percentage of total grassland burned in Marshall and Chase counties.

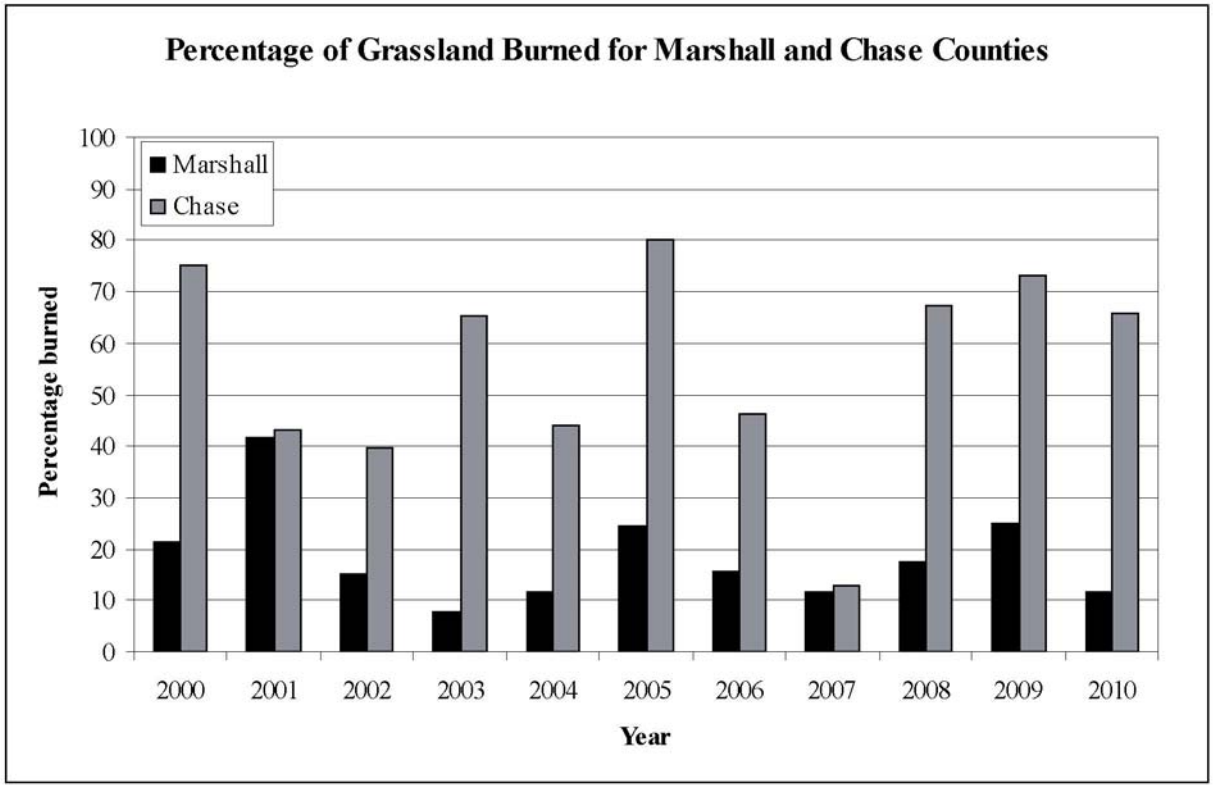

7.3.2.3 Burn Frequency

When the frequency of burning (in the context of total county area) is tabulated and examined for all counties in the study area, several patterns emerge (Table 7.9). First, the majority of the area in some counties, such as Marshall, Marion and Kay, often remains unburned in a given year. Additionally, burned areas in these counties are burned less frequently, with most being burned only one to three years out of eleven. As discussed in section 7.3.2.2 above, this is likely due to the existence of these counties on the periphery of the Flint Hills, and the associated characteristics of their grasslands. In contrast to this, counties with larger percentages of their area in grassland (which also have larger grassland tracts) show relatively little area that is burned between one and three years out of eleven, compared to area that is burned between four and nine years out of eleven. In fact, the number of hectares that went unburned during the entire eleven-year study (31,138) in Chase county is only slightly larger than the number of hectares burned exactly eight of the eleven years of the study (25,444) in that county. Additionally, more than 20,000 hectares are also burned at a frequencies of six, seven, and nine years.

Table 7.9: Total hectares burned by burn frequency for all 18 counties.

County	0	1	2	3	4	5	6	7	8	9	10	11
Marshall	163,306	29,356	17,238	10,550	6,188	3,081	1,594	706	381	144	138	75
Riley	73,169	14,225	11,481	11,138	9,788	8,438	8,600	7,219	5,675	4,194	4,019	1,350
Pottawatomie	87,881	33,475	25,638	20,144	15,863	12,706	8,506	6,956	5,850	3,131	1,238	444
Geary	45,631	10,894	10,619	10,506	9,331	6,313	4,250	2,775	2,063	1,931	1,656	788
Wabaunsee	52,525	14,706	13,744	13,831	15,363	17,819	18,569	18,069	15,244	11,269	8,856	6,838
Morris	78,813	19,831	14,300	11,288	9,569	8,913	8,494	7,138	8,169	9,013	4,375	1,269
Lyon	84,013	17,050	18,088	17,569	16,925	15,031	13,081	11,644	10,900	8,688	6,563	2,963
Marion	178,994	21,313	12,919	10,075	6,806	5,169	3,800	2,031	1,575	419	306	69
Chase	31,138	6,513	8,506	10,806	13,556	18,081	22,100	24,869	25,444	22,931	9,675	4,119
Coffey	85,631	15,994	13,969	12,394	10,744	9,450	7,200	6,050	4,275	3,056	1,238	663
Greenwood	68,594	27,775	27,575	27,706	26,538	24,594	25,694	22,344	20,306	15,656	6,763	2,700
Butler	152,419	39,325	36,744	33,269	28,075	23,919	17,238	17,506	13,394	9,031	4,738	744
Woodson	55,531	14,050	12,863	10,838	8,344	6,575	5,238	4,881	4,950	7,156	1,069	294
Elk	54,244	17,269	15,894	13,956	12,356	11,225	11,163	8,938	8,275	7,138	5,856	994
Cowley	141,763	31,500	24,881	20,206	18,306	17,856	13,806	8,938	7,506	5,194	731	363
Chautauqua	70,231	18,894	17,038	15,450	12,756	10,838	8,275	5,131	2,888	1,000	425	200
Osage (OK)	283,738	70,394	55,819	48,244	35,281	25,769	22,731	16,013	16,938	9,913	3,306	325
Kay (OK)	197,594	16,431	9,331	6,956	4,644	3,044	2,394	1,006	519	181	231	113

It was noted in section 7.3.2.2 that counties with lower grassland percentages typically have a lower percentage of that grassland burned each year than do counties with high grassland percentages. This trend is related to the frequency with which grasslands are burned in a given county. Specifically, grassland areas in counties with high grassland percentages are burned much more frequently than are grasslands in counties with low grassland percentages. This supports an obvious conclusion: in any given year, grasslands are more likely to be burned in a county where they are more plentiful, and less likely to be burned where they are less plentiful. This means that, in areas where grasslands are not plentiful, a relatively small percentage of total grassland is burned each year, and areas that are burned are likely to be different from year to year. Additionally, it is possible that this phenomenon causes the lower than expected overall (study area-wide) burn frequency that was described in section 7.3.1.3, as counties with low percentages of grassland lower the average over the entire study area.

Table 7.10: Percent of grassland burned by burn frequency (years) for all 18 counties. Grass % column is the 11-year average percent of each county's grassland area that was burned.

County	Grass (ha)	Grass %	1	2	3	4	5	6	7	8	9	10	11
Marshall	77,514	18	38	22	14	8	4	2	1	0	0	0	0
Riley	101,515	35	14	11	11	10	8	8	7	6	4	4	1
Pottawatomie	154,836	27	22	17	13	10	8	5	4	4	2	1	0
Geary	71,259	30	15	15	15	13	9	6	4	3	3	2	1
Wabaunsee	165,161	47	9	8	8	9	11	11	11	9	7	5	4
Morris	132,198	32	15	11	9	7	7	6	5	6	7	3	1
Lyon	149,519	41	11	12	12	11	10	9	8	7	6	4	2
Marion	116,515	15	18	11	9	6	4	3	2	1	0	0	0
Chase	172,128	56	4	5	6	8	11	13	14	15	13	6	2
Coffey	96,821	32	17	14	13	11	10	7	6	4	3	1	1
Greenwood	252,354	40	11	11	11	11	10	10	9	8	6	3	1
Butler	269,743	31	15	14	12	10	9	6	6	5	3	2	0
Woodson	85,772	34	16	15	13	10	8	6	6	6	8	1	0
Elk	138,170	35	12	12	10	9	8	8	6	6	5	4	1
Cowley	193,548	27	16	13	10	9	9	7	5	4	3	0	0
Chautauqua	132,105	23	14	13	12	10	8	6	4	2	1	0	0
Osage (OK)	369,597	27	19	15	13	10	7	6	4	5	3	1	0
Kay (OK)	96,340	11	17	10	7	5	3	2	1	1	0	0	0

Figure 7.5: Comparison of burn frequencies for Marshall and Chase Counties.

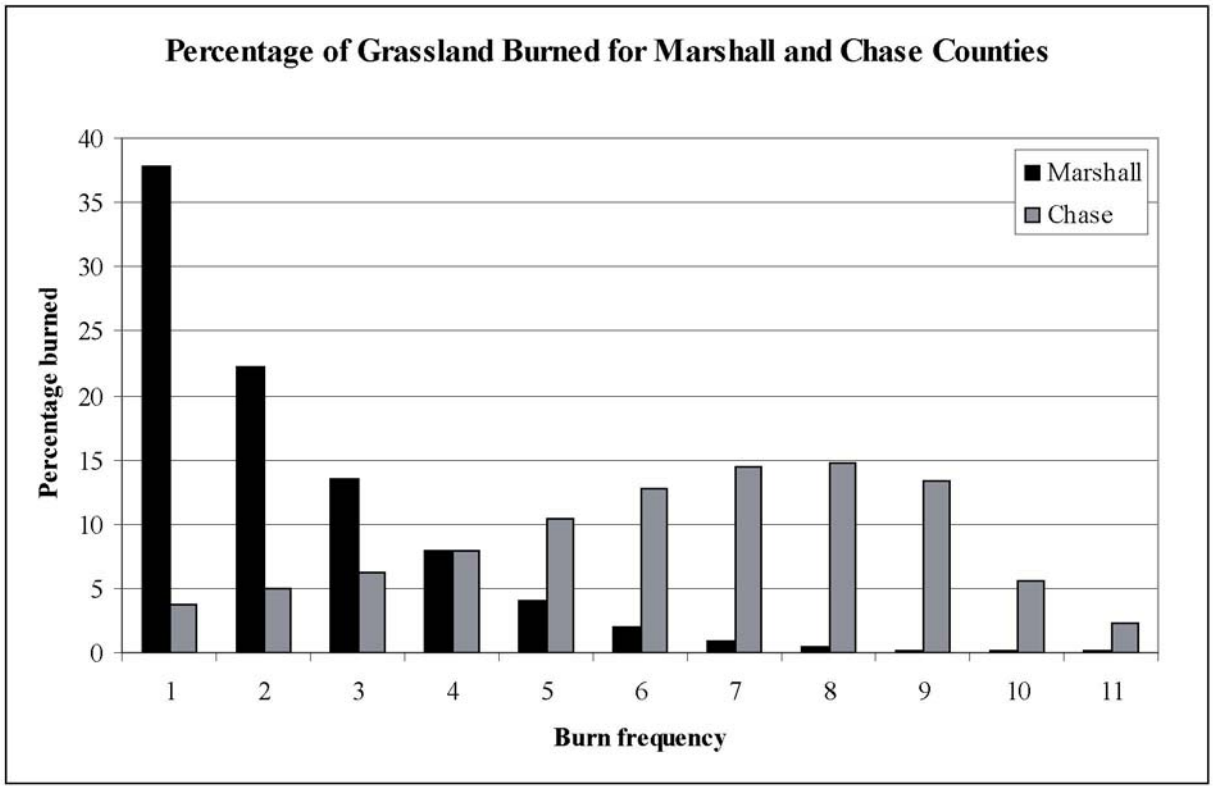

7.4 Conclusions

This chapter described the reconstruction of the spatio-temporal fire history of the Flint Hills from 2000 through 2010, which was done by classifying MODIS 250 m resolution red and NIR data with a supervised minimum distance technique. Results showed that the total amount of burned area in the Flint Hills was highly variable from year-to-year, but that no increase or decrease in area burned existed over the period of study. They also showed spatial variation in burned areas across the Flint Hills. This was particularly true in 2006 and 2007, where the majority of burning activity took place in the northern half of the study area. The results also showed that most burning takes place in April, though some additional burning taking place in March and May. With regard to burn frequency, most pixels that were burned at all were burned in only one to three years of the total eleven. This trend is somewhat surprising, considering the benefits of frequent burning to livestock production outlined in Chapter 1. However, this trend varied across the study area, with some counties showing a decidedly opposite trend.

County-level analysis showed that counties with high percentages of burned areas were most often counties with high percentages of grassland, which is not at all surprising. What was somewhat surprising was that a high percentage of grassland within a county correlated with high percentages of grassland being burned. Therefore, counties with more grass are more likely to burn a higher percentage of it. This is related to burn frequency, as areas with more grassland are burned more often, thereby accounting for their higher likelihood of being burned in a given year. Finally, the tendency of counties with little grassland to burn it less often than counties with more grassland might be responsible for lower than expected burn frequencies over the entire study area.

CHAPTER 8 - Assessment of Burned Area and Active Fire Product Quality

8.1 Introduction

The fifth and final objective of this study was to compare the burned area maps of the Flint Hills produced in the previous chapter to MODIS active fire product and to MODIS burned area product. In order to accomplish this objective, two hypotheses would be tested. First, that the locally produced burned area maps will depict burned areas more accurately than active fire product. This hypothesis is based on the fact that active fire product does not account for total area burned, and is calculated at a much coarser spatial resolution of 500 m. The second hypothesis is that locally produced burned area maps will depict burned areas more accurately than the monthly burned area product. This hypothesis is based on the fact that monthly burned area maps are calculated at a much coarser spatial resolution of 1 km. Both of these hypotheses were tested using both a simple comparison of supposed burned area as well as a chi-square test.

The active fire product used in this chapter is produced by detecting and recording thermal anomaly pixels, then placing these pixels into one of three categories based the level of confidence in that particular pixel actually being a fire. Additionally, cloudy and unknown pixels are recorded as well (Giglio 2010). Because active fire products rely on thermal bands, they are available at a maximum resolution of 1 km. A more detailed description of thermal anomaly/active fire data can be found in Giglio (2010).

The burned area product evaluated in this chapter uses a burn detection algorithm whereby changes in the surface are recorded on a daily basis. Specifically, drops in reflectance are mapped, then burned areas are separated from other causes of reduced albedo through temporal analysis (e.g., clouds should be only temporary) and through spectral properties (e.g., burned areas behave differently in MODIS band 7 than do cloud shadows (Boschetti *et al.* 2009). These criteria are used to produce a product that depicts burned areas globally. Because these products use MODIS bands besides red and NIR, they are available at a maximum spatial resolution of only 500 m. A more detailed description of the MODIS monthly burned area product, including its detection algorithms, can be found in Boschetti *et al.* (2009).

8.2 Methods

8.2.1 Product Acquisition and Processing

Monthly burned area products (MCD45A1) for all years from 2001 through 2010 (except 2006) were downloaded through WIST and processed with the MRT in the same manner as all other MODIS imagery, including being subset to the study area. Monthly burned area product from 2000 was not used in this analysis because the data for this year, being the first year of MODIS, were of poor quality. Furthermore, product for 2006 was not available, and so this year was not used either. Four months covered the entire study period in each year: February, March, April, and May. In the case of some years, no burned areas were present within the study area for certain months, and these were not included in the analysis (Table 8.1). For each month in each year, the band that showed on which Julian date an area was burned was reclassified so that burned areas were depicted as 1 and unburned areas were depicted as 0, resulting in a burned/not burned binary image. All months in a given year were summed and resampled so that burned and unburned areas were represented by values of 1 and 0, respectively. This yielded a percentage of burned and unburned area within the study area for each year.

Table 8.1: Monthly burned area product used for each year. All months used in a given year were summed to get total burned area for that year.

Year	Months used
2001	February, March, April
2002	March, April, May
2003	February, March, April
2004	February, March, April, May
2005	February, March, April, May
2006	NA
2007	February, March, April, May
2008	February, March, April, May
2009	February, March, April, May
2010	February, March, April, May

Two versions of the active fire product were downloaded through WIST and processed in the same manner as were the burned area products. Again, 2000 was not used due to quality issues, though active fire product for 2006 was available. The first product was an 8-day composite (MOD14A2 and MYD14A2 for Terra and Aqua, respectively) that showed all pixels classified as being thermal anomalies (which is taken to mean active fires) during that 8-day period. The second product was the daily version (MOD14A1 and MYD14A1 for Terra and

Aqua, respectively) of the 8-day product. This version was used to fill in beginning and end dates not covered by the 8-day composites (covering these dates with 8-day composites could lead to overestimation because active fires outside of the study period could be counted).

Each daily and 8-day scene for each year for each sensor (Table 8.2) was reclassified to a binary classification, where 1 represented fire pixels and 0 represented all other pixels. Although the original data classified fire pixels into three types, low-confidence fire, nominal-confidence fire, and high-confidence fire, all fire types were combined here into the same class. All scenes for a given year were then summed and reclassified, which yielded a binary image for each year that depicted all fire pixels with a value of 1, and all non-fire pixels with a value of 0. This scene yielded the percentage of fire and non-fire pixels within the study area for each year.

Table 8.2: Dates of fire product used in each year to produce a composite of active fire pixels for each of the study years.

Year	Study Period	8-Day (range)	Daily Aqua	Daily Terra
2001	Mar. 8-May 9	Mar. 14-Apr. 30	NA	Mar. 9, 10, 13
2002	Feb. 28-May 9	Mar. 6-May 8	NA	None
2003	Mar. 2-May 5	Mar. 6-Apr. 30	May 2, 4	May 2, 4
2004	Mar. 7-Apr.27	Mar. 13-Apr. 21	Mar. 9-12, Apr. 25, 27	Mar. 8-12, Apr. 25-27
2005	Mar. 1-May 4	Mar. 6-Apr. 30	Mar. 1-5, May 2-4	Mar. 2-5, May 3
2006	Mar. 2-Apr. 27	Mar. 6-Apr. 22	Apr. 23, 26, 27	Mar. 3, Apr. 26, 27
2007	Mar. 3-Apr. 29	Mar. 6-Apr. 22	Mar. 5, Apr. 23, 28, 29	Mar. 4, 5, Apr. 23, 28, 29
2008	Mar. 1-May 3	Mar. 5-Apr. 29	Feb. 27, 29, Mar. 1, May 2, 3	Feb. 27, 29, May 3
2009	Mar. 1-May 8	Mar. 6-May 8	Mar. 5	Mar. 4
2010	Mar. 2-Apr. 29	Mar. 6-Apr. 22	Mar. 2-4, Apr. 23, 27, 29	Mar. 2-5, Apr. 26

8.2.2 Method of Comparison

Burned areas were compared to active fire and burned areas products in two ways. First, the percentage of the total area that was burned as estimated from each of the two products for each year was compared to the same percentages as estimated from the burned area maps developed in Chapter 7.

Additionally, the similarity of the burned area estimates from the two products was also compared statistically to the estimates from the Chapter 7 maps using a goodness-of-fit chi-square test. In this case, the burned area estimates from Chapter 7 represented the theoretical burned area amounts, while the burned area estimates from the two products were evaluated for

their fit to this theoretical estimate. The hypothesis stated that burned area frequency distribution for each year from either the active fire or burned area product did differed significantly from the distribution indicated by the Chapter 7 maps of burned area for the same year.

To perform the chi-square test, 200 pixels were selected at random from each product in each year. The status of these (burned or unburned) was recorded and formed the observed frequency distribution for the two products that was used in the chi-square analysis. The theoretical frequency distribution was the proportion of total pixels burned in each year as indicated by Chapter 7 burned area classifications. Chi-square was calculated as

$$X^2 = \sum_{i=1}^{n} O_i - E_i)^2 / E_i \tag{8.1}$$

where X^2 is the chi-square test statistic, O is the observed frequency, E is the expected frequency, n is the number of cells in the table, and i denotes the cell in question. The hypothesis was accepted if X^2 fell within the range 0.004 to 3.841, as these are the upper and lower critical values with one degree of freedom at the 95% confidence interval.

8.3 Results and Discussion

The comparison of total burned area percentages as calculated from both the active fire and burned area products to those from the Chapter 7 burned area maps showed that neither product could not detect all or even most of the burned area within the study area. This was especially true in 2001 and 2002, where only one MODIS sensor was in operation (on board the Terra satellite). Even in the best case in 2009, only 63 and 60 percent of the total burned area was found by the active fire and burned area products, respectively. In all years, the active fire product performed better than the burned area product did. This is somewhat surprising, given its coarser spatial resolution, but the performance of either product is still far poorer than the method developed in Chapter 6 and applied in Chapter 7 of this paper.

Table 8.3: Total burned area and percent of burned area found by each product in each of the 11 years of the study.

Year	Burn maps (ha)	Active fire (ha)	% found	Burned area (ha)	% found
2001	760,769	117,500	15	12,500	2
2002	543,119	39,800	7	125	0
2003	1,077,588	639,600	59	344,450	32
2004	696,594	279,700	40	165,700	24
2005	1,320,556	619,800	47	375,250	28
2006	755,813	346,200	46		
2007	414,456	188,200	45	23,275	6
2008	1,074,944	614,200	57	477,025	44
2009	1,212,281	762,700	63	728,125	60
2010	905,738	529,600	58	292,100	32

Chi-square analysis supported the conclusions suggested by the comparison of burned area percentages. Specifically, the frequency of detected burned areas from both the active fire and burned area products was not statistically similar to the theoretical distribution provided by the burned area maps produced in Chapter 7. In only one case, using active fire data in 2008, was the hypothesis close to being rejected ($X^2 = 4.39$, $p = 0.036$). This analysis also supports two other findings of the simple percentage burned comparison between the classifications and the products. First, that burn detection was poor when only one MODIS image per day was available. Second, that active fire product was better able to detect burned areas than burned area product, though the performance of both was generally very poor. All X^2 statistics and probabilities are given in Table 8.4.

Table 8.4: Chi-square and *p*-values for each product and each year used in the study.

	Expected		Active Fire				Burned Area			
Year	Burned	Unburned	Burned	Unburned	X^2	*p*	Burned	Unburned	X^2	*p*
2001	18	82	4	196	34.69	< 0.001	2	198	39.16	< 0.001
2002	13	87	0	200	29.89	< 0.001	0	200	29.89	< 0.001
2003	26	74	26	174	17.57	< 0.001	14	186	37.53	< 0.001
2004	17	83	11	189	18.75	< 0.001	6	194	27.78	< 0.001
2005	31	69	27	173	28.64	< 0.001	16	184	49.46	< 0.001
2006	18	82	18	182	10.98	<0.001				
2007	10	90	7	193	9.39	0.0022	0	200	22.22	< 0.001
2008	26	74	39	161	4.39	0.036	23	177	21.86	< 0.001
2009	29	71	29	171	2042	< 0.001	31	169	17.70	< 0.001
2010	22	78	23	177	12.85	< 0.001	13	187	28.00	< 0. 001

8.4 Conclusions

Comparison of burned area estimates from burned area products and active fire products to estimates from the burned area maps produced in Chapter 7 shows that the two products could not detect many of the burned areas depicted in by the classification technique. In fact, the active fire product was never able to detect more than 63% of the burned area indicated by the classification technique from Chapter 7. The burned product performed even poorer, as it was only able to detect 60% of burned area in the best case, and failed to detect even 1% of total burned area in 2002. These results were supported by a chi-square goodness-of-fit test, where the hypothesis was consistently accepted regardless of which product was compared to the Chapter 7 classifications. This indicated that the frequency distribution of burned areas in all years with both products was not statistically similar to the theoretical distribution provided by the classifications. Given that the estimated accuracy of the burned areas classifications produced in Chapter 7 were 90% or better, these findings support the hypotheses outlined at the beginning of this chapter, which stated that neither product would be able to map burned areas as accurately than the technique developed in Chapter 6 of this study. Specifically, the high rate of Type II error in both products is far greater than the maximum 10% error that could be expected based on the Chapter 7 classifications.

The poor performance of the two products was likely caused by two factors. First, the two products were available at 500 m and 1 km spatial resolution, compared to the 250 m spatial resolution of the classification technique used in Chapter 7. Performance of the two products was also likely poor due to the fact that these products are calibrated to account for fires and burn scars in a variety of land cover types, and do not take into account the specific requirements of burned area mapping in tallgrass prairie. Consequently, the use of these products in tallgrass prairie or similar cover types should be done with caution, and with the realization that many burned areas have likely gone undetected. This finding supports the ideas of discussed in section 2.2.2, where many published works have cautioned about the accuracy of these products.

CHAPTER 9 - Summary of Major Findings and Future Work

9.1 Summary of Major Findings

9.1.1 Study Background

Prescribed burning in tallgrass prairie is important for several reasons. First, it preserves the tallgrass prairie ecosystem by limiting the growth of woody vegetation and non-native grass species, which affects the heterogeneity of the prairie plant communities, and increases productivity of matrix species. Both plant community dynamics and productivity are related closely to grazing. Fire in tallgrass prairies also affects wildlife, and these effects can be both positive and negative, depending on the scale at which burning takes place. Finally, prescribed burning can affect human health by releasing particulates and combustion chemicals into the air.

This study developed a process for creating accurate burned area maps in tallgrass prairie, as this was a critical step toward managing tallgrass prairie ecosystems using sound scientific principals, and with the interests of all stakeholders in mind. This goal was reached by completing several separate objectives, such as identifying suitable spectral ranges and indices for burned area mapping in tallgrass prairie though *in situ* hyperspectral analysis and satellite-based remote sensing, developing a technique that used suitable spectral ranges and indices to classify burned areas and assessing its accuracy, classifying historical burned areas in the Flint Hills using this technique, and comparing this technique to available burned area and active fire products.

9.1.2 Chapter 4: In Situ Hyperspectral Analysis

Various bands and indices were simulated from hyperspectral radiometer data taken *in situ* from both burned and unburned tallgrass prairie. These bands and indices were tested for their ability to differentiate between burned and unburned areas through the burning season and during subsequent vegetation regrowth. Because they were unable to differentiate between burned and unburned areas for an adequate length of time, the GEMI, GEMI-B, and NBR indices, as well as the LMIR band, were deemed unsuitable for burned area mapping in tallgrass prairie. Another interesting finding is that, when measured with NDVI, the relationship between burned and unburned areas differs depending on the state of vegetation regrowth. This renders NDVI impractical for burned area mapping in tallgrass prairie, as *a priori* knowledge must be

available for all burned areas in an image, and this is unlikely to be the case. Simulated bands such as NIR, LNIR, and SMIR, as well as simulated indices such as BAI and MIRBI, were able to differentiate burned from unburned areas for a sufficient length of time to be deemed useful for burned area mapping in tallgrass prairie. Consequently, they were retained for analysis in subsequent chapters.

9.1.3 Chapter 5: Normalized Distance Analysis

Those bands and indices that were effective at differentiating burned from unburned areas with the *in situ* hyperspectral data were tested for their ability to do the same at the wider, satellite image scale. This allowed comparison between the utility of each band or index for burned area mapping at the field level with its utility at the satellite level. Each band or index was evaluated using two pairs of burned and unburned areas and a normalized distance technique. Those bands and indices that were able to differentiate between burned and unburned areas well with the field level analysis excelled at doing the same at the satellite scale. The exception to this was SMIR, which performed very poorly at the satellite scale, despite its excellent performance when simulated with radiometer data. Overall, testing at the satellite-scale resulted in shorter time periods over which bands or indices were able to effectively differentiate burned from unburned areas, and this was likely due to the differences in the two sampling and evaluation techniques. Finally, no appreciable difference existed between the TM and MODIS sensors. All band and indices tested, with the exception of SMIR, were retained for analysis in the next chapter.

9.1.4 Chapter 6: Image Classification and Accuracy Assessment

Using those bands and indices that were able to differentiate burned from unburned areas in the preceding two chapters, several classification scenarios were created using both single-band and multiple-band/index images from TM and MODIS. These were classified using both an object-based and a minimum distance pixel-based classification technique. The results of this procedure identified the most suitable bands and/or index (singly or in combination), the best classification technique, and the best sensor, for burned area mapping in tallgrass prairie. Classification results were evaluated using both error matrices and by comparing specific burned areas to their area as measured *in situ*. This comparison suggested that classifying MODIS 250 m spatial resolution data provides the best mix of temporal and spatial resolution, and that using

the red and NIR band in combination can detect burned areas at 90% accuracy as long as those burned areas are less than 2-3 weeks old, with more recent burned areas being more accurately represented. Additionally, classification should be done with pixel-based methods, as object-based methods did not improve accuracy significantly in any case, and actually reduced accuracy in some instances.

9.1.5 Chapter 7: Flint Hills Burn History

The fire history of the Flint Hills was reconstructed from 2000 to 2010 using the method that was most likely to yield the most accurate results (based on previous chapters). Burned area maps were expected to have an accuracy of 90% or better. Total area burned and total grassland burned varied greatly from year to year, though no overall trend existed throughout the study period. Burning varied spatially from year to year as well, particularly in the southern half of the study area. Burn frequency showed that approximately 55% of the study area was burned at least once during the 11-year study period. However, most area that was burned was not burned at a frequency of at least 2-3 years, as is in line with accepted best management practices. Additionally, the areas that were burned most frequently were in areas with greater percentages of grasslands. This was demonstrated by county-level data, where counties with more grassland tended to burn that grassland more often than counties with less grassland. Therefore, counties with less grassland tended to burn different patches from year to year. Finally, this historical burned area reconstruction showed that most burning is distributed temporally throughout the month of April, with a small percentage of prescribed burning occurring in March and May.

9.1.6 Chapter 8: Burned Area and Active Fire Product Quality Assessment

Comparison of both burned area and active fire products to results from the burned area maps produced in Chapter 7 showed that neither of these products could accurately detect many burned areas in tallgrass prairie. This was likely due in part to the coarser resolution of these two products, and to the fact the products are calibrated to perform well in a variety of land cover types, but do not specialize in any cover type; especially cover types such as tallgrass prairie where burn scar recovery is rapid. As a result, the use of these products in tallgrass prairie, or other specific cover types, should be done with caution, and with the realization that significant underestimation is certain.

9.2 Future Work

Although this work was intended to be a relatively definitive guide to burned area mapping in tallgrass prairie, it raises several additional questions and provides several opportunities for related research. With regard to the hyperspectral analysis performed in Chapter 4, future work should strive to understand the effects of topography and the position of grasslands on the performance of the various bands and indices tested. Whereas this work sought to control these variables in order to characterize the effect of others (burn duration, grazing presence, etc.), future work that addresses the effects of these variables would contribute to a more thorough understanding of how burned areas change spectrally through time, and how these changes affect their ease of detection.

The possibility of using the existing hyperspectral data to seek out additional relationships between burned and unburned areas should be given attention in the future as well. Specifically, where only currently published spectral regions and indices were tested in this work, other spectral regions and indices that have not been used to map burned areas should be tested in the future. Doing this would require little additional investment in time, as the data have already been collected. Furthermore, exposing the merits of previously untested spectral regions might lead to new methods of mapping burned areas in a variety of other cover types, in addition to tallgrass prairie.

Additional work should also better establish the link between the ability of bands and indices to differentiate burned from unburned areas at the field-scale and their ability to do so at the satellite-level scale. This was illustrated in Chapter 5, where the better-performing bands and indices were able to differentiate burned from unburned areas for less time than in the field-level analysis of Chapter 4. Although this could be due to differences between the two evaluation techniques, it is almost certainly related to within-burn variation, and so is also tied to the issues mentioned in the first paragraph of this section. This work would also help to identify links between the burn detection capabilities of different sensors, which would be important if one or both of the MODIS sensors failed, and another sensor had to take its place.

Related to the above issues is the slight rebound in the normalized distance values in Chapter 5 near the end of the sampling period in August. This occurred only for sample pair #2, and occurred only with BAI, Red, and NIR. The fact that these particular indices are involved is not surprising, as the latter two are components of the first. This phenomenon provides several

avenues for future work. First, the record could be extended further into the fall to see if the trend continues. Additionally, other bands and indices could be evaluated with regard to this trend. Addressing both of these issues might help solve the overarching question of exactly what causes the trend, and why is it present in one sample pair and not the other.

Another important question raised by this work is whether coarser resolution imagery, such as the 500 m resolution imagery used in this study, could better estimate burned areas if pixels that represented a mixture of burned and unburned areas could be classified as such. This might allow detection of smaller, previously undetected burned areas with 500 m resolution imagery, as well as prevent the loss of information from pixels on the edge of burned areas. If this is true, a much larger selection of bands and indices can be used for burned area mapping in tallgrass prairie. Furthermore, the advantages that come with those bands, such as the ability to identify burned areas through light smoke and clouds, could be used as well. Minimizing the effect of smoke is especially important for this work, as smoke is very likely to be present in the imagery for obvious reasons. One way to calibrate the mechanism for separating the components of mixed pixels is to use existing, higher-resolution data, such as a concurrent classification from TM, or ground-cover data such as the National Land Cover Data (NLCD).

Future work should also focus on fine-tuning the classification technique used in this study. Although it is apparent that object-based classification shows little promise for burned area classification in tallgrass prairie, other pixel-based classification techniques might. For example, minimum distance classification was used in this work because within-class variation was expected to be great, and because this technique allowed consistency between single and multi-band scenarios. However, focusing on the detection of recent burned areas, as well as masking cover types other than burned and unburned grassland, might reduce within-class variation enough to allow a maximum likelihood technique to be used. Furthermore, this is especially true since the best-performing classification scenario contained multiple bands.

Additional work should also focus on identifying why the percentage of grassland burned is greater in counties with a larger percent of their total area in grassland. This could be done by searching for traits in counties with low grassland percentages that might contribute to this phenomenon. As mentioned in section 7.3.2.2, these traits could include, but are certainly not limited to, high rates of CRP occurrence, increased cropland burning, the fractured nature of these grasslands, safety and insurance/liability reasons, land ownership/tenure reasons, and

possible burning moratoriums. Further analysis should search for links between these and other factors and low rates of grassland burning. Additionally, this phenomenon should be examined in the context of burn frequencies across the entire study area being much lower on average than the accepted best management practices.

The burned area mapping techniques developed in this work should be used and applied to studies in other fields. Many of these are mentioned in Chapter 2, and include air quality analysis, biological analysis, human health, and range management, as well as many others. In using these techniques and burned area maps, the spatial nature of burning in the Flint Hills could also be examined. For example features such as patch homogeneity, patch pattern, and patch size could be examined in the context of species affected.

The final focus of future work that warrants mentioning is the need to automate the classification technique that was applied in Chapter 7. Not only could this provide timely burned area maps and reduce human labor costs, but it might also eliminate some of the subjectivity of the process. It should be noted that automating this technique, because of the need to select training data and the need to avoid areas of cloud cover, would be extremely difficult, though automating even portions of the technique would prove worthwhile.

References

Abrams, M. D., and L. C. Hulbert. 1987. Effect of topographic position and fire on species composition in tallgrass prairie in northeast Kansas. *American Midland Naturalist* 117:442-5.

Al-Rawi, K. R., J. L. Casanova, and A. Calle. 2001. Burned area mapping system and fire detection system, based on neural networks and NOAA-AVHRR imagery. *International Journal of Remote Sensing* 22:2015-32.

Anderson, R. C. 1990. The historic role of fire in the North American grassland. In S. L. Collins and L. L. Wallace, (eds.) *Fire in North American tallgrass prairies*. (pp. 8-18). Norman: University of Oklahoma Press.

Anderson, R. H., S. D. Fuhlendorf, and D. M Engle. 2006. Soil nitrogen availability in tallgrass prairie under the fire-grazing interaction. *Rangeland Ecology and Management* 59:625-31.

Baatz, M., U. Benz, S. Deghani, S. Heynen, A. Holtje, P. Hoffman, I. Ingenfelder, M. Mimler, M. Sohlbach, M. Weber, and G. Willhauck. 2004. eCognition user's guide v. 4.0. Definiens, A. G. Munich.

Benz, U. P., P. Hoffman, G. Willhauck, I. Lingenfelder, and M. Heynen. 2004. Multi-resolution, object-oriented fuzzy analysis of remote sensing data for GIS-ready information. *ISPRS Journal of Photogrammetry and Remote Sensing* 58:239-58.

Bernardo, D. J., D. M. Engle, and E. T. McCollum. 1988. An economic assessment of risk and returns from prescribed burning on tallgrass prairie. *Journal of Range Management* 41:178-83.

Boschetti, L., H. D. Eva, P. A. Brivio, and J. M. Gregoire. 2004. Lessons to be learned from the comparison of three satellite-derived biomass burning products. *Geophysical Research Letters* 31: Article L21501.

Boschetti, L., D. Roy, P. Barbosa, R. Boca, and C. Justice. 2008. A MODIS assessment of the summer 2007 extent burned in Greece. *International Journal of Remote Sensing* 29:2433-6.

Boschetti, L., D. Roy, and A. A. Hoffmann. 2009. MODIS collection 5 burned area product—MCD45—user's guide version 2.0. http://modis-fire.umd.edu/BA_usermanual.html

Bragg, T. B., and L. C. Hulbert. 1976. Woody plant invasion of unburned Kansas bluestem prairie. *Journal of Range Management* 29:19-24.

Cao, X., J. Chen, B. Matsushita, H. Imura, and L. Wang. 2009. An automatic method for burn scar mapping using support vector machines. *International Journal of Remote Sensing* 30:577-94.

Chandler, G., and B. Markham. 2003. Revised Landsat-5 TM radiometric calibration procedures and postcalibration dynamic ranges. *IEEE Transactions on Geoscience and Remote Sensing* 40:2674-7.

Chuvieco, E., and R. G. Cognalton. 1988. Mapping and inventory of forest fires from digital processing of TM data. *Geocarto International* 4:41-53.

Chuvieco, E., S., M. P. Martin, and A. Palacios. 2002. Assessment of different spectral indices in the red-near-infrared spectral domain for burned land discrimination. *International Journal of Remote Sensing* 23:5103-10.

Chuvieco, E., S. Opazo, W. Sione, H. Del Valle, J. Anaya, C. Di Bella, I. Cruz, L. Manzo, G. Lopez, N. Mari, F. Gonzalez-Alonso, F. Morelli, A. Setzer, I. Csiszar, J. A. Kanpandegi, A. Bastarrika, and R. Libonati. 2008. Global burned-land estimation in Latin America using MODIS composite data. *Ecological Applications* 18:64-79.

Collins, S. L. 1987. Interaction of disturbances in tallgrass prairie: a field experiment. *Ecology* 68:1243-50.

Collins, S. L. 1989. Experimental analysis of patch dynamics and community heterogeneity in tallgrass prairie. *Vegetatio* 85:57-66.

Collins, S. L. 1992. Fire frequency and community heterogeneity in tallgrass prairie vegetation. *Ecology* 73:2001-6.

Collins, S. L., and E. M. Steinauer. 1998. Disturbance, diversity, and species interactions in tallgrass prairie. In A. K. Knapp, J. M. Briggs, D. C. Hartnett, and S. L. Collins, (eds.) *Grassland dynamics: Long-term ecological research in tallgrass prairie.* (pp. 140-156). New York: Oxford University Press.

Collins, S. L., and M. D. Smith. 2006. Scale-dependent interaction of fire and grazing on community heterogeneity in tallgrass prairie. *Ecology* 87:2058-67.

Congalton, R. G., R. G. Oderwald, and R. A. Mead. 1983. Assessing Landsat classification accuracy using discrete multivariate analysis statistical techniques. *Photogrammetric Engineering and Remote Sensing* 49:1671-8.

Coppedge, B. R. and J. H. Shaw. 1998. Bison grazing patterns on seasonally burned tallgrass prairie. *Journal of Range Management* 51:258-64.

Dempewolf, J., S. Trigg, R. S. DeFries, and S. Eby. 2007. Burned-area mapping of the Serengeti-Mara region using MODIS reflectance data. *IEEE Geoscience and Remote Sensing Letters* 4:312-6.

Dennis, A., M. Fraser, S. Anderson, and D. Allen. 2002. Air pollution emissions associated with forest, grassland, and agricultural burning in Texas. *Atmospheric Environment* 36:3779-96.

Ebi, K. L., and G. McGregor. 2008. Climate change, tropospheric ozone and particulate matter, and health impacts. *Environmental Health Perspectives* 116:1449-55.

Engle, D. M., R. L. Mitchell, and R. L. Stevens. 1998. Late growing-season fire effects in mid-successional tallgrass prairies. *Journal of Range Management* 51:115-21.

Engle, D. M., and T. G. Bidwell. 2001. The response of central North American prairies to seasonal fire. *Journal of Range Management* 54:2-10.

Eva, H., and E. F. Lambin. 1998. Remote sensing of biomass burning in tropical regions: sampling issues and multisensor approach. *Remote Sensing of Environment* 64:292-315.

Evans, E. W. 1984. Fire as a natural disturbance to grasshopper assemblages of tallgrass prairie. *Oikos* 43:9-16.

Evans, E. W. 1988. Grasshopper (Insecta: Orthoptera: Acrididae) assemblages of tallgrass prairie: influences of fire frequency, topography, and vegetation. *Canadian Journal of Zoology* 66:1495-501.

Freeman, C. C. 1998. The flora of Konza Prairie: a historical review and contemporary patterns. In A. K. Knapp, J. M. Briggs, D. C. Hartnett, and S. L. Collins, (eds.) *Grassland dynamics: Long-term ecological research in tallgrass prairie.* (pp. 69-80). New York: Oxford University Press.

Fuhlendorf, S. D., W. C.Harrell, D. M. Engle, R. G. Hamilton, C. A. Davis, and D. M. Leslie Jr. 2006. Should heterogeneity be the basis for conservation grassland bird response to fire and grazing. *Ecological Applications* 16:1706-16.

Giglio, L., G. R. Van Der Werf, J. T. Randerson, G. J. Collatz, and P. Kasibhatla. 2006. Global estimation of burned area using MODIS active fire. *Atmospheric Chemistry and Physics* 6:957-74.

Giglio, L., T. Loboda, D. P. Roy, B. Quayle, and C. O. Justice. 2009. An active-fire based burned area maping algorithm for the MODIS sensor. *Remote Sensing of Environment* 113:408-20.

Giglio, L. 2010. MODIS collection 5 active fire product user's guide version 2.4. http://modis-fire.umd.edu/AF_usermanual.html

Gitas, I. Z., G. H. Mitri, and G. Ventura. 2004. Object-based classification for burned area mapping of Creus Cape, Spain, using NOAA-AVHRR imagery. *Remote Sensing of Environment* 92:409-13.

Gitas, I. Z., A. Polychronaki, T. Katagis, and G. Mallinis. 2008. Contribution of remote sensing to disaster management activities: a case study of the large fires in the Peloponnese, Greece. *International Journal of Remote Sensing* 29:1847-53.

Glenn, S. M., S. L. Collins, and D. J. Gibson. 1992. Disturbances in tallgrass prairie: local and regional effects on community heterogeneity. *Landscape Ecology* 7:243-51.

Hartnett, D. C., K. R. Hickman, and L. E. Fischer Walter. 1996. Effects of bison grazing, fire, and topography on floristic diversity in tallgrass prairie. *Journal of Range Management* 49:413-20.

Hartnett, D. C., and P. A. Fay. 1998. Plant populations: patterns and processes. In A. K. Knapp, J. M. Briggs, D. C. Hartnett, and S. L. Collins, (eds.) *Grassland dynamics: Long-term ecological research in tallgrass prairie.* (pp. 81-100). New York: Oxford University Press.

Hay, G. J., D. J. Marceau, P. Dube, and A. Bouchard. 2001. A multiscale framework for landscape analysis: object-specific analysis and upscaling. *Landscape Ecology* 16:471-90.

Hayden, B. P. 1998. Regional climate and the distribution of tallgrass prairie. In A. K. Knapp, J. M. Briggs, D. C. Hartnett, and S. L. Collins, (eds.) *Grassland dynamics: Long-term ecological research in tallgrass prairie.* (pp. 19-34). New York: Oxford University Press.

Heisler, J. L., and A. K. Knapp. 2008. Temporal coherence of aboveground net primary productivity in mesic grasslands. *Ecography* 31:408-16.

Hickman, K. R., D. C. Hartnett, R. C. Cochran, and C. E. Owensby. 2004. Grazing management effects on plant species diversity in tallgrass prairie. *Journal of Range Management* 57:58-65.

Hobbs, N. T., D. S. Schimel, C. E. Owensby, and D. S. Ojima. 1991. Fire and grazing in the tallgrass prairie: contingent effects on nitrogen budgets. *Ecology* 72:1374-82.

Hudak, A. T., and B. H. Brockett. 2004. Mapping fire scars in a southern African savannah using Landsat imagery. *International Journal of Remote Sensing* 25:3231-43.

Jonas, J. L., and A. Joern. 2007. Grasshopper (Orthoptera: Acrididae) communities respond to fire, bison grazing, and weather in North American tallgrass prairie: a long-term study. *Oecologia* 153:699-711.

Kansas Applied Remote Sensing Program. 2001. GAP Analysis Program Raster. http://www.KansasGIS.org

Kaufman, D. W., E. J. Finck, and G. A. Daufman. 1990. Small mammals and grassland fires. In S. L. Collins and L. L. Wallace, (eds.) *Fire in North American tallgrass prairies*. (pp. 46-80). Norman: University of Oklahoma Press.

Kaufman, D. W., P. A. Fay, G. A. Kaufman, and J. L. Zimmerman. 1998a. Diversity of terrestrial macrofauna. In A. K. Knapp, J. M. Briggs, D. C. Hartnett, and S. L. Collins, (eds.) *Grassland dynamics: Long-term ecological research in tallgrass prairie.* (pp. 101-112). New York: Oxford University Press.

Kaufman, D. W., G. A. Kaufman, P. A. Fay, J. L. Zimmerman, and E. W. Evans. 1998b. Animal populations and communities. In A. K. Knapp, J. M. Briggs, D. C. Hartnett, and S. L. Collins, (eds.) *Grassland dynamics: Long-term ecological research in tallgrass prairie.* (pp. 113-139). New York: Oxford University Press.

Kaufman, Y. J., and L. A. Remer. 1994. Detection of forests using mid-IR reflectance: an application for aerosol studies. *IEEE Transactions on Geoscience and Remote Sensing* 32:672-83.

Knapp, A. K. 1984. Post-burn differences in solar radiation, leaf temperature and water stress influencing production in a lowland tallgrass prairie. *American Journal of Botany* 71:220-7.

Knapp, A. K. 1985. Effect of fire and drought on the ecophysiology of *Andropogon gerardii* and *Panicum virgatum* in tallgrass prairie. *Ecology* 66:1309-20.

Knapp, A. K., and T. R. Seastedt. 1986. Detritus accumulation limits productivity of tallgrass prairie. *BioScience* 36:662-8.

Knapp, A. K., and T. R. Seastedt. 1998. Introduction: grasslands, Konza Prairie, and long-term ecological research. In A. K. Knapp, J. M. Briggs, D. C. Hartnett, and S. L. Collins, (eds.) *Grassland dynamics: Long-term ecological research in tallgrass prairie.* (pp. 3-18). New York: Oxford University Press.

Kollmorgen, W. M., and D. S. Simonett. 1965. Grazing operations in the Flint Hills-Bluestem Pastures of Chase County, Kansas. *Annals of the Association of American Geographers*, 55:260-90.

Koutsias, N., and M. Karteris. 1998. Logistic regression modeling of multitemporal Thematic Mpper data for burned area mapping. *International Journal of Remote Sensing* 19:3499-514.

Li, R-R., Y. J. Kaufman, W. M. Hao, J. M. Salmon, and B-C. Gao. 2004. A technique for detecting burn scars using MODIS data. *IEEE Transactions on Geoscience and Remote Sensing* 42:1300-7.

Loboda, T., K. J. O'Neal, and I. Csiszar. 2007. Regionally adaptable dNBR-based algorithm for burned area mapping from MODIS data. *Remote Sensing of Environment* 109:429-42.

Lopez-Garcia, M. J., and V. Caselles. 1991. Mapping burns and natural reforestation using Thematic Mapper data. *Geocarto International* 6:31-7.

Meng, Z., D. Dabdub, and J. H. Seinfeld. 1997. Chemical coupling between atmospheric ozone and particulate matter. *Science* 277:116-9.

Mitri, G. H., and I. Z. Gitas. 2004a. A semi-automated object-oriented model for burned area mapping in the Mediterranean region using Landsat-TM imagery. *International Journal of Wildland Fire* 13:367-76.

Mitri, G. H., and I. Z. Gitas. 2004b. A performance evaluation of a burned area object-based classification model when applied to topographically and non-topographically corrected TM imagery. *International Journal of Remote Sensing* 25:2863-70.

Mitri, G. H., and I. Z. Gitas. 2006. Fire type mapping using object-based classification of Ikonos imagery. *International Journal of Wildland Fire* 15:457-62.

Mitri, G. H., and I. Z. Gitas. 2008. Mapping the severity of fire using object-based classification of IKONOS imagery. *International Journal of Wildland Fire* 17:431-42.

Mohler, R. L., and D. G. Goodin. 2010. A comparison of red, NIR, and NDVI for monitoring temporal burn signature change in tallgrass prairie. *Remote Sensing Letters* 1:3-9.

Nieme, J. V., H. Tervahattu, H. Vehkamaki, J. Martikainen, L. Laakso, M. Kulmala, Pl Asrnio, T. Koskentalo, S. Sillanpaa, and U. Makkonen. 2005. Characterization of aerosol particle episodes in Finland caused by wildfires in Eastern Europe. *Atmospheric Chemistry and Physics* 5:2299-310.

Pereira, J. M. C., E. Chuvieco, A. Beaudoin, and N. Desbois. 1997. Remote sensing of burned areas: a review. In E. Chuvieco (ed.) *A review of remote sensing methods for the study of large wildland fires.* (pp. 127-184). Alcalá de Henares, Spain: Departamento de Geografía Universidad de Alcalá.

Pereira, J. M. C. 1999. A comparative evaluation of NOAA/AVHRR vegetation idexes for burned surface detection and mapping. *IEEE Transactions on Geoscience and Remote Sensing* 37:217-26.

Pereira, J. M. C. 2003. Remote sensing of burned areas in tropical savannas. *International Journal of Wildland Fire* 12:259-70.

Pinty, B., and M. M. Verstraete. 1992. GEMI: a non-linear index to monitor global vegetation from satellites. *Vegetatio* 101:15-20.

Pope, C. A. III, R. T. Burnett, M. J. Thun, E. E. Calle, D. Krewski, K. Ito, and G. D. Thurston. 2002. Lung cancer, cardiopulmonary mortality, and long-term exposure to fine particulate air pollution. *Journal of the American Medical Association* 287:1132-41.

Pu, R., and P. Gong. 2004. Determination of burnt scars using logistic regression and neural network techniques from a single post-fire Landsat 7 ETM+ image. *Photogrammetric Engineering and Remote Sensing* 70:841-50.

Radke, L. F., D. E. Ward, and P. J. Riggan. 2001. A prescription for controlling the air pollution resulting from the use of prescribed biomass fire: clouds. *International Journal of Wildland Fire* 10:103-11.

Rahman, A. F., and J. A. Gamon. 2004. Detecting biophysical properties of a semi-arid grassland and distinguishing burned from unburned areas with hyperspectral reflectance. *Journal of Arid Environments* 58:597-610.

Roy, D. P., P. E. Lewis, and C. O. Justice. 2002. Burned area mapping using multi-temporal moderate spatial resolution data—a bi-directional reflectance model-based expectation approach. *Remote Sensing of Environment* 83:263-86.

Roy, D. P., Y. Jin, P. E. Lewis, and C. O. Justice. 2005. Prototyping a global algorithm for systematic fire-affected area mapping using MODIS time series data. *Remote Sensing of Environment* 97:137-62.

Sa, A. C. L., J. M. C. Pereira, M. J. P. Vasconcelos, J. M. N. Silva, N. Ribeiro, and A. Awasse. Assessing the feasibility of sub-pixel burned area mapping in miombo woodlands of northern Mozambique using MODIS imagery. *International Journal of Remote Sensing* 24:1782-96.

Shao, G., and B. W. Duncan. 2007. Effects of band combinations and GIS masking on fire-scar mapping at local scales in east-central Florida, USA. *Canadian Journal of Remote Sensing* 33:250-9.

Silva, J. M. N., J. F. C. L. Cadima, J. M. C. Pereira, and J-M Gregoire. 2004. Assessing the feasibility of a global model for multi-temporal burned area mapping using SPOT-VEGETATION data. *International Journal of Remote Sensing* 25:4889-913.

Simmons, M. T., S. Windhager, P. Power, J. Lott, R. K. Lyons, and C. Schwope. 2007. Selective and non-selective control of invasive plants: the short-term effects of growing-season prescribed fire, herbicide, and mowing in two Texas prairies. *Restoration Ecology* 15:662-9.

Smith, M. D., and A. K. Knapp. 1999. Exotic plant species in a C_4-dominated grassland: invisibility, disturbance, and community structure. *Oecologia* 120:605-12.

Stroppiana, D., S. Pinnock, J. M. C. Pereira, and J-M Gregoire. 2002. Radiometric analysis of SPOT-VEGETATION images for burnt area detection in Northern Australia. *Remote Sensing of Environment* 82:21-37.

Stroppiana, D., K. Tansey, J-M. Gregoire, and J. M. C. Pereira. 2003. An algorithm for mapping burnt areas in Australia using SPOT-VEGETATION data. *IEEE Transactions on Geoscience and Remote Sensing* 41:907-9.

Stroppiana, D., M. Boschetti, P. Zaffaroni, and P. A. Brivio. 2009. Analysis and interpretation of spectral indices for soft multicriteria burned-area mapping in Mediterranean regions. *IEEE Geoscience and Remote Sensing Letters* 6:499-503.

Svejcar, T. J., and J. A. Browning. 1988. Growth and gas exchange of *Andropogon gerardii* as influenced by burning. *Journal of* Range Management 41:239-44.

Svejcar, T. J. 1990. Response of Andropogon gerardii to fire in the tallgrass prairie. In S. L. Collins and L. L. Wallace, (eds.) *Fire in North American tallgrass prairies.* (pp. 19-27). Norman: University of Oklahoma Press.

Tanaka, S., H. Kimura, and Y. Suga. 1983. Preparation of a 1:25 000 Landsat map for assessment of burnt area on Etajima Island. *International Journal of Remote Sensing* 4:17-31.

Towne, E. G., and K. E. Kemp. 2003. Vegetation dynamics from annually burning tallgrass prairie in different seasons. *Journal of Range Management* 56:185-92.

Towne, E. G., and C. Owensby. 1984. Long-term effects of annual burning at different dates in ungrazed Kansas tallgrass prairie. *Journal of Range Management* 37:392-7.

Trigg, S., and S. Flasse. 2000. Characterizing the spectral-temporal response of burned savannah using *in situ* spectroradiometry and infrared thermometry. *International Journal of Remote Sensing* 21:3161-8.

Trigg, S., and S. Flasse. 2001. An evaluation of different bi-spectral spaces for discriminating burned shrub-savannah. *International Journal of Remote Sensing* 22:2641-7.

United States Department of Agriculture, National Agricultural Statistics Service (USDA-NASS). 2011. Bluestem Pasture Report. http://www.nass.usda.gov/Statistics_by_State/Kansas/Kansas/Publications/Economics_and_Misc/Bluestem/index.asp.

Van Dyke, F., J. D. Schmeling, S. Starkenburg, S. H. Yoo, and P. W. Stewart. 2007. Responses of plant and bird communities to prescribed burning in tallgrass prairies. *Biodiversity and Conservation* 16:827-39.

Vinton, M. A., D. C. Hartnett, E. J. Finck, and J. M. Briggs. 1993. Interactive effects of fire, bison (Bison bison) grazing and plant community composition in tallgrass prairie. *American Midland Naturalist* 129:10-8.

Wilgers, D. J., and E. A. Horne. 2006. Effects of different burn regimes on tallgrass prairie herpetofaunal species diversity and community composition in the Flint Hills, Kansas. *Journal of Herpetology* 40:73-84.

With, K. A., A. W. King, and W. E. Jensen. 2008. Remaining large grasslands may not be sufficient to prevent grassland bird declines. *Biological Conservation* 141:3152-67.

Zimmerman, J. L. 1992. Density-independent factors affecting the avian diversity of the tallgrass prairie community. *Wilson Bulletin* 104:85-94.